The mid-Cretaceous coastal catastrophe along the eastern margin of Eurasia reconstructed by sedimentological analysis and chronostratigraphic correlation

A thesis presented by

Aya Kubota

to

Department of Earth and Planetary Science

Graduate School of Sciences

Hokkaido University

for the degree of Doctor of Science

2019 March

学位論文

The mid-Cretaceous coastal catastrophe along the eastern margin of Eurasia reconstructed by sedimentological analysis and chronostratigraphic correlation

堆積物の未固結時変形構造と複合年代層序対比を用いた

白亜紀中期沿岸域大規模崩壊イベントの復元

2019 年 3 月

北海道大学大学院理学院

自然史科学専攻

地球惑星システム科学講座

久保田　彩

要旨

地球表層で発生したイベントの発見の多くは，元素・有機物濃集や不整合面など地層中の（1）“異質性”の認識に因る．この異質性を提示した先駆的な研究を出発点として，（2）現象と要因の解読・解明や（3）時空間的規模の解明を目指した研究がこれまで展開されてきた．これらの情報が蓄積した結果，グローバルな海洋無酸素事変や巨大隕石衝突など地球表層環境を大きく変えるイベントの全貌が明らかになってきた．本研究は，重力流堆積物を中心に様々に様相を変化させる堆積物の異質性に着目し，新規的な手法と着眼点から，それぞれの詳細な形成プロセスを復元することに成功した．その結果，大規模津波や巨大な生物礁の破壊・崩落などを提唱，さらに高精度な複合年代層序学的手法で，これら複数のイベントの同期性を示し，前期白亜紀アプチアン最末期のユーラシア大陸東縁部において大規模かつ広域的な沿岸域の物理的破壊イベントが繰り返し発生していたことを突き止めた．

地質記録において，津波や地震など短期間で大規模破壊を起こすイベントは，そのほとんどが認識されていない（できていない）．これは，破壊（侵食）プロセスがほとんど地層中に保存されないこと，後背地や砕屑物供給経路によって同一現象でも堆積相が多様になる点など様々な要因がある．加えて，従来の層序対比は，同一岩相・物質・生物相の追跡が基本であり，多様な堆積相を呈するイベント堆積物は広域対比されずに，ローカルな現象として見過ごされてきた．本論文では，多様に岩相を変える異質な地層を認識，解読，対比することで，地質記録に隠されてきた地球表層イベントの新たな抽出に挑んだ．

km オーダーで同時代・同層準の堆積物が，泥質スランプ，礫質重力流堆積物，オリストストロームなど多様な岩相に変化することを明らかにした（第二ー三章）．さらに，津

波堆積物（第一章）の 200 km 南方では，古くから知られる巨大地すべり堆積物の重要性に着目し，これの岩相層序調査，年代測定（U-Pb 年代測定，Sr 同位体測定）を行った．さらに含まれる異地性石灰岩の未固結時変形構造から，大規模津波と同期して，白亜紀の北太平洋における最大の浅海生物礁が大規模に破壊・崩落する現象が発生したことを明らかにした（第四章）．

本研究では，このようにアプチアン最末期に，北海道北部－中央部の 200 km 範囲において，従来の地質・堆積学では復元不可能であった規模，かつ多様な破壊現象を統一的なイベントとして提唱することに成功した．この研究は，樹脂や石灰岩の未固結時変形構造可視化などの新規的なアプローチから，従来の堆積学，層序学的観点からは抽出不可能な破壊・運搬過程を見出している．復元されたアプチアン末期の沿岸域大規模崩壊イベントは，休止期を含めると約 200 万年もの長期間に断続的に発生していたことが示された．このイベントは，前弧海盆砕屑物供給システムの転換期や礁性生物群の絶滅イベントとも同期しており，これらとの関連性とその重要性も指摘した．km オーダーで同時代・同層準の堆積物が，泥質スランプ，礫質重力流堆積物，オリストストロームなど多様な岩相に変化することを明らかにした（第二－三章）．さらに，津波堆積物（第一章）の 200 km 南方では，古くから知られる巨大地すべり堆積物の重要性に着目し，これの岩相層序調査，年代測定（U-Pb 年代測定，Sr 同位体測定）を行った．さらに含まれる異地性石灰岩の未固結時変形構造から，大規模津波と同期して，白亜紀の北太平洋における最大の浅海生物礁が大規模に破壊・崩落する現象が発生したことを明らかにした（第四章）．

本研究では，このようにアプチアン最末期に，北海道北部－中央部の 200 km 範囲において，従来の地質・堆積学では復元不可能であった規模，かつ多様な破壊現象を統一的なイベントとして提唱することに成功した．この研究は，樹脂や石灰岩の未固結時変形構造可視化などの新規的なアプローチから，従来の堆積学，層序学的観点からは抽出不可能な破壊・運搬過程を見出している．復元されたアプチアン末期の沿岸域大規模崩壊イベントは，

休止期を含めると約 200 万年もの長期間に断続的に発生していたことが示された．このイベントは，前弧海盆砕屑物供給システムの転換期や礫性生物群の絶滅イベントとも同期しており，これらとの関連性とその重要性も指摘した．

Extended Abstract

The first step for elucidation Earth's surface events in a geological record starts with recognizing enigmatic deposits. And then the following researches try to reconstruct their detail process in high resolution and geographical scales by sedimentary, geologically, geochemical, and chronological analyses. Destructive events such as tsunamis, earthquakes, and landslides, have been, however, hardly recognized although they should have occurred repeatedly in the geological past. This is due to difficulty of enigmatic deposit identification and its poor preservation potential, and low-resolution of chronostratigraphy.

Purpose of this study is to reveal large-scale destructive events on Earth's surface in the geological record by novel approaches. In Chapter 1, the latest Aptian tsunamis archived in hemi-pelagic deposits are reconstructed by sedimentary structure of amber-concentrated turbidites at the boundary between the Sorachi and Yezo groups in northern Hokkaido, Japan. In Chapter 2 and 3, chaotic deposits at the lowest part of the Yezo Group, which have various litho-facies are recognized and these are correlated with tsunami deposits in a 20 km- (Chapter 2) and a 100 km-scale (Chapter 3, 4). At the boundary between the Sorachi and Yezo groups, drastic change of the litho-facies from volcanoclastic and siliceous sediments to terrigenous sediments are considered as a result of a remarkable shift of the tectonic setting of the hinterland from an oceanic island arc to the active continental margin along the Eurasia. In this study, it is cleared that

the deposition of the Yezo Group in northern Hokkaido started with catastrophic deposition. The supply of the organic rich siliciclastic sediments had lasted continuously until the Maastrichtian.

In Chapter 4, collapse event of the huge "living" carbonate platform is reconstructed in central Hokkaido by multiple chronostratigraphy and sedimentological analysis that focusing on soft-sediment deformation structures of sedimentary carbonate. In previous studies, drastic disappearance of typical Cretaceous Tethyan biota in Northwest Pacific in the latest Aptian has been proposed. The carbonate platform biota had not appeared in the Northwest Pacific during the Middle Albian to Paleocene interval. The wide destruction of their habitats can be a conceivable factor of those biotic events.

In conclusion, these chaotic deposits, which distributed sporadically in a 200 km scale are correlated by integrated stratigraphy. A coastal catastrophe including large-scale tsunamis, submarine landslides and a collapse of carbonate platform occurred in the latest Aptian (about 114 Ma), Early Cretaceous are proposed.

CONTENTS

Chapter 1

Amber mines in the deep sea: evidence for large-scale tsunamis in the Early Cretaceous

ABSTRACT

Large-scale tsunamis destroy coastal area and rapidly transport huge amounts of material over long distances. Sediments related to tsunamis have rarely been recognized in the geological record, they are difficult to identify and have a poor preservation potential. Tsunami deposits have been studied in coastal areas for late Quaternary sediments. They are, however, rarely preserved due to strong erosion. In this study, we focus on hemi-pelagic settings as potential archives of large-scale tsunami events. Here we show enigmatic occurrences of abundant amber (fossilized plant resins) in Lower Cretaceous (about 117–114 Ma) hemi-pelagic sediments north of Japan. Soft-"resin" deformation structures revealed large-scaled land forest destructions and rapid transportation of organic remains from the continent to marine hemi-pelagic environments. Sedimentological features like large pieces of driftwood provide further evidence for a transport via large-scale tsunamis. This study sheds new light on large-scaled tsunamis as a rapid mass-transportation system from continents to oceans in the geological record.

INTRODUCTION

Tsunamis are catastrophic sea waves caused by earthquakes, submarine slides, volcanic eruptions and bolide impacts (Dawson and Stewart, 2007). They attract much attention from the standpoint of disaster prevention, and have therefore been studied intensively from late Quaternary coastal deposits for evaluating their damage to society. Though sediments of paleo-tsunamis should be a common feature in pre Quaternary settings, they are hard to recognize for three reasons. Firstly, robust criteria of tsunami deposits have not yet been established due to the difficulty of distinguishing tsunamis from other high-energy coastal events such cyclones (Shanmugam, 2012). Secondly, coastal tsunami deposits would be easily erased in a short time, because of intense erosional processes (Dawson and Stewart, 2007). Thirdly, the information of original landforms and hinterlands are difficult to recognize in the geological record. So far only mega scaled tsunamis like those induced by asteroid impacts received attention (Dawson and Stewart, 2007), while another ones and their significance for the Earth's surface system has not been discussed at all.

In this study, large-scale tsunamis have been identified in the deep past (over 100 million years ago, Early Cretaceous) by sedimentological findings. We focus on extraordinary rich amber (fossilized resin) concentrations intercalated in marine hemi-pelagic siliciclastic successions, north of Japan. This finding suggests a fast and rapid sedimentation process, which transported the soft amber from the coast lands of an adjoining continent into the ocean. This study reveals the importance of hemi-pelagic settings as possible archives of large-scale paleo-tsunami events.

GEOLOGICAL SETTINGS

The geology of Hokkaido Island (northern Japan) is characterized by an ophiolite-based fore-arc basin sequence of Jurassic–Paleogene age. The rocks consist of a piece of basaltic oceanic crust, volcanogenic and siliceous sediments, and thick and fossiliferous siliciclastic sediments in ascending order (e.g., Takashima et al., 2004; Ueda, 2016). The remarkable lithofacies change from the underlying volcanogenic rocks of the Sorachi Group to the thick siliciclastic deposits of the Yezo Group indicates a shift of the tectonic setting. The hinterland situation changed from an oceanic island arc to an active continental margin on the eastern rim of the Asian Continent (e.g., Niida and Kito, 1986; Takashima et al., 2017).

The enigmatic amber-rich siliciclastic deposits occur near the boundary of the Sorachi and Yezo groups in the Shimonakagawa Quarry (44°49'39.8"N, 142°06'45.1"E), Nakagawa area, northern Hokkaido (Figs. 1–3). The approximately 150 m thick sequence is divided into four litho-stratigraphic units (Fig. 1). Units 1 and 3 are characterized by gray-, dark gray- and dark green-colored claystones (Figs. 1–2). A parallel lamination caused by layers of radiolarians is well developed, ash-fall tuff horizons without bioturbation are intercalated in the claystones. Units 2 and 4 are composed of alternating beds of sandstone and dark gray-colored siltstone (Figs. 1–2). The amber and plant debris are generally concentrated in the sandstone beds (Fig. 3), most of which are interpreted as distal turbidites (Fig. 2). Units 1 and 4 are correlated to the uppermost part of the Sorachi Group and the lowermost part of the Yezo Group,

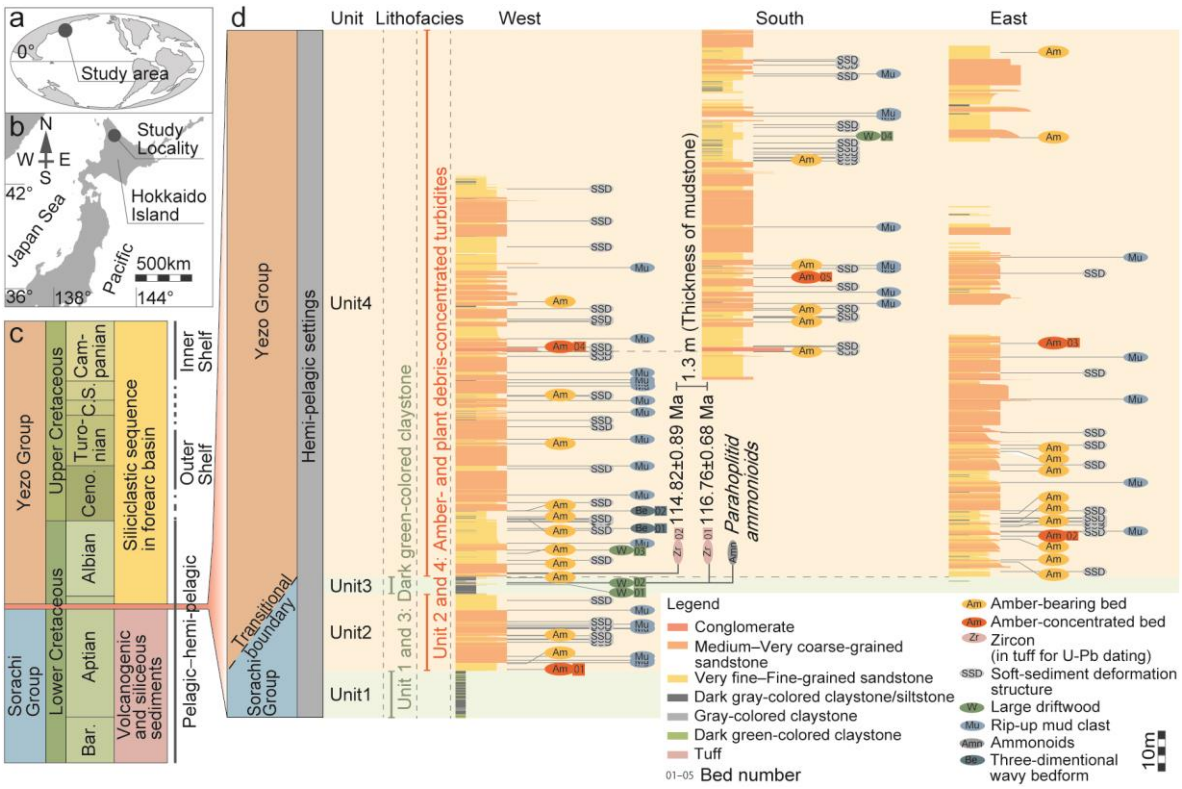

Fig. 1 Locality and stratigraphic distribution of amber-concentrated beds in the Shimonakagawa Quarry, Nakagawa area, northern Hokkaido, northern Japan. a–b: Locality map. Cretaceous paleomap is modified from Iba et al. (2011). c: Stratigraphic scheme and general trend of depositional settings of the Cretaceous siliciclastic sequence in the Nakagawa area (modified from Iba et al. (2011)). Bar.–Barremian. Ceno.–Cenomanian. C.–Coniacian. S.–Santonian. d: Columnar sections in the west, south, and east portions of the Shimonakagawa Quarry (Fig. 2). The horizons of amber highly-concentrated (over 10%) beds, tuff layers used for zircon U-Pb dating, large driftwood are also shown with each bed number.

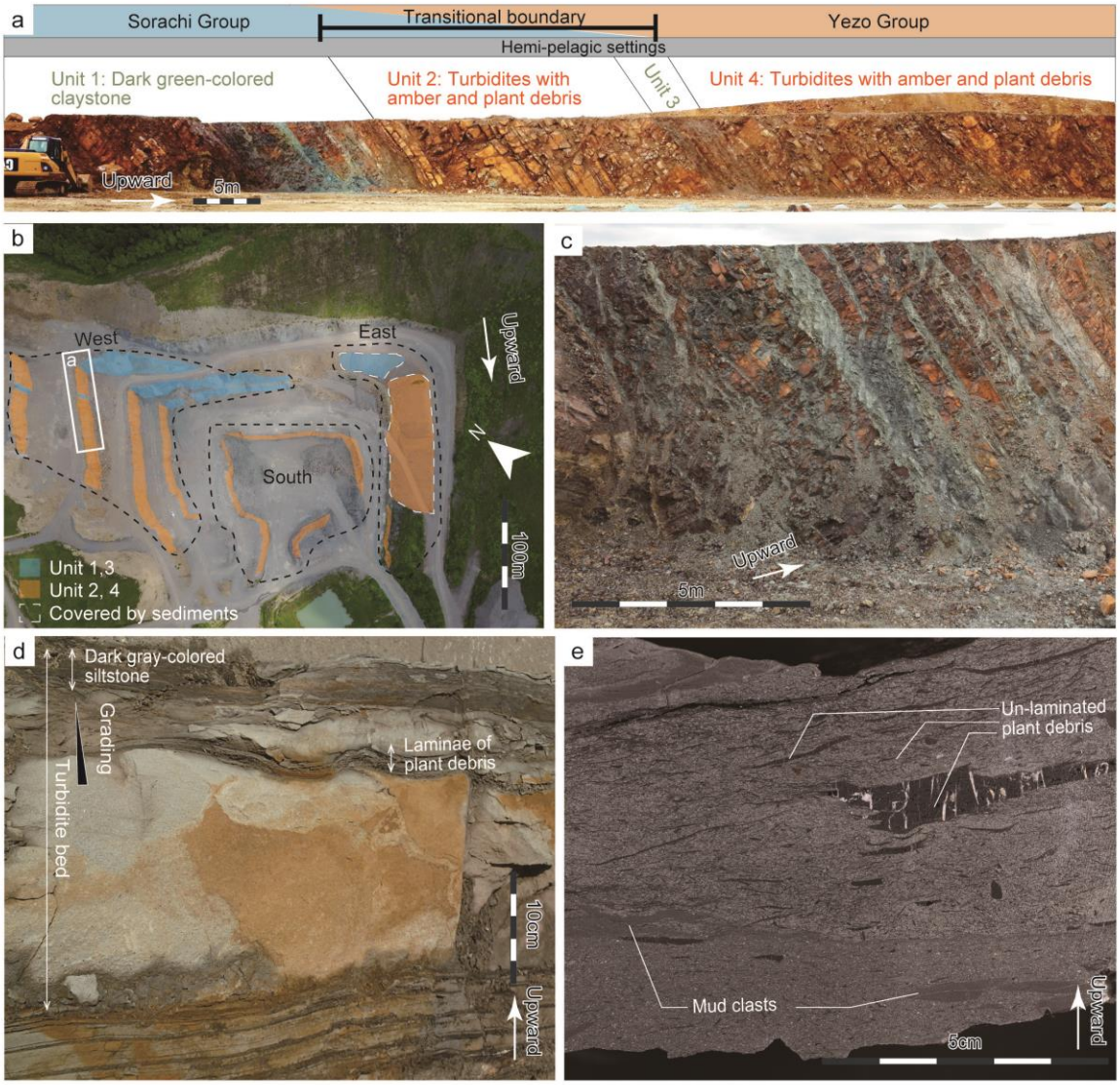

Fig. 2 The outcrops in the study locality and the mode of occurrence of sandstone beds. a: The outcrops representing the transitional boundary between the Sorachi and Yezo groups in the quarry. b: Top view of the quarry. Three columnar sections in Figure 1 have been logged for the south, west and east side of the quarry, respectively, by combining multiple columnar sections. White dot line areas are the outcrops covered by sediments at present. c: Dark green-colored claystone in Unit 1. d: A turbidite bed (type 1) in Unit 4. e: A poorly sorted silty sandstone bed including plant debris and very angular rip-up clasts (type 2).

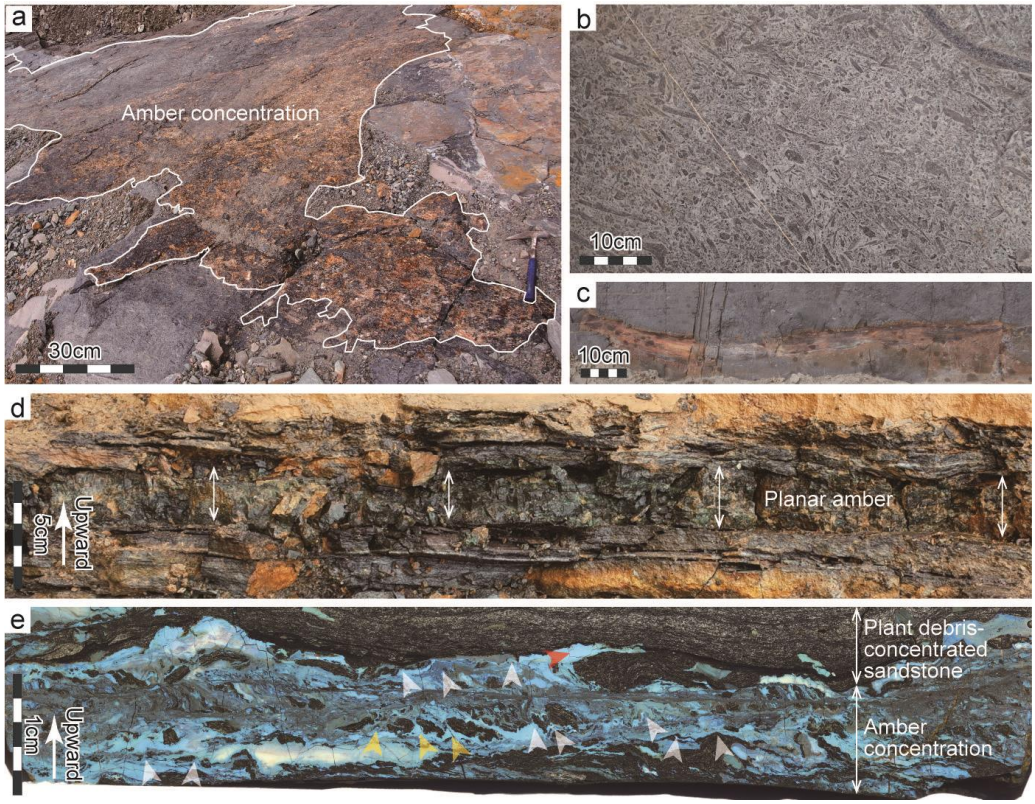

Fig. 3 The mode of occurrences of amber and associated sedimentary structures. a: Amber concentration in Am 02 widely exposed on the bedding plane. b: Concentration of plant debris on the bedding plane of the turbidite bed of W 04. c: A large driftwood in claystone bed of W 02. d: A planar-shaped amber in the bed of Am 01. Cross section. e: A fluorescence tomogram showing soft- "resin" deformation structures in amber-concentrated bed of Am 01. Cross section. Photographed under the UV and white lights at same time. White arrows show the flame structures; a red arrow shows a horizontally-oriented flame structures; yellow arrows show the ball-and-pillow structures. Stratigraphically upward is the proximal side of the surfaces in photographs (a–c), and upper side of photographs (d–e). See Figure 1-d for accurate horizons of a–e.

respectively. Units 2 and 3 represent the transitional boundary between the Sorachi and Yezo groups. Units 3 and 4 are assigned to the latest Aptian according to the occurrences of age-diagnostic Parahoplitid ammonoids (Fig. 1).

MATERIALS AND METHODS

Amber-concentrated beds: The mode of occurrence of the amber and associated material (e.g., plant debris), and sedimentary structures were described in detail in the quarry. The amount of amber was estimated in cross sections and bedding planes in the field. Here we regard horizons with > 10% amber as amber-concentrated beds.

Zircon U-Pb dating: The zircons from the tuff layers (Zr 01 in Unit 3 and Zr 02 in Unit 4, Fig. 1) were analyzed for U-Pb dating. Zircon grains were separated by crushing and sieving the rock samples. Heavy mineral separation was achieved via heavy liquid and hand-picking under a binocular microscope. Zircons were then mounted for each sample in epoxy and polished to expose approximate centers of the zircon grains. Backscattered electron (BSE) and cathodoluminescence (CL) images of individual zircon grains were obtained using a JEOL JSM-6610LV scanning electron microscope at the Korea Basic Science Institute (KBSI, Ochang, Republic of Korea), and were used for choosing analytical spots.

The zircons were analyzed for U-Pb isotopes using SHRIMP Ⅱ-e/MC (sensitive high resolution ion microprobe) at the KBSI following standard procedures (Williams, 1998 and references therein). FC1 (1099.0 Ma; Paces and Miller, 1993) and SL13 (U = 238 ppm) standard zircon were used for calibrating of measured $^{206}Pb/^{238}U$ ratio and U

concentrations, respectively. A primary negative ion oxygen beam (O_2^-) was 2–5 nA in intensity and ca. 25 μm in spot size. Each analysis consisted of five scans through mass measurements for each isotope. Common Pb contributions were corrected using the measured ^{207}Pb amount using the model common Pb composition (Stacey and Kramers, 1975). SQUID 2.50 and ISOPLOT programs (Ludwig, 2008, 2009) were used for reduction and plotting of the U-Pb data.

Visualization of internal sedimentary structures of amber: The mode of occurrences and internal sedimentary structures of amber supply remarkable clues for reconstructing their sedimentary process. X-ray computed tomography proved to be the most successful method in tomography. It has, however, a strong limitation with samples of low-density differences, such as limestone (Pascual-Cebrian et al., 2013) and our material. In addition, tomograms by X-ray CT are gray-scale and low-resolution. In contrast, we visualized the detailed structures in amber using a novel technique, so called “Grinding Tomography”. This method is based on automatic serial grinding and the subsequent serial full-color imaging. This technique using automatic serial grinding and imaging is recently applied for fossil materials, and its basic mechanism was explained in pioneering studies of Götz (2007).

We used the following procedures in this analysis at the Paleobiology Laboratory, Department of Earth and Planetary Sciences, Hokkaido University (Sapporo, Japan). Rock samples have been grinded down by an automatic machine, new surfaces have been photographed with a high-resolution digital camera (Canon 5Ds: 50.6-megapixel) in 40 μm intervals. Every photo shooting was taken under two types of light at the same

time. White light was used for the visualization of siliciclastic sediment parts, UV light (wavelength 365 nm) for visualization of amber. Amber shows its strong autofluorescence under UV light, which is very helpful for visualizing its internal structures. The new technique of "Fluorescence Grinding Tomography" was applied to two vertical sections of samples from amber-concentrated beds Am 01 and Am 02 (Figs. 1 and 3). A total of 5935 full-size images (JPG and Raw image formats) have been archived as digital specimens in the Kyushu University Museum.

RESULTS

1. Description of sandstone beds

Units 2 and 4 of the sequence exposed in the Shimonakagawa Quarry consist of alternating beds of sandstone and dark gray-colored siltstone (Fig. 1). Sandstone beds are generally divided into two lithofacies. Most sandstone beds (type 1; Fig. 2-d) are typically very fine to medium-grained and about 0.5 cm−4 m thick. Their thickness changes laterally, and some beds thin out within a 100 m length. Thinning upward cycles occur every 5−20 m. Each sandstone bed is divided into three units vertically. The bottom unit is generally flat at its base without erosional surface. The middle unit is massive and rarely shows grading. The upper unit is graded upward and generally contains parallel lamination of plant debris. In the bottom to medium units, subangular to subrounded, coarse- to very coarse-grained clasts were occasionally observed. Pebble-sized (7 mm in maximum diameter) clasts are rare. Type 1 sandstones, which

show a fine-grained matrix, lack erosional features at their bottom are interpreted as distal turbidites. Type 2 sandstones (Fig. 2-e) are poorly-sorted silty to fine-grained sandstone. Un-laminated plant debris and rip-up mud clasts are concentrated. They are interpreted as cohesive debris-flow deposits.

2. The mode of occurrences of amber in the siliciclastic sequence

Amber occur in the sandstone beds of Unit 2 and 4 (Fig. 1). A total of 32 amber-bearing beds were recognized in the outcrop. Five amber-rich beds, with amber concentrations of 10–80% on specific bedding planes and in cross-section, have been recognized (Am 01 to 05 in Figs. 1, 3 and Table 1). Amber is especially abundant in layers Am 01 (3 cm-thick in average) and Am 02 (3–7 cm in thickness). Am 02 is widely exposed on a 10 m × 10 m sized bedding plane (Figs. 3-a and 4), Am 01 occurs in the lowermost turbidite bed in Unit 2 (Fig. 1).

3. Zircon U-Pb dating

Sample Zr 01 (Figs. 5-a, 6-a and Table 2): Zircon grains typically occur as short stubby to long prismatic, almost completely un-rounded and subhedral to euhedral. Their aspect ratio ranges from 1 to 4. Their length ranges from 80–220 μm. Many zircons show oscillatory and sector zoning in CL images, which is usually interpreted as

Table 1 Content rate of amber-concentrated beds. See Am in Figure 1-d for specific horizons. Amber concentration was estimated in the field as an area ratio of amber and sandstone of the exposed part as cross-sections and bedding planes.

Bed number	Exposed area	Typical content rate (%)		Thickness of the planar amber	Extension
		Cross section	Bedding plane		
Am 01	cross section	80	–	3 cm in average	Continue 50 cm laterally in cross section
Am 02	bedding plane and cross section	30	50	3–7 cm in thickness	10 × 10 m on bedding plane
Am 03	bedding plane and cross section	20	40	3 cm in average	3 × 3 m on bedding plane
Am 04	bedding plane	10	40	–	–
Am 05	bedding plane	–	50	–	–

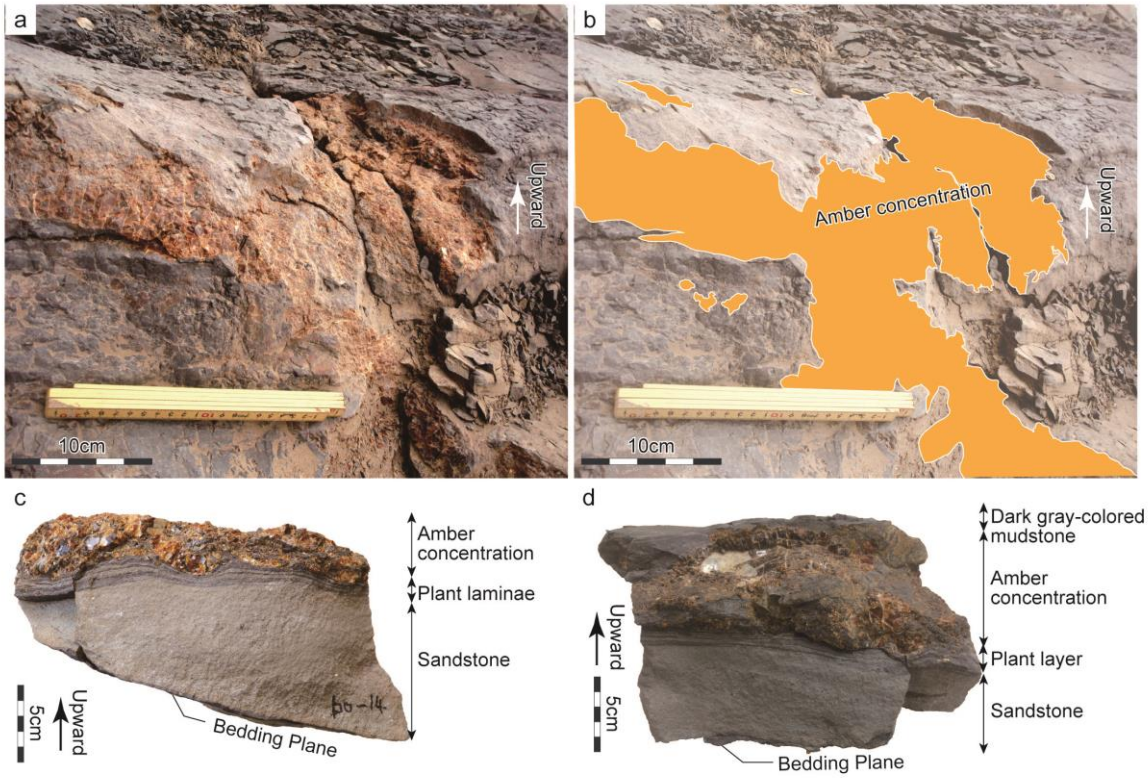

Fig. 4 The mode of occurrence of amber-concentrated bed of Am 02. a−b: The amber concentration. c−d: Rock samples of the amber-bearing turbidite. Amber is concentrated in the upper part of the turbidite.

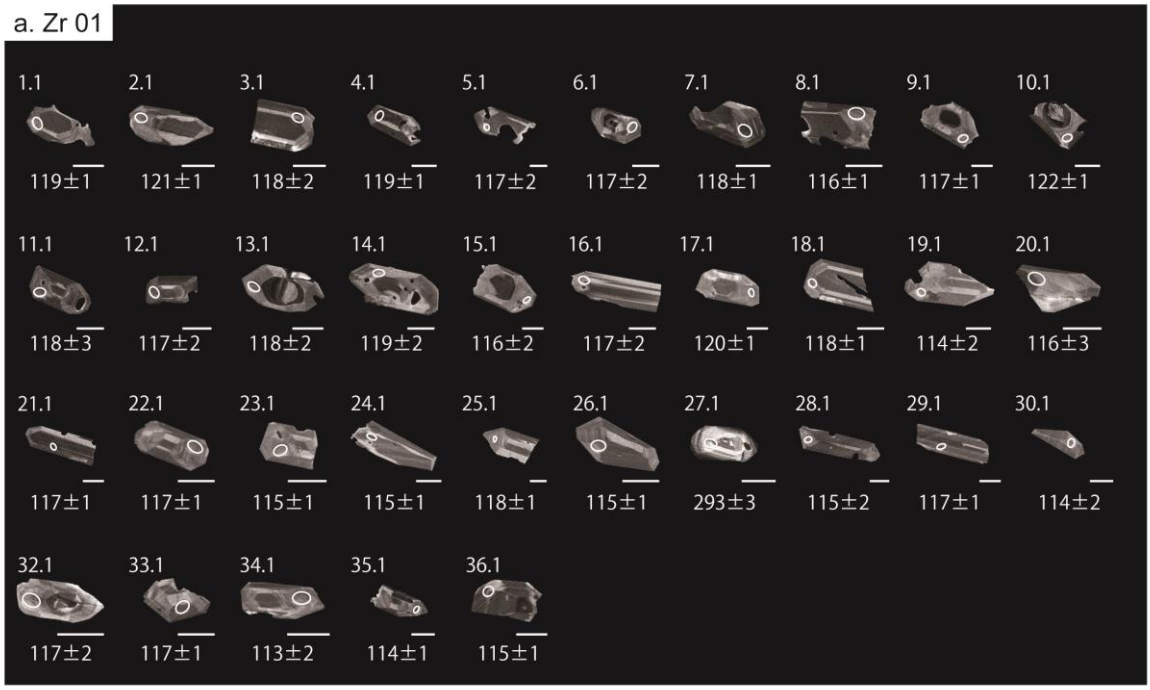

Fig. 5 Cathodoluminescence images of zircon grains from studied samples. See Zr in Fig. 1-d for their horizons. a: Zr 01 and b: Zr 02 recording analysis spots and U-Pb ages (in Ma); ages are based on $^{206}Pb/^{238}U$ ages. Scale bars are 50 μm.

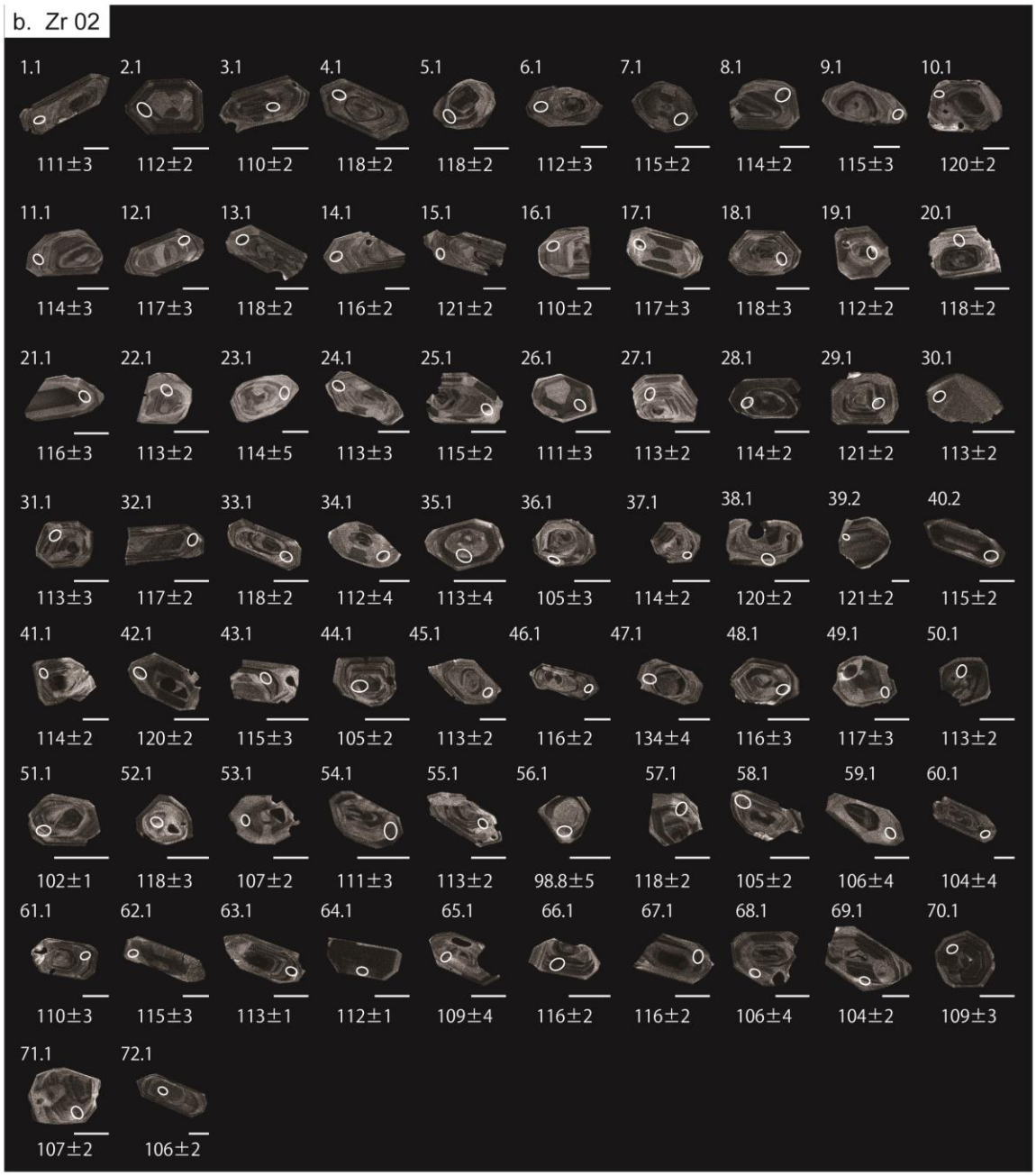

Fig. 5 (*continued*)

Table 2 Summary of SHRIMP U-Pb isotopic compositions of zircon.

Spot number	Common ^{206}Pb (%)	U (ppm)	Th (ppm)	$^{206}Pb/^{238}U$ Age (Ma)*	$^{238}U/^{206}Pb^{\dagger}$	± (%)‡	$^{207}Pb/^{206}Pb^{\dagger}$	± (%)‡
Zr01								
0724-01_1.1	--	167	62	119 ±1	53.3	1.1	0.0502	3.2
0724-01_2.1	--	169	64	121 ±1	53.1	1.1	0.0470	3.1
0724-01_3.1	--	184	78	118 ±2	54.5	1.7	0.0442	3.6
0724-01_4.1	0.04	251	142	119 ±1	53.8	1.1	0.0484	2.1
0724-01_5.1	0.66	114	43	117 ±2	54.0	1.8	0.0552	2.8
0724-01_6.1	0.22	141	55	117 ±2	54.4	1.7	0.0505	2.7
0724-01_7.1	--	239	115	118 ±1	54.3	1.1	0.0461	2.2
0724-01_8.1	--	149	53	116 ±1	55.4	1.1	0.0450	4.5
0724-01_9.1	--	129	48	117 ±1	54.7	1.1	0.0451	2.9
0724-01_10.1	--	139	49	122 ±1	52.7	1.1	0.0463	5.2
0724-01_11.1	--	167	68	118 ±3	54.2	2.5	0.0460	2.9
0724-01_12.1	0.02	171	70	117 ±2	54.7	1.5	0.0482	2.5
0724-01_13.1	0.23	140	50	118 ±2	53.9	1.8	0.0497	4.3
0724-01_14.1	0.02	156	59	119 ±2	53.8	2.1	0.0486	2.9
0724-01_15.1	0.24	162	64	116 ±2	54.9	1.5	0.0476	2.6
0724-01_16.1	0.07	156	60	117 ±2	54.7	1.7	0.0500	2.6
0724-01_17.1	--	195	84	120 ±1	53.4	1.1	0.0462	4.4
0724-01_18.1	0.00	176	67	118 ±1	53.9	1.3	0.0506	2.3
0724-01_19.1	0.02	148	52	114 ±2	56.1	1.8	0.0493	2.8
0724-01_20.1	0.34	167	65	116 ±3	54.6	2.6	0.0525	3.5
0724-01_21.1	0.03	347	221	117 ±1	54.8	1.1	0.0486	2.2
0724-01_22.1	0.17	200	85	117 ±1	54.5	1.1	0.0483	2.3
0724-01_23.1	--	204	89	115 ±1	55.7	1.1	0.0485	3.4
0724-01_24.1	--	198	94	115 ±1	55.7	1.1	0.0454	2.5
0724-01_25.1	0.00	194	82	118 ±1	54.0	1.1	0.0475	2.5
0724-01_26.1	0.13	190	75	115 ±1	55.3	1.1	0.0503	2.2
0724-01_27.1	0.09	65	36	293 ±3	21.3	1.3	0.0580	2.4
0724-01_28.1	0.26	134	47	115 ±2	55.8	1.5	0.0465	4.5
0724-01_29.1	--	198	103	117 ±1	54.6	1.3	0.0473	2.5
0724-01_30.1	--	180	73	114 ±2	56.4	1.5	0.0431	2.7
0724-01_32.1	0.23	166	65	117 ±2	54.6	1.7	0.0487	2.6
0724-01_33.1	--	214	116	117 ±1	54.9	1.1	0.0463	2.5
0724-01_34.1	0.55	161	68	113 ±2	56.4	1.5	0.0491	2.6
0724-01_35.1	0.44	160	63	114 ±1	56.1	1.1	0.0491	2.5
0724-01_36.1	--	169	79	115 ±1	55.6	1.1	0.0479	2.6
Zr02								
SNG03_1.1	2.29	156	87	111 ±3	56.9	2.8	0.0560	10.5
SNG03_2.1	1.30	322	210	112 ±2	57.2	2.5	0.0468	5.1
SNG03_3.1	1.54	259	148	110 ±2	58.1	2.0	0.0477	4.8
SNG03_4.1	1.38	314	175	118 ±2	54.3	2.3	0.0471	5.1
SNG03_5.1	1.32	276	141	118 ±2	54.2	1.5	0.0483	4.0
SNG03_6.1	1.75	240	126	112 ±3	56.9	3.0	0.0502	4.8
SNG03_7.1	1.39	282	154	115 ±2	55.4	2.2	0.0527	4.6
SNG03_8.1	1.31	248	167	114 ±2	57.0	2.5	0.0379	9.7
SNG03_9.1	1.35	171	89	115 ±3	55.6	2.6	0.0471	12.0
SNG03_10.1	1.38	197	96	120 ±2	52.9	1.6	0.0538	8.2
SNG03_11.1	2.08	261	132	114 ±3	55.5	2.7	0.0538	4.5
SNG03_12.1	1.42	210	110	117 ±3	54.3	3.0	0.0509	4.9
SNG03_13.1	1.05	278	156	118 ±2	54.1	1.9	0.0501	4.2
SNG03_14.1	2.54	149	69	116 ±2	54.8	1.8	0.0503	14.0
SNG03_15.1	1.56	165	86	121 ±2	52.8	1.7	0.0490	12.9
SNG03_16.1	1.58	188	91	110 ±2	58.0	1.7	0.0458	5.7
SNG03_17.1	2.65	164	98	117 ±3	54.3	2.7	0.0543	9.7

SNG03_18.1	2.31	177	87	118 ±3	53.8	2.8	0.0527	5.4
SNG03_19.1	0.87	235	154	112 ±2	57.0	1.6	0.0456	5.2
SNG03_20.1	1.12	221	136	118 ±2	54.0	2.3	0.0483	5.7
SNG03_21.1	2.08	223	107	116 ±3	55.3	2.9	0.0484	5.6
SNG03_22.1	2.23	214	110	113 ±2	56.8	1.8	0.0448	11.0
SNG03_23.1	1.50	231	125	114 ±5	55.8	4.7	0.0490	6.1
SNG03_24.1	1.97	192	99	113 ±3	56.5	2.6	0.0500	10.2
SNG03_25.1	2.53	144	67	115 ±2	55.0	1.7	0.0602	4.9
SNG03_26.1	0.39	403	270	111 ±3	57.4	2.6	0.0495	5.2
SNG03_27.1	1.21	213	136	113 ±2	56.5	2.5	0.0470	5.6
SNG03_28.1	0.36	638	376	114 ±2	56.2	1.8	0.0489	2.7
SNG03_29.1	0.42	300	186	121 ±2	52.9	1.8	0.0435	6.4
SNG03_30.1	1.65	172	108	113 ±2	56.4	2.1	0.0500	6.6
SNG03_31.1	1.32	174	100	113 ±3	55.9	2.6	0.0572	4.7
SNG03_32.1	0.47	318	194	117 ±2	54.9	2.3	0.0428	4.9
SNG03_33.1	0.64	278	168	118 ±2	54.0	2.3	0.0479	4.2
SNG03_34.1	1.58	182	92	112 ±4	57.0	3.5	0.0514	5.6
SNG03_35.1	0.42	399	290	113 ±4	56.7	4.1	0.0459	5.4
SNG03_36.1	1.42	218	116	105 ±3	60.1	3.1	0.0565	4.4
SNG03_37.1	2.46	211	150	114 ±2	54.6	1.9	0.0682	6.4
SNG03_38.1	21.52	151	82	120 ±2	54.0	2.5	0.0357	18.1
SNG03_39.2	1.30	194	121	121 ±2	52.8	1.7	0.0501	5.9
SNG03_40.2	0.08	973	941	115 ±2	55.5	2.5	0.0520	4.8
SNG03_41.1	0.94	215	103	114 ±2	56.5	2.0	0.0450	5.3
SNG03_42.1	1.31	188	98	120 ±2	53.1	1.6	0.0512	4.3
SNG03_43.1	0.84	325	197	115 ±3	55.5	2.9	0.0506	4.1
SNG03_44.1	0.47	362	241	105 ±2	60.4	2.7	0.0532	5.7
SNG03_45.1	1.43	162	85	113 ±2	56.8	2.3	0.0447	6.1
SNG03_46.1	0.81	402	270	116 ±2	55.5	1.6	0.0424	4.8
SNG03_47.1	1.32	248	117	134 ±4	47.1	3.2	0.0578	3.7
SNG03_48.1	1.27	233	135	116 ±3	54.8	3.1	0.0500	4.9
SNG03_49.1	0.90	297	148	117 ±3	54.8	2.5	0.0440	4.8
SNG03_50.1	--	584	445	113 ±2	56.5	2.2	0.0500	4.1
SNG03_51.1	1.37	232	130	102 ±1	62.7	1.6	0.0473	5.2
SNG03_52.1	1.66	257	130	118 ±3	54.6	2.9	0.0437	5.3
SNG03_53.1	0.70	227	125	107 ±2	59.3	2.2	0.0522	4.3
SNG03_54.1	1.18	269	146	111 ±3	57.8	2.8	0.0434	5.5
SNG03_55.1	1.33	233	126	113 ±2	56.7	1.6	0.0476	7.6
SNG03_56.1	1.77	146	77	98.8 ±5	64.4	6.1	0.0519	7.6
SNG03_57.1	0.98	187	88	118 ±2	54.2	1.7	0.0455	8.2
SNG03_58.1	0.58	167	75	105 ±2	61.1	1.8	0.0447	5.3
SNG03_59.1	1.99	139	75	106 ±4	60.4	4.5	0.0486	7.8
SNG03_60.1	1.02	241	125	104 ±4	61.5	3.9	0.0483	5.9
SNG03_61.1	0.53	267	148	110 ±3	58.3	2.8	0.0462	4.5
SNG03_62.1	2.01	167	82	115 ±3	55.1	2.5	0.0547	5.1
SNG03_63.1	1.01	335	207	113 ±1	55.9	1.5	0.0556	3.5
SNG03_64.1	0.60	557	394	112 ±1	57.1	1.5	0.0483	3.8
SNG03_65.1	0.68	152	75	109 ±4	58.8	4.0	0.0460	6.2
SNG03_66.1	1.04	362	283	116 ±2	54.7	2.0	0.0526	4.6
SNG03_67.1	1.19	173	79	116 ±2	55.4	1.6	0.0466	5.0
SNG03-68.1	5.02	163	89	106 ±4	60.7	4.1	0.0407	22.0
SNG03-69.1	1.66	139	88	104 ±2	61.0	2.6	0.0536	6.0
SNG03-70.1	0.82	378	178	109 ±3	57.9	3.1	0.0584	3.5
SNG03_71.1	2.76	160	70	107 ±2	59.2	2.5	0.0546	5.5
SNG03_72.1	0.87	252	197	106 ±2	60.5	2.2	0.0429	7.3

*Common Pb corrected by assuming 206Pb/238U-207Pb/235U age-concordance

†Common Pb corrected by assuming 206Pb/238U-208Pb/232Th age-concordance

‡All errors are percent, 1σ errors.

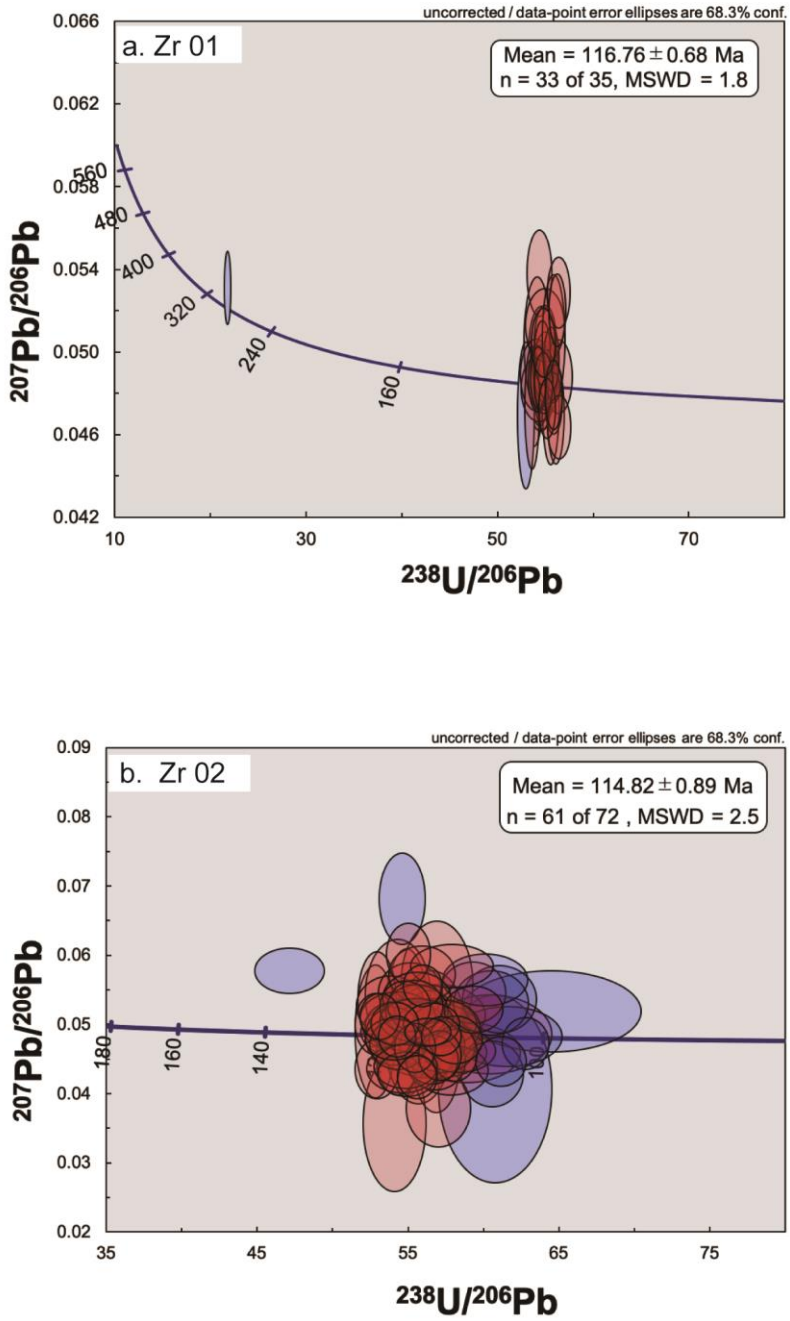

Fig. 6 Concordia diagrams showing SHRIMP zircon U-Pb data with weighted mean $^{206}Pb/^{238}U$ ages and uncertainties at the 95% confidence level. Error ellipses are at the 1-sigma level. MSWD–mean square of weighted deviates. a: Zr 01. b: Zr 02.

primary igneous zoning. Most U-Pb zircon ages (n = 33 of 35) are an approximately concordant population with a mean $^{207}Pb/^{206}Pb$ age of 116.76±0.68 Ma.

Sample Zr 02 (Figs. 5-b, 6-b and Table 2): Zircon grains typically occur as short stubby to short prismatic, almost completely unrounded to very poorly rounded and subhedral to euhedral. Their aspect ratio ranges from 1 to 4. Their length ranges from 60–200 μm. Many zircons show strong oscillatory zoning in CL images; some also sector zoning. Most U-Pb zircon ages (n = 61 of 72) are an approximately concordant population with a mean $^{207}Pb/^{206}Pb$ age of 114.82±0.89 Ma. These data indicate an latest Aptian age (Ogg et al., 2016), which is in accordance with the occurrence of the age-diagnostic ammonite, Parahoplitidae from Unit 3 (Fig. 1).

4. Soft- "resin" deformation structures in amber

The morphology of the amber pieces varies from spherical (less than 1 cm to 3 cm in diameter), to planar (Figs. 3 and 7–9). Angular to sub-angular fragments (less than 1mm to 5 mm in diameter), the typical shapes of amber (Seyfullah et al., 2018), are common (Figs. 8-a–b and 9-b). Horizontally continuous planer-shaped amber generally occur in the upper part of turbidite beds with a large amount of plant debris (Figs. 3-a, d–e and 4).

The amber shows distinctive internal sedimentary structures, suggesting soft-sediment deformation (Figs. 3-e and 7). At the interface of planar amber and the overlying turbidite in Am 01, upward projecting flame and ball-and-pillow structures

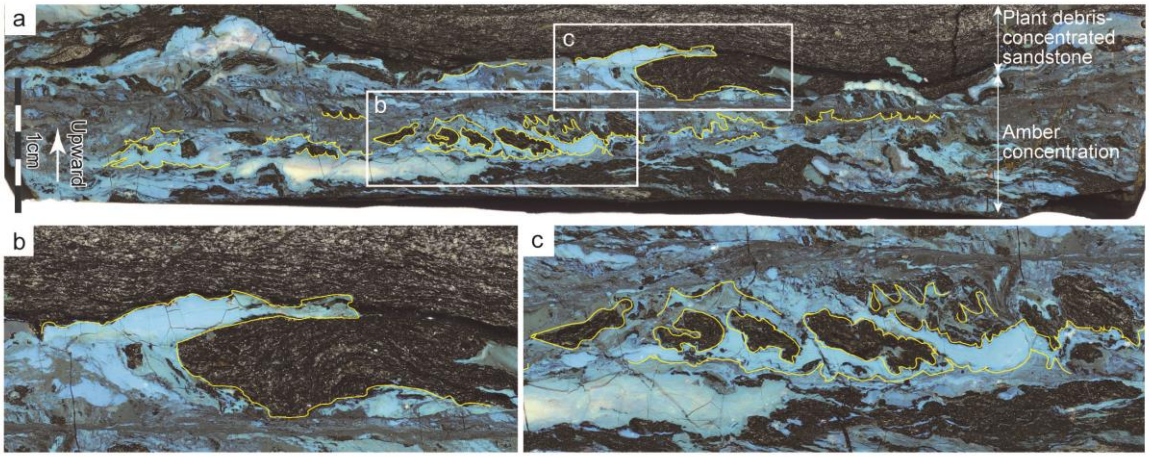

Fig. 7 Fluorescent tomograms showing soft-resin deformation structures of a planar-shaped amber of Am 01. a: Complex internal structures of a planar-shaped amber. b: Horizontally-oriented flame structures on the interface between sandstones and amber. c: Flame structures and ball-and-pillow structures of amber.

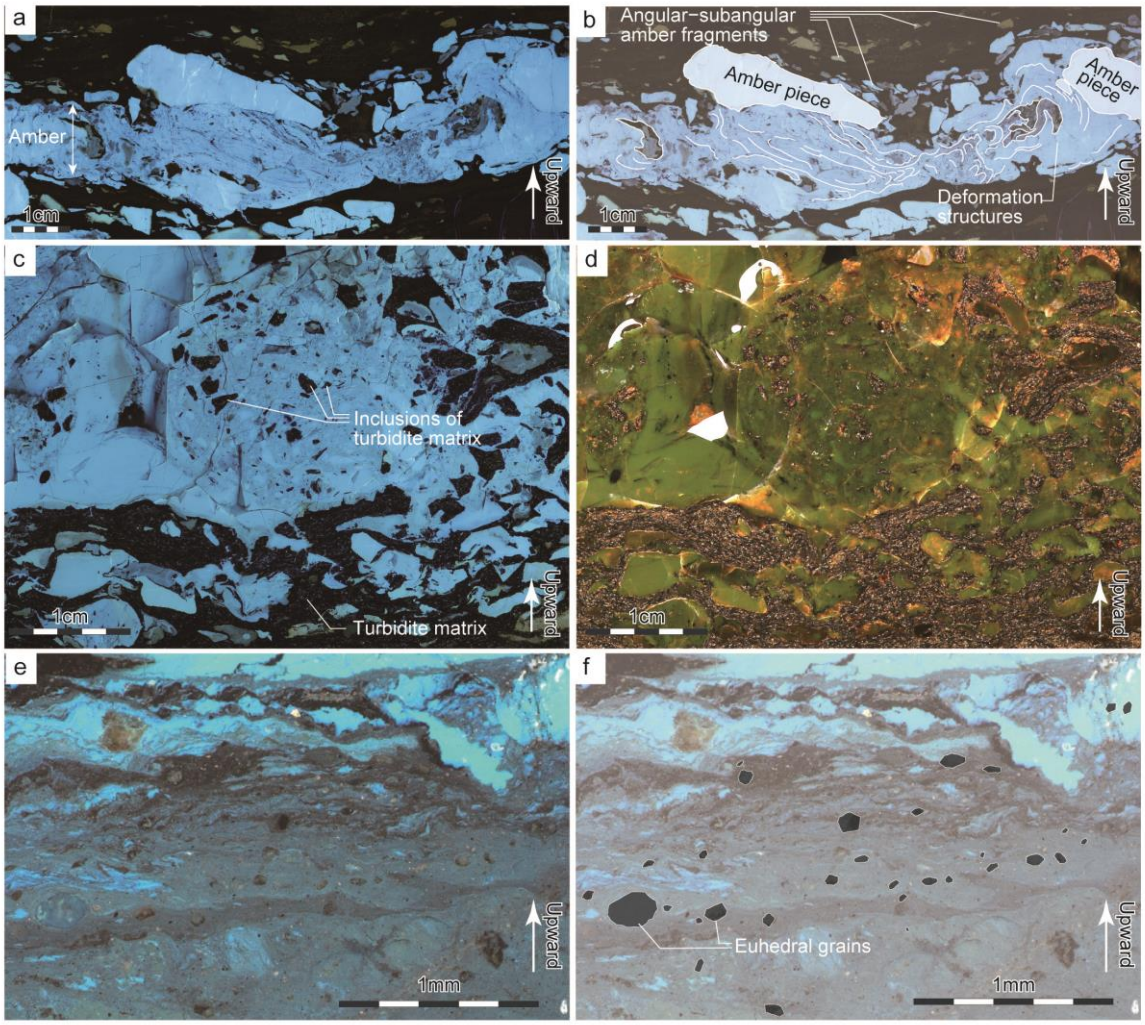

Fig. 8 Tomograms of soft-resin deformation structures. All structures support the soft condition of resin when they were deposited on the hemi-pelagic sea floor. a−b: Amber concentrations (Am 02 in Fig. 1-d) under the UV light (wavelength 365nm). Amber, which is laterally elongated, fills up the surrounding spaces of other amber fragments and pieces which had been solidified when deposited. This photo was not taken by grinding tomography, but from a single polished slab sample. c−d: Amber including clasts of turbidite (Am 02) under UV light (c) and white light (d). e−f: Muddy sediments containing euhedral opaque mineral grains larger than the grains of the turbidite matrix intercalated in planer-shaped amber (Am 01). Photo was taken under a digital zoom microscope (Zeiss Axio Zoom. V16; wavelength 365 nm).

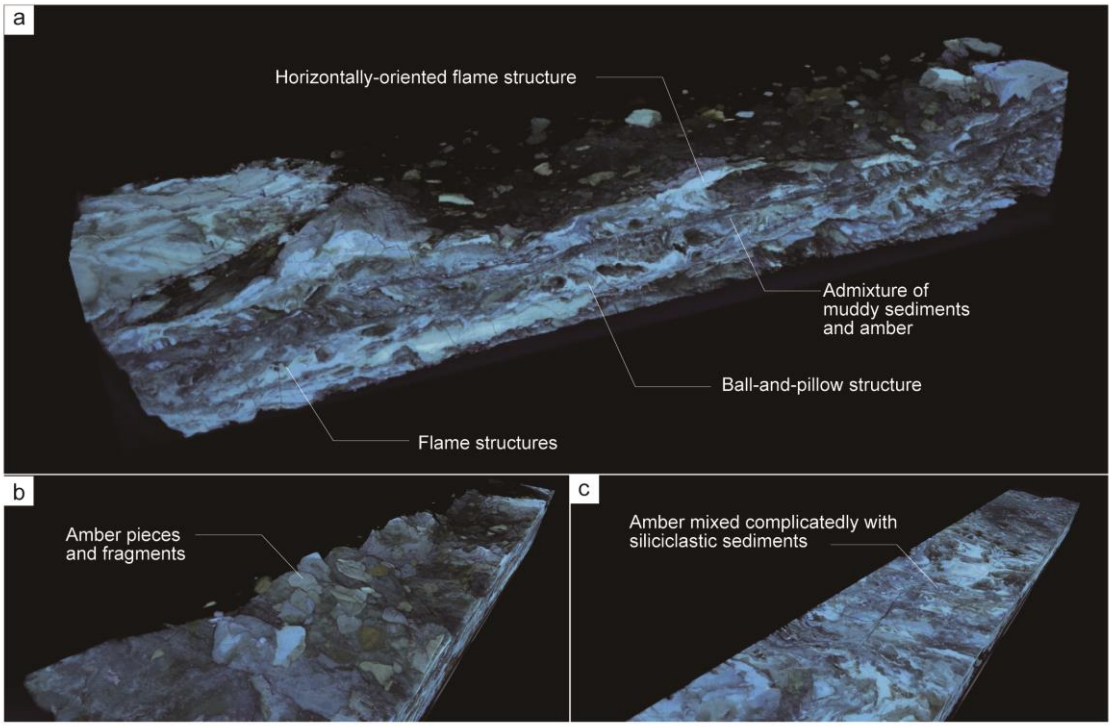

Fig. 9 Three dimensional mode of occurrence of ambers (Am01). a. The whole shape of Samples. b. Upper part of ambers. Amber pieces and fragments are dominant. c. Horizontal section of the amber.

are well-developed (Figs. 3-e, 7 and 9). Some projections extend horizontally (Fig. 7-b). The planar amber yields common siliciclastic clasts (Fig. 8).

5. Sedimentary structures associated with amber-concentrated beds

Various sedimentary structures related to a transport and deposition by a tsunami (e.g., Dawson and Stewart, 2007), have been observed in Units 2–4 (Figs. 10–13).

a. Large driftwood (Figs. 3-c and 10): The average size of highly-concentrated plant debris in turbidites is several hundred micrometers to 30 mm in length (Fig. 3-c). Robust fossil wood (over 30 cm and up to 1.3 m in length) without bio-erosion occurs both in sandstone beds and in claystones (W in Fig. 1-d, and 2-c).

b. Large rip-up mud clasts (Fig. 11): Large rip-up mud clasts (over 1 m in maximum diameter) frequently occur in the turbidites (Mu in Fig. 1-d) in Units 2 and 4. Mud clasts typically consist of dark gray-colored siltstone. Their shapes vary from very angular to well-rounded.

c. Soft-sediment deformation structures (Fig. 12): Soft-sediment deformation structures, such as millimeter to meter-scale sand injections, small-scale diapirs, flame structures, complex convolutions, slump structures, and tightly folding structures, are common in the turbidites of Units 2 and 4 (SSD in Fig. 1-d).

d. Three-dimensional wavy bedforms (Fig. 13): Arrays of three-dimensional wavy bedforms (1.5–2 m in length) occur in two turbiditic horizons in the lower part of Unit 4 in the Shimonakagawa Quarry (Fig. 13). They show radially symmetric mound-like structures, sloping at low angles, and are intervened by curvilinear hollows. Abundant

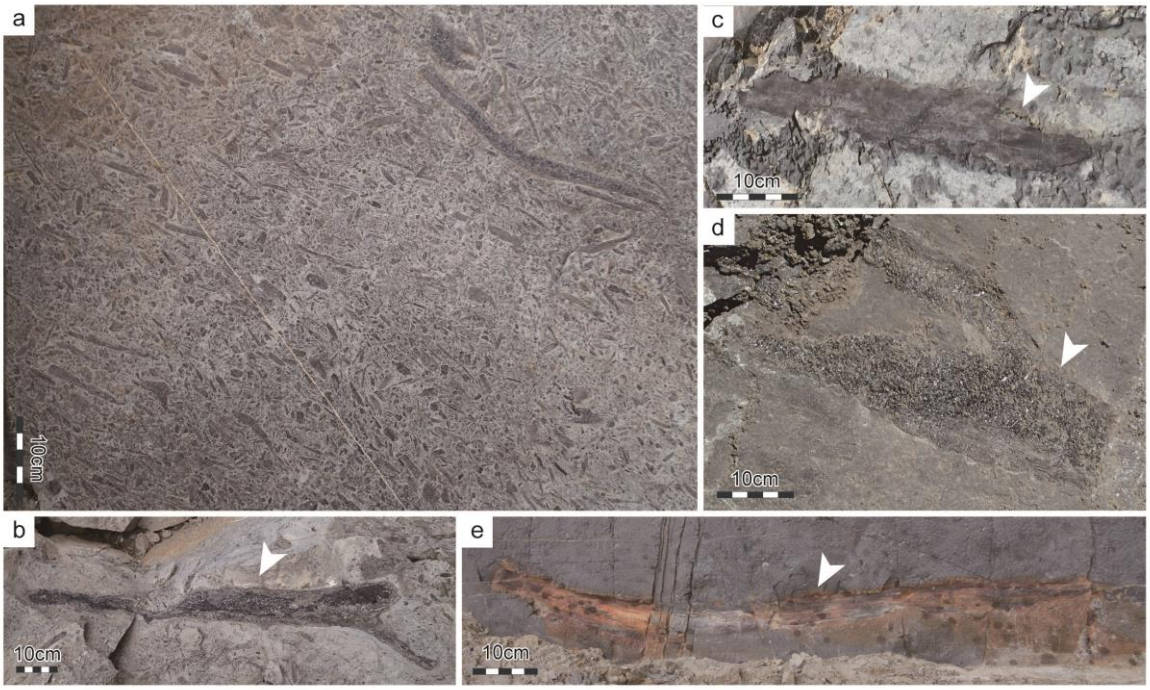

Fig. 10 Plant debris concentration and large driftwood in Units 2–4. Proximal side of the surfaces in photographs is upward. a: Concentration of plant debris on the bedding plane of turbidite bed W 04. b−e: Large driftwood. See W in Fig. 1-d for accurate horizons. The driftwood indicates that it has not been transported by turbidity currents, but by drift. b: Largest (about 1.3 m long) driftwood (W 04 in Fig. 1-d). c−e: Large driftwood in the mudstone (c: W 01, d: W 03 and e: W 02 in Fig. 1-d).

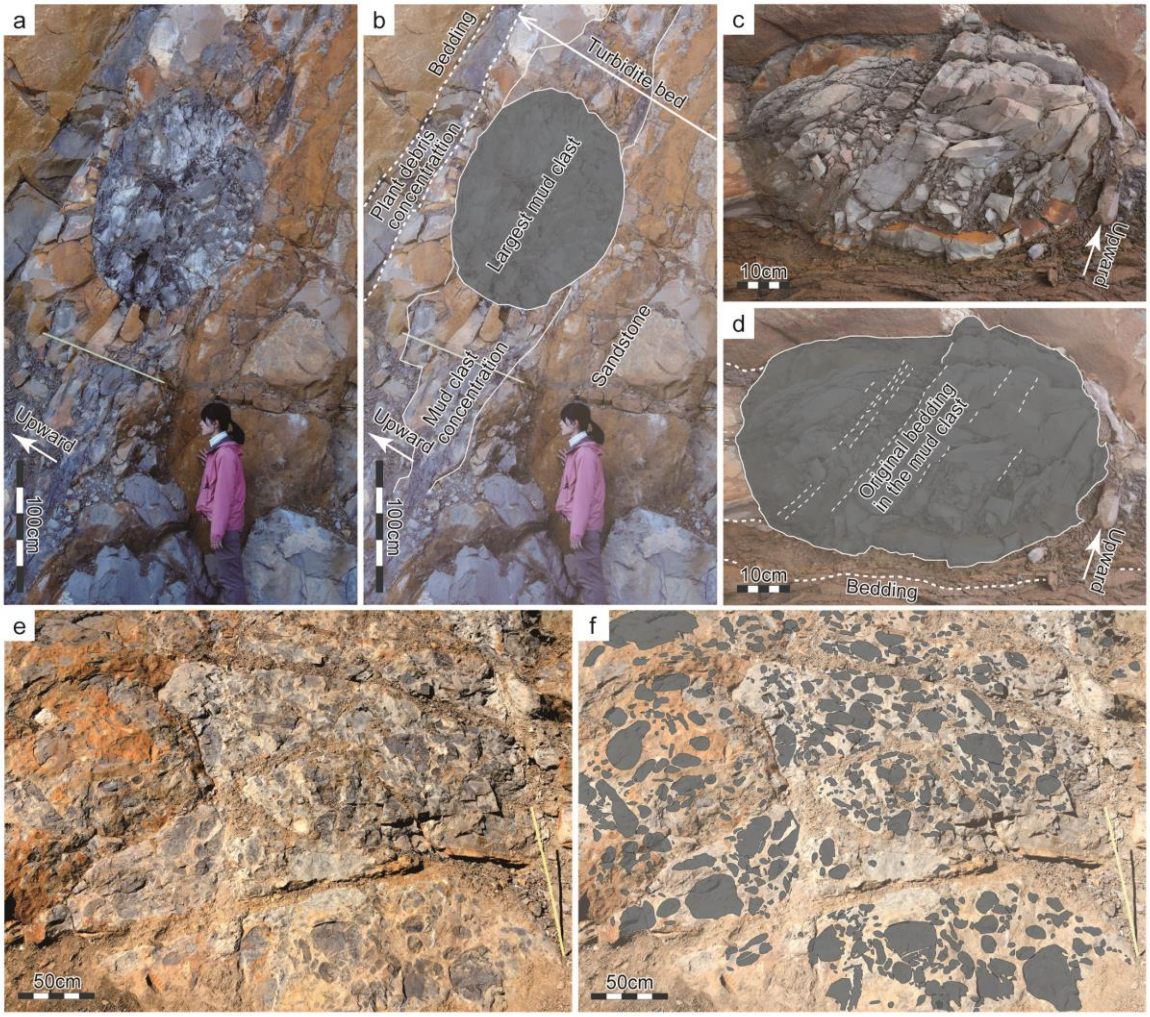

Fig. 11 Large rip-up mud clast concentrated in turbidites. See Mu in Figure 1-d for the accurate horizons. a−b: Largest mud clast. c−d: Large clasts of the dark gray-colored siltstone, preserving original bedding structures. e−f: Mud clast-concentrated bed. Proximal side of the surfaces in photographs is upward.

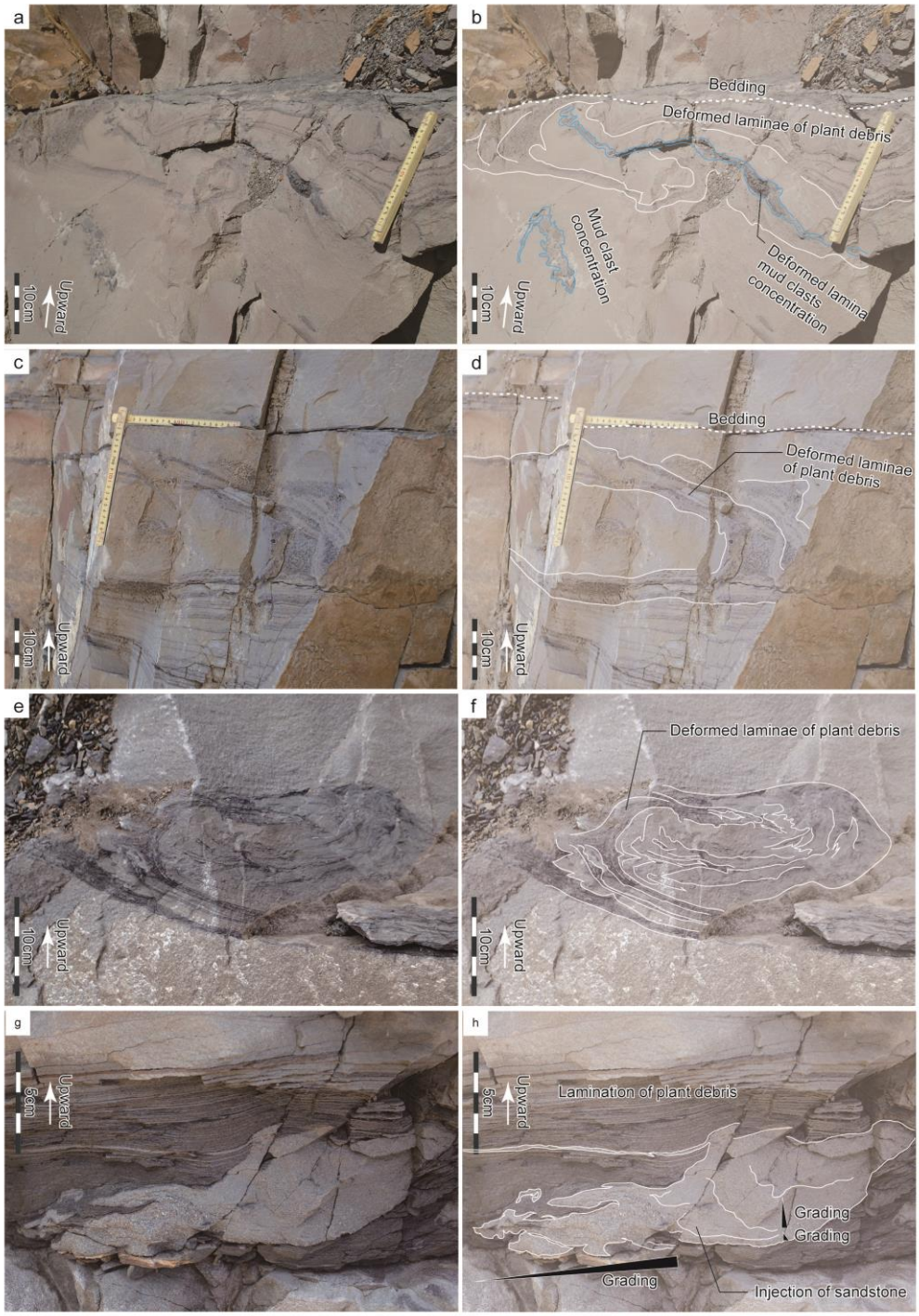

Fig. 12 Soft-sediment deformation structures. See SSDS in Fig. 1-d for their horizons. a−f: Deformed laminae of plant debris. a−b: Mud clasts are interbedded in SSDS as a layer and a patch. c−d: A roll structure of laminae of plant debris. e−f: Fold of laminae of plant debris. g−h: Injection of sandstone penetrating the plant debris in a condensed layer. i−j: Slumping beds. Injection of sandstone layer, the deformed laminae of plant debris and mudstone layers are recognized.

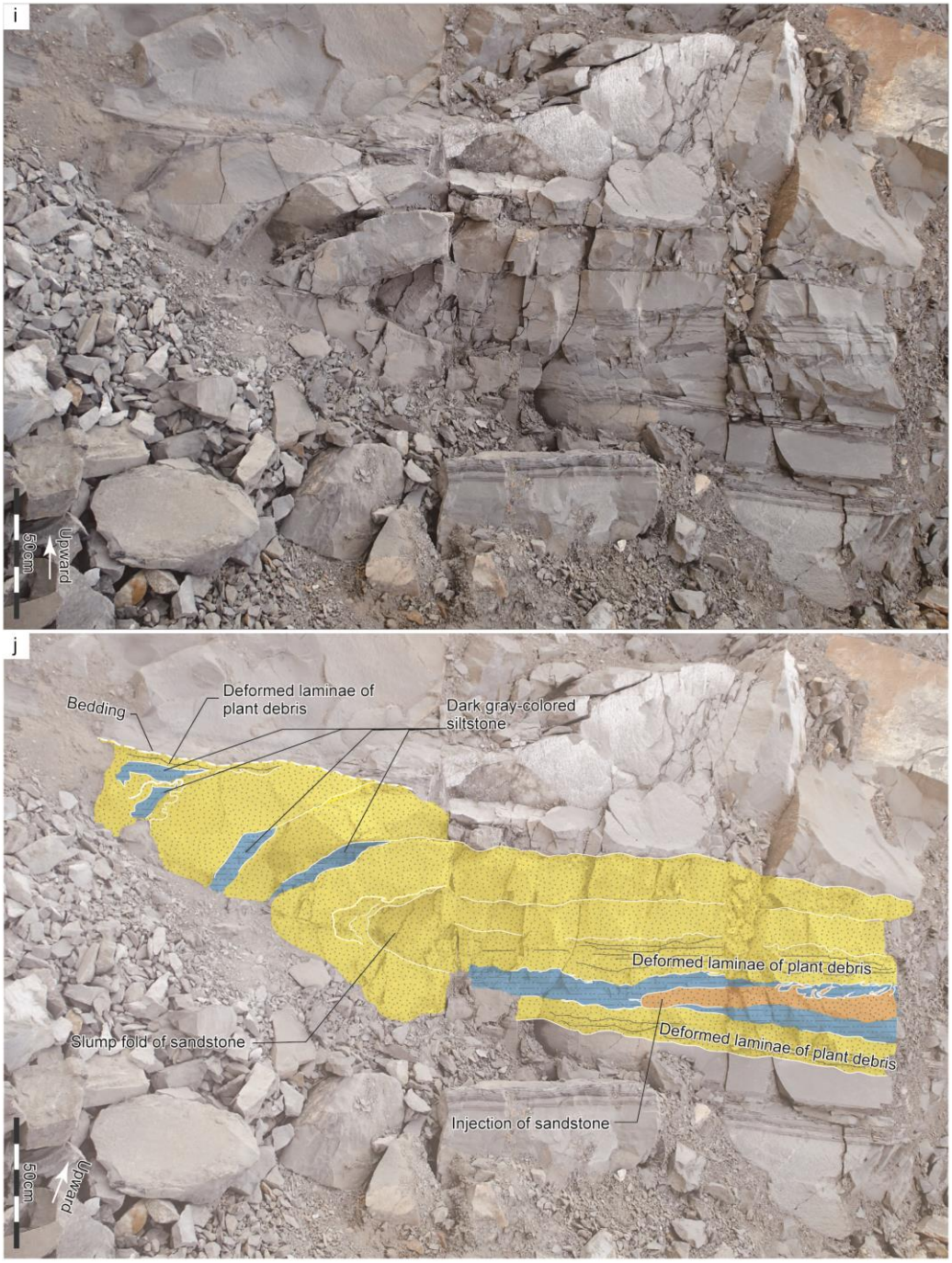

Fig. 12 (*continued*)

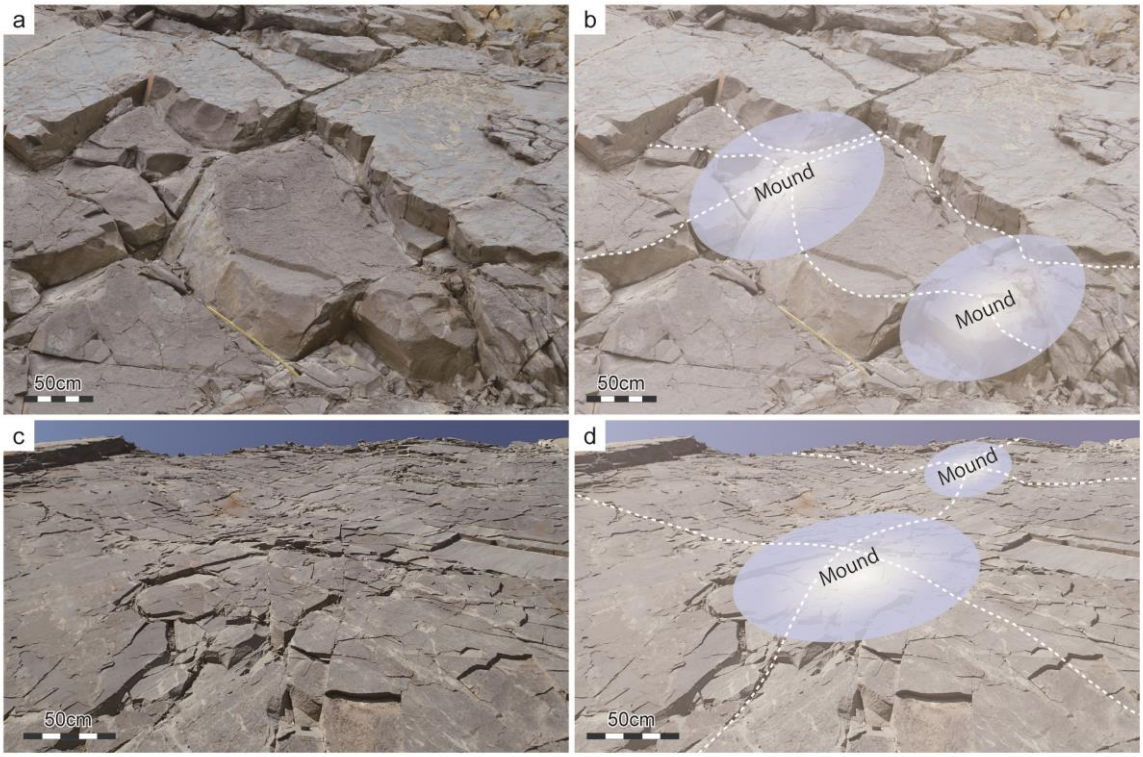

Fig. 13 Three-dimensional wavy bedforms. a–b: Be 01. c–d: Be 02. The wavelength of the bedforms is about 1.5 m and 2 m, respectively. Proximal side of the surfaces in photographs is upward. See Be in Figure 1-d for the accurate horizons.

plant debris forms stratifications, which are concordant with the surface of the bedforms, though truncation and cross-stratification are uncommon in their vertical sections. The long axis of the plant debris on the surfaces is aligned. This orientation is parallel to the trend of current lineation, which is developed on the surface of bedform Be 02 in Unit 4 (Be in Fig. 1-d).

DISCUSSION

1. Amber deposited in hemi-pelagic environments

No reliable sedimentary structure indicating water depth below the storm wave base. Benthic foraminifera assemblages are often used to discuss paleobathymetry in the Cenozoic (e.g., Hayward, 2004; Van Hinsbergen et al., 2005). It however, is the fact that benthic foraminifera are poor preserved by dissolution in the deep pelagic sea bottom, and actually missing in our sediments. The ichnofacies index, which had been widely used for bathymetric evaluations, could not be applied because distribution of benthic biota is not only affected by water depth but also other multiple factors such as substrate condition, dissolved oxygen level, food resources (e.g., Kotake, 2014).

Megafossils are very rare in the siliciclastic sequence of the studied quarry. Only a few shell-dissolved ammonoid fossils were recovered (Fig. 1). Most sandstone beds in Units 2 and 4 are interpreted as distal turbidites. A well-developed lamination caused by radiolarian skeletons and thin ash-fall tuff layers in the claystones of Units 1 and 3 indicate a calm depositional environment and very slow sedimentation rates. The thickness of the mudstones, excluding the amber-concentrated sandstones, is estimated

to represent the background sedimentation rate of the sequence. Zircon U-Pb ages of two ash tuff layers (Zr 01 in Unit 3 and Zr 02 in Unit 4, Fig. 1), which vary by 1.3 m in thickness, are here used for calculating a sedimentation rate of 0.38−3.66 mm/kyr. This rate is on the same magnitude as that of the pelagic bedded cherts (ca. 0.4−5.3 mm/kyr; Table 3). Both, paleontological and sedimentological data indicate that the amber was probably deposited in a hemi-pelagic environment.

2. Amber was transported in a soft condition

Over 100 amber (fossilized resin) localities have been reported for the last 320 Ma (Late Carboniferous–late Pleistocene) of the geological past (Langenheim, 2003). These occurrences are restricted to terrestrial (e.g., marsh and fluvial settings) and shallow marine environments (Martínez-Delclòs et al., 2004). In this study we report on amber and plant debris, which comonly occurs in hemi-pelagic deep-sea deposits. The amber-rich bed Am 01, which occurs in the lowermost turbidite of Unit 2 (Figs. 1 and 3), documents that amber had been transported into the hemi-pelagic setting from an early phase onwards.

Resins have a unique nature, they rapidly harden with losing volatile materials shortly after their secretion to the air in a soft condition (Langenheim, 2003). Due to its rapid solidification directly after exudation from trees, amber typically forms drops, tubes or spherical shapes (Seyfullah et al., 2018). When modern resins are exposed to air they solidify in about one week (Schmidt and Dilcher, 2007). Field experiments show, that resins which are covered by water obtain their soft condition unless they are

Table 3 Summary of sedimentation rates in the geologic record.

Reference	Locality	Geological age	Lithology	Average sedimentation rate (mm/kyr)	Min – Max sedimentation rate (mm/kyr)
Kumon et al., 1997	Miyama Fm, Shimanto Belt, Kii Peninsula, Japan	Hauterivian-Barremian to Turonian-early Coniacian, Upper Cretaceous	chert	0.4	
Murray et al., 1991	F-RLP section, Fransiscan Complex, northern California	Kimmeridgean, Upper Jurassic	bedded chert	~1(minninum)	
Murray et al., 1991	F-MH section, Fransiscan Complex, Martin Headlands, California	Lower Jurassic to middle Cretaceous	radiolarian ribbon chert	0.82	
Murray et al., 1991	F-MH section, Fransiscan Complex, Martin Headlands, California	Lower Jurassic to middle Cretaceous	radiolarian ribbon chert	~2	
Iijima et al., 1989	Adoyama chert, Kuzuh area in the southeast of the Ashio Mountains, northern Kanto, central Japan	Triassic to Lower Jurassic	radiolarian bedded chert	2.1	
Ikeda et al., 2010	Tamba Belt, Inuyama, Japan	middle Triassic	chert-shale couplet	1.8	1.6–2.1
Ikeda et al., 2010	Tamba Belt, Inuyama, Japan	Ladinian	chert-shale couplet	1.1	0.6–2.4
Ikeda et al., 2010	Tamba Belt, Inuyama, Japan	Anisian	chert-shale couplet	2.8	1.7–5.3
Matsuda et al., 1980	Tamba Belt, Inuyama, Japan	Upper Triassic	chert-shale couplet	2.8	
Hori et al., 1993	Tamba Belt, Inuyama, Japan	Lower Jurassic	chert-shale couplet	1	

exposed to air (Schmidt and Dilcher, 2007). The observation of common planar shaped amber in our material (Figs. 3-d–e and 7–9) strongly indicates that the resin (=amber) was still soft, when deposited. The deformation to plane pieces occurred after deposition on the seafloor due to sedimentary overburden. Upward projecting flame and ball-and-pillow structures of the amber were probably formed by the density-inversion at the interface of resin and clastic sediments (Figs. 7 and 9). Horizontally-oriented projections of amber indicate that the amber could still change its shape caused by water flow on the surface of the sediment. The observation that deformed planar amber is directly in contact with angular amber fragments (Fig. 8-a–b) excludes that the deformation of the planar amber occurred by high temperature and pressure during the late diagenesis process. The flame structures can be interpreted as syn-sedimentary deformations (e.g., Matsumoto et al., 2008), they strongly indicate that the resin (=amber) was still soft after its burial for quite some time.

The soft condition of the amber suggests that all sedimentary processes recorded here took place underwater. “Soft-resin sedimentology” therefore provides the clue to understand the pre- and syn-transport and syn-sedimentary processes of amber. Numerous fresh soft resin, which were secreted from host woods, were rapidly covered by water, and immediately transported into the hemi-pelagic seafloor without air-exposed process.

3. Amber-concentrated deposits driven by tsunamis?

This study documents the repeated tranpsort of soft resin into hemi-pelagic settings. Our findings indicate that a wide range of land forests close to the coast was destroyed. Large quantities of terrigenous material, documented by plant material and resin, was transported directly and repeatedly into hemi-pelagic seafloors. Large-scale tsunami seem to be a more plausible cause.

Certain sedimentary features, which have been recognized in the amber-concentrated sandstone beds of this study, have already been proposed as tsunami related (e.g., Dawson and Stewart, 2007). These features include mega rip-up mud clasts, abundant plant debris and soft-sediment deformation structures (Figs. 10–12). Large trunks of driftwood without any bio-erosion features indicates a rapid deposition (Fig. 10). Their occurence in the claystone shows that they were not transported by turbidity currents, but rather by tsunami events. Other events, which possibly supply terrigenous materials directly into ocean, are floods. Although the flood-induced hyperpycnal flows can transport land plants into the ocean, the typical sedimentary structures of their deposits, such as climbing ripples and reverse grading, have not been observed in the studied sequence.

The three-dimensional wavy bedform, called HCS-mimics (Rust and Gibling, 1990), has been reported from various deposits, such as fluvial sandstones, tidal deposits, flood deposits, and channel-fill turbidites. The unidirectional, upper regime flow (Froude number exceed 1.3) with highly abundant suspension is usually considered as the

environment where this bedform is deposited (e.g., Rust and Gibling, 1990; Yagishita, 1995; Yokokawa et al., 1999).

The bedforms observed in this locality show typical sedimentary features of the HCS-mimics (Fig. 13). The current lineation on the bedform of Be 02 in Unit 4 indicates the presence of an upper regime flow (Froude number exceed about 0.75; Allen, 1964). They are parallel to the estimated paleocurrent, based on the orientation of plant debris on the bedform surface, and the dominant paleocurrents (south to north) throughout the sequence. This evidence implies that the bedforms were formed by a unidirectional flow (Rust and Gibling, 1990). The stratification of abundant plant debris, concordant with bedform surface, and the lack of truncation and cross-stratification can be caused by a highly abundant suspension setting (Rust and Gibling, 1990).

The formation conditions are concordant to the nature of tsunamis. Tsunami waves are characterized by an extraordinary long wave period and an enormous wavelength of 15−100 minutes and hundreds of kilometers in the typical case of the Pacific (Apel, 1987). It is supposed that the orbital motion of tsunami waves reaches hemi-pelagic seafloors directly (Dawson and Stewart, 2007) and that the highly abundant suspension is typically stirred up by tsunami passing (Dawson and Stewart, 2007). It is unclear whether large-scale tsunamis can form the bedforms of hemi-pelagic seafloors. Further studies about the property of near bottom currents of large-scale tsunamis in hemi-pelagic settings are needed (e.g., Kastens and Cita, 1981).

In summary, we reconstruct several phases of tsunami events, which are recorded in the amber-concentrated deposits in the studied quarry, as follows (Fig. 14): (1)

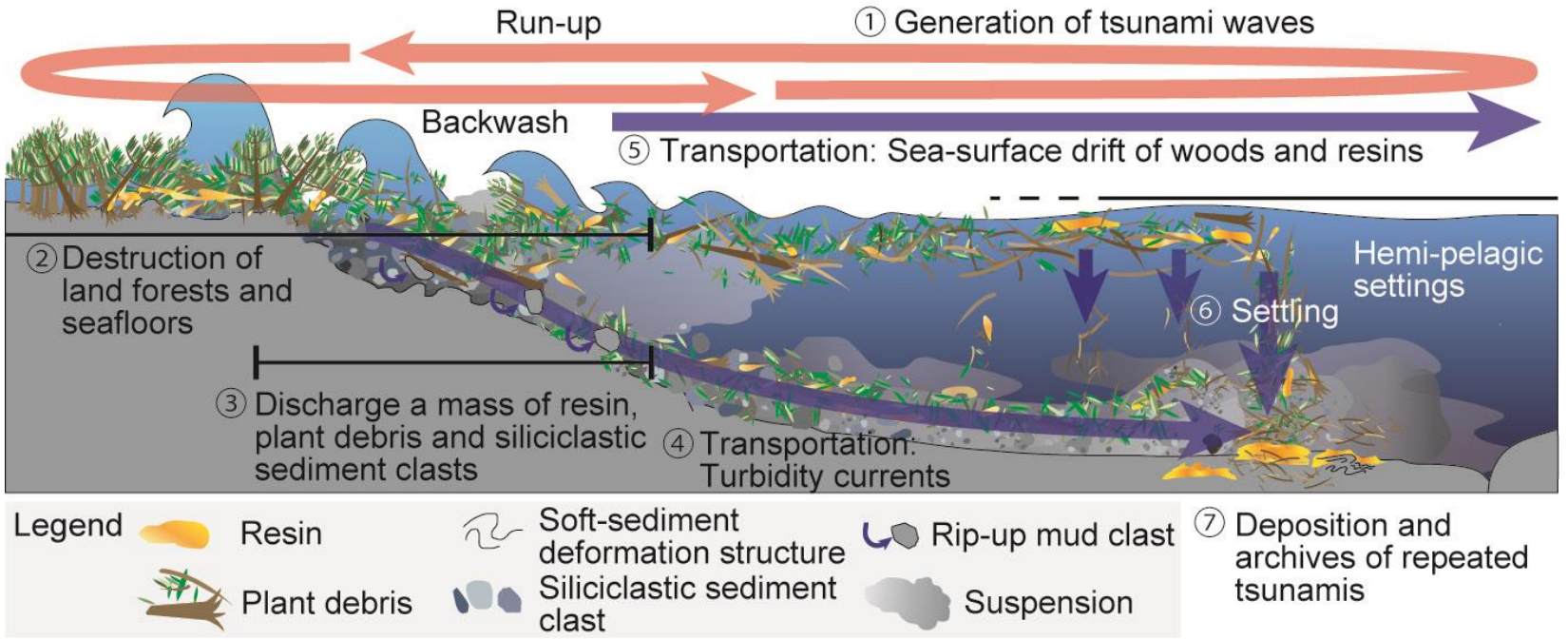

Fig. 14 Mass-transportation process of Early Cretaceous large-scale tsunamis reconstructed in this study. (1) Earthquakes probably generate the tsunamis. (2) Tsunamis largely destroy land forests and seafloors, and (3) discharge a mass of resin, plant debris and rip-up mud clasts into the ocean. (4) Tsunami-induced turbidity currents transport them directly into the hemi-pelagic seafloors. (5) Woods and resins drift and (6) sink into the seafloors. (7) The resins and other materials from lands and shallow sea, and soft-sediment deformation structures derived from repeated tsunamis are archived in hemi-pelagic deposits over 100 million of years.

Earthquakes probably generated repeatedly tsunamis, (2) tsunamis destroyed a wide range of coastal forests and seafloors, (3) they discharged a mass of resins, plant debris and unconsolidated to semi-lithified siliciclastic sediments into the ocean, (4) Tsunami-induced turbidity currents transported the resin, plant debris and siliciclastic sediments directly to the seafloor, and simultaneously, (5) wood and resin drifted on the sea surface, and (6) later sank to the hemi-pelagic seafloor, (7) the resin and other material from land and the shallow sea, and soft-sediment deformation structures derived from repeated tsunamis are archived in hemi-pelagic deposits over 100 million of years.

CONCLUDING REMARKS

This study reveals that large-scale tsunami events can be clearly recorded and recognized in hemi-pelagic sediments. The hemi-pelagic setting is the environment where depositional processes are dominant, contrary to the land and shallow marine areas, which are exposed to the strong erosion process. Hemi-pelagic sequences have therefore a large potential for archiving large-scaled tsunami events of the geological past. This study also implies that large-scale tsunamis probably transported large amount of materials from coastal and shallow marine environments to relative deep oceanic settings in a short time. This process can be considered as an important and so far underrated mass transportation system linking land and ocean. The role of large-scale tsunami events in the Earth's surface system should be validated in future works.

REFERENCES CITED

Allen, J.R.L., 1964, Primary current lineation in the Lower Old Red Sandstone (Devonian), Anglo-Welsh Basin: Sedimentology, v. 3, p. 89–108, doi: 10.1111/j.1365-3091.1964.tb00635.x.

Apel, J.R., 1987, Principles of ocean physics, Volume 38: Academic Press, 634p.

Dawson, A.G., and Stewart, I., 2007, Tsunami deposits in the geological record: Sedimentary Geology, v. 200, p. 166–183, doi: 10.1016/j.sedgeo.2007.01.002.

Götz, S., 2007, Inside rudist ecosystems: growth, reproduction and population dynamics, *in* Scott, R.W., ed., Cretaceous Rudists and Carbonate Platforms: Environmental Feedback, SEPM Special Publication, Society for Sedimentary Geology, v. 87, p. 97–113.

Hayward, W.B., 2004, Foraminifera-based estimates of paleobathymetry using Modern Analogue Technique, and the subsidence history of the early Miocene Waitemata Basin: New Zealand Journal of Geology and Geophysics, v. 47, p. 749–767, doi: 10.1080/00288306.2004.9515087.

Hori, S.R., Cho, C.F., and Umeda, H., 1993, Origin of cyclicity in Triassic-Jurassic radiolarian bedded cherts of the Mino accretionary complex from Japan: Island Arc, v. 2, p. 170–180, doi: 10.1111/j.1440-1738.1993.tb00084.x.

Iba, Y., Mutterlose, J., Tanabe, K., Sano, S., Misaki, A., and Terabe, K., 2011, Belemnite extinction and the origin of modern cephalopods 35 m.y. prior to the

Cretaceous–Paleogene event: Geology, v. 39, p. 483–486, doi: 10.1130/G3 1724.1.

Iijima, A., Kakuwa, Y., and Matsuda, H., 1989, Silicified wood from the Adoyama chert, Kuzuh, Central Honshu, and its bearing on compaction and depositional environment of radiolarian bedded chert: Siliceous deposits of the Tethys and Pacific Regions, New York, Springer, p. 151–168, doi: 10.1007/978-1-461 2-3494-4_11.

Ikeda, M., Tada, R., and Sakuma, H., 2010, Astronomical cycle origin of bedded chert: a middle Triassic bedded chert sequence, Inuyama, Japan: Earth and Planetary Science Letters, v. 297, p. 369–378, doi: 10.1016/j.epsl.2010.06.027.

Kastens, K.A., and Cita, M.B., 1981, Tsunami-induced sediment transport in the abyssal Mediterranean Sea: Geological Society of America Bulletin, v. 92, p. 845–857, doi: 10.1130/0016-7606(1981)92<845:TSTITA>2.0.CO;2.

Kotake, N., 2014, Changes in lifestyle and habitat of Zoophycos-producing animals related to evolution of phytoplankton during the Late Mesozoic: geological evidence for the ‘benthic-pelagic coupling model’: Lethaia, v. 47, p. 165–175, doi: 10.1111/let.12046.

Kumon, F., Matsuyama, H., and Musashino, M., 1997, An oceanic fragment in the Upper Cretaceous Miyama Formation of the Shimanto Belt, Kii Peninsula, Japan: The Memoir of the Geological Society of Japan, v. 48, p. 100–109.

Langenheim, J.H., 2003, Plant resins−Chemistry, evolution, ecology, and ethnobotany: Portland, Oregon, Timber Press, 586p.

Ludwig, K.R., 2008, User's manual for Isoplot 3.6: a geochronological toolkit for Microsoft Excel: Berkeley Geochronology Center Special, Publication, v. 4, p. 77.

Ludwig, K.R., 2009, User's manual for Squid 2.50: Berkeley Geochronology Center Special, Publication, v. 5, p. 110.

Martínez-Delclòs, X., Briggs, D.E.G., and Peñalver, E., 2004, Taphonomy of insects in carbonates and amber: Palaeogeography, Palaeoclimatology, Palaeoecology, v. 203, p. 19–64, doi: 10.1016/S0031-0182(03)00643-6.

Matsuda, T., Isozaki, Y., and Yao, A., 1980, Stratigraphic relation of the Triassic−Jurassic rocks in Inuyama area Mino belt: Geological Society of Japan Abstract with Program 107.

Matsumoto, D., Naruse, H., Fujino, S., Surphawajruksakul, A., Jarupongsakul, T., Sakakura, N., and Murayama, M., 2008, Truncated flame structures within a deposit of the Indian Ocean Tsunami: evidence of syn-sedimentary deformation: Sedimentology, v. 55, p. 1559–1570, doi; 10.1111/j.1365-3091.2008.00957.x.

Murray, W.R., Ten Brink, M.R.B., Gerlach D.C., Russ Ⅲ G.P., and Jones D.L., 1991, Rare earth, major, and trace elements in chert from the Franciscan Complex and Monterey Group, California: Assessing REE sources to fine-grained marine sediments: Geochemical et Cosmochimica Acta, v. 55, p. 1875–1895, doi: 10.1016/0016-7037(91)90030-9.

Niida, K., and Kito, N., 1986, Cretaceous arc-trench system in Hokkaido: Monograph of the Association of Geological Collaboration, Japan, v. 31, p. 379–402.

Ogg, J., Ogg, G., and Gradstein, F., 2016, A Concise Geologic Time Scale 2016: Amsterdam, Netherlands, Elsevier, 234 p., doi: 10.1016/B978-0-444-59467-9.00001-7.

Paces, J.B., and Miller Jr., J.D., 1993, Precise U-Pb ages of Duluth Complex and related mafic intrusions, northeastern Minnesota: Geochronological insights to physical, petrogenetic, paleomagnetic, and tectonomagmatic processes associated with the 1.1 Ga Midcontinent Rift System: Journal of Geophysical Research, Solid Earth, v. 98, p. 13997–14013, doi: 10.1029/93JB01159.

Pascual-Cebrian, E., Hennhöfer, D.K., and Götz, S., 2013, 3D morphometry of polyconitid rudist bivalves based on grinding tomography: Facies, v. 59, p. 347–358, doi:10.1007/s10347-012-0310-8.

Rust, B.R., and Gibling, M.R., 1990, Three-dimensional antidunes as HCS mimics in a fluvial sandstone; the Pennsylvanian South Bar Formation near Sydney, Nova Scotia: Journal of Sedimentary Research, v. 60, p. 540–548, doi: 10.2110/60.4.540.

Schmidt, A.R., and Dilcher, D.L., 2007, Aquatic organisms as amber inclusions and examples from a modern swamp forest: Proceedings of the National Academy of Sciences, v. 104, p. 16581–16585, doi: 10.1073/pnas.0707949104.

Seyfullah, L.J., Beimforde, C., Corso, J.D., Perrichot, V., Rikkinen, J., and Schmidt, A.R., 2018: Production and preservation of resins–past and present: Biological Reviews, v. 93, p. 1684–1714, doi: 10.1111/brv.12414.

Shanmugam, G., 2012, Process-sedimentological challenges in distinguishing paleo-tsunami deposits: Natural Hazards, v. 63, p. 5–30, doi: 10.1007/s11069-011-9766-z.

Stacey, J.S., and Kramers, J.D., 1975, Approximation of terrestrial lead isotope evolution by a two-stage model: Earth and Planetary Science Letters, v. 26, p. 207–221, doi: 10.1016/0012-821X(75)90088-6.

Takashima, R., Kawabe, F., Nishi, H., Moriya, K., Wani, R., and Ando, H., 2004, Geology and stratigraphy of fore-arc basin sediments in Hokkaido, Japan: Cretaceous environmental events on the north-west Pacific margin: Cretaceous Research, v. 25, p. 365–390, doi: 10.1016/j.cretres.2004.02.004.

Takashima, R., Nishi, H., and Yoshida, T., 2017, Stratigraphic and Petrological Insights into the Late Jurassic–Early Cretaceous Tectonic Framework of the Northwest Pacific Margin: Dynamics of Arc Migration and Amalgamation-Architectural Examples from the NW Pacific Margin, InTech., doi: 10.5772/intechopen.68289.

Ueda, H., 2016, Hokkaido, *in* Moreno, T., Wallis, S., Kojima, T., and Gibbons, W., eds., The Geology of Japan: Geological Society, London, p. 201–221.

Van Hinsbergen, D.J.J., Kouwenhoven, T. J., and Van der Zwaan, G.J., 2005, Paleobathymetry in the backstripping procedure: Correction for oxygenation effects on depth estimates: Palaeogeography, Palaeoclimatology, Palaeoecology, v. 221, p. 245–265, doi: 10.1016/j.palaeo.2005.02.013.

Williams, I.S., 1998 U-Th-Pb geochronology by ion micro probe, *in* McKibben, M.A., et al., eds., Applications of microanalytical techniques to understanding mineralizing processes: Reviews in Economic Geology, v. 7, p. 1–35.

Yagishita, K., 1995, Antidunes in a small gorge on the beach sand, the Sanriku Coast, northeast Japan: Journal of the Sedimentological Society of Japan, v. 42, p. 21–28, doi: 10.4096/jssj1995.42.21.

Yokokawa, M., Masuda, F., Sakai, F., Endo, T., and Kubo, Y., 1999, Sedimentary structures generated in upper-flow-regime with sediment supply: Antidune cross-stratification (HCS mimics) in a flume: Land-sea link in Asia, STA (JISTEC) and Geological Survey of Japan, v. 55, p. 49–57, doi: 10.4116/j aqua.55.49.

Chapter 2

The destruction events recorded in the lowest part of the Yezo Group in the Nakagawa area, northern Hokkaido

ABSTRACT

The Yezo Group is a thick terrestrial siliciclastic fore-arc basin deposit (Late Aptian to Paleocene), which is distributed from southern Hokkaido to Sakhalin, deposited along with the eastern margin of Eurasia. In the Nakagawa area, northern Hokkaido, lithofacies and biostratigraphy of the middle to the upper part of the Yezo Group have been established based on fossiliferous and continuous strata. Those of the lowest part of the Yezo Group are, however, still unclear because of lack of fossil occurrence and limitation of exposure of strata. In Chapter 1, amber- and plant debris-concentrated turbidites at the boundary between the Sorachi Group and the Yezo Group, and in the lowermost part of the Yezo Group were described in the Shimonakagawa Quarry. In some other localities in the Nakagawa area, chaotic deposits such as conglomerate beds and slumps inserted in siliceous mudstone have been sporadically recognized.

The purpose of this chapter is to integrate the lithostratigraphy of the uppermost part of the Sorachi Group and the lowermost part of the Yezo Group in the Nakagawa area, focusing on the chaotic deposits. Results show that the chaotic deposits such as slump deposits are concentrated in the lowermost part of the Yezo Group. They strongly indicate that the presence of instability relating the destruction of the hinterland in a 20 km scale in the Nakagawa area, latest Aptian.

Chapter 2

The destruction events recorded in the lowest part of the Yezo Group in the Nakagawa area, northern Hokkaido

ABSTRACT

The Yezo Group is a thick terrestrial siliciclastic fore-arc basin deposit (Late Aptian to Paleocene), which is distributed from southern Hokkaido to Sakhalin, deposited along with the eastern margin of Eurasia. In the Nakagawa area, northern Hokkaido, lithofacies and biostratigraphy of the middle to the upper part of the Yezo Group have been established based on fossiliferous and continuous strata. Those of the lowest part of the Yezo Group are, however, still unclear because of lack of fossil occurrence and limitation of exposure of strata. In Chapter 1, amber- and plant debris-concentrated turbidites at the boundary between the Sorachi Group and the Yezo Group, and in the lowermost part of the Yezo Group were described in the Shimonakagawa Quarry. In some other localities in the Nakagawa area, chaotic deposits such as conglomerate beds and slumps inserted in siliceous mudstone have been sporadically recognized.

The purpose of this chapter is to integrate the lithostratigraphy of the uppermost part of the Sorachi Group and the lowermost part of the Yezo Group in the Nakagawa area, focusing on the chaotic deposits. Results show that the chaotic deposits such as slump deposits are concentrated in the lowermost part of the Yezo Group. They strongly indicate that the presence of instability relating the destruction of the hinterland in a 20 km scale in the Nakagawa area, latest Aptian.

INTRODUCTION

A Jurasso–Paleogene ophiolite-based fore-arc basin sequence that deposited in the eastern margin of Eurasia is widely distributed in a north–south axis area of Hokkaido Island, northern Japan (Takashima et al., 2004) (Fig. 1). They are called the Sorachi Group and the Yezo Group. In Chapter 1, amber and plant debris-concentrated turbidites in the boundary between the Sorachi Group and the Yezo Group, and the lowermost part of the Yezo Group were reported from a new section; this section is exposed in a quarry in the Shimonakagawa area, northern Nakagawa. The chaotic deposits indicate the presence of large-scale tsunamis, which destroy the wide range of land forests and transport its remains into the hemi-pelagic settings.

The boundary between the Sorachi Group and the Yezo Group is defined as the transition from the green-colored mudstone to black-colored mudstone (Kawaguchi et al., 1997). This stratigraphic scheme is widely accepted entire Hokkaido (e.g., Kiminami et al., 1992, Takashima et al., 2004, Iba et al., 2005). The lowermost part of the Yezo Group is characterized by the terrigenous siliciclastic sediments (Ueda, 2016). The lowermost part of the Yezo Group in the Nakagawa area, chaotic siliciclastic deposits has been recognized such as a conglomerate bed and slump deposits intercalated in the terrigenous siliciclastic sediments. The conglomerate bed has been recognized sporadically in the Nakagawa area (e.g., Ijima and Shinada, 1952) and classified as the “Onodera conglomerate and sandstone Member” of the Kamiji Formation (e.g., Taki et al., 2011). In addition, muddy slump deposits in the Chirashinaigawa Creek has been recently reported (Taki et al., 2011). Although they have been reported in previous studies, the integrated interpretation of their causes has not been mentioned. The purpose of this chapter is to integrate the lithostratigraphy and

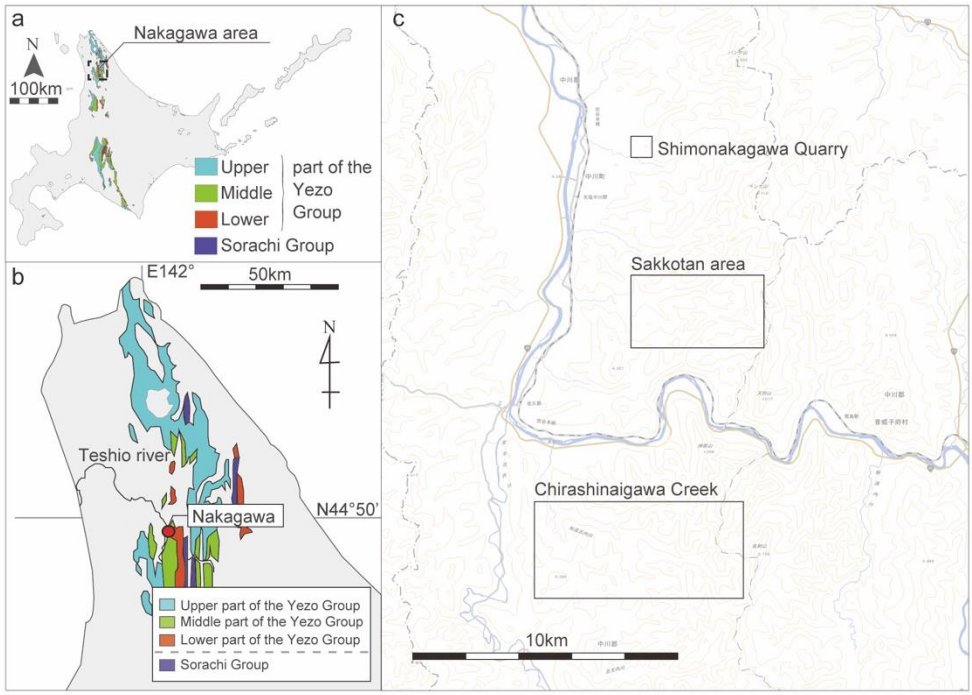

Fig. 1 The study localities. a–b: Nakagawa area in northern Hokkaido. c: The study localities in the Nakagawa area.

understand depositional process of the lowermost part of the Yezo Group in the Nakagawa area, toward for tracing tsunamites in Chapter 1 at regional 20 km scale.

GEOLOGICAL SETTINGS AND METHODS

The upper Cretaceous regional stratigraphy in the Nakagawa area has been established in previous studies (e.g., Matsumoto, 1942, 1943; Ijima and Shinada, 1952; Nagao, 1962; Hashimoto et al., 1967; Takahashi et al., 2003; Taki et al., 2011). The Sorachi Group in the Nakagawa area consists of the pillow lava, volcaniclastic sediments and siliceous sediments, in ascending order (e.g., Kawaguchi, 1997). The group is subdivided into four formations; The Onisashigawa, Osashima, Monomanaigawa, and Pechikunnai formations in ascending order (Kawaguchi, 1997). The Pechikunnai Formaiton is the uppermost part of the Sorachi Group and consist siliceous claystone and volcaniclastic sandstone. The Yezo Group is subdivided into nine formations and they are organized in three parts; the Kamiji Formation in the lower part, the Moihoro, Shirataki, Sakkotandake, Sakugawa, and Saku formations in the middle part, the Nishichirashinai, Omagari, and Osoushinai in the upper part (Kawaguchi, 1997; Takahashi, 2003). The Kamiji Formation conformably overly the Pechikunnai Formation (Sorachi Group) and stratigraphically represents the lower part of the Yezo Group (Iba et al., 2005). The formation consists mainly dark gray-colored mudstone and alternating beds of sandstone and mudstone, and subdivided into nine units (Kj1 to Kj8 in ascending order; Hashimoto et al., 1967).

The boundary between the Sorachi and Yezo groups (The Pechikunnai Formation and the Kamiji Formation, respectively) is defined as a gradual transition green- to black-colored mudstone (Kawaguchi, 1997). That can be traced over 300 km from the

Nakagawa area in northern Hokkaido to the Urakawa area in southern Hokkaido (Kanie et al., 1981). The group boundary is considered as a period of drastic tectonic changes, such as paleo-backland shifts by orogeny of hinterlands (e.g., Niida and Kito, 1986; Kiminami et al., 1992).

The age of the uppermost part of the Sorachi Group in the Nakagawa area has been estimated as the Barremian age by last occurrence of radiolarian species, "*Cecrops*" *sertemporatus* (Taketani and Kanie, 1992; Kawaguchi, 1997; Mitsugi and Hirano, 1998). The age of the lowermost part of the Yezo Group is estimated as the Late Aptian by larger benthic foraminifera *Mesorbitolina parva* from limestone pebbles in a conglomeratic gravity flow deposit (the lowest Kj1Member; 11 m above the group boundary) (Iba et al., 2005; Iba and Sano, 2006). It is concordant to the other occurrence from the lower part of the Yezo Group by rare occurrence of megafossils from the Kamiji Formation; Late Aptian ammonite *Parahoplites colossus* (Kj2 Member; Matsumoto, 1984), the late Early Albian ammonite *Douvilleiceras* sp. (Kj3 Member; Yoshida et al., 2010), calcareous red algae, and *Neithea syriaca amanoi* (a Tethyan non-rudist bivalve *sensu* Dhondt, 1992; Kj3 Member; Iba and Sano, 2007), Albian ammonite *Ammonoceratites* (Kj7 Member; Hayakawa, 1999). In addition, the ammonoid *Acanthohoplites* sp. and the SHRIMP U-Pb ages (114.82±0.89 Ma and 116.76±0.68 Ma; latest Aptian) from zircon in ash-fall tuff were newly reported from the boundary between the Sorahi and Yezo groups (Chapter 1).

In this chapter, lithostratigraphic and sedimentological research, which are especially focused on chaotic deposits was examined in the Nakagawa area. Three sections of the Shimonakagawa quarry, the Sakkotan area, and the Chirashinaigawa Creek, were selected (Fig. 1). In three sections, the boundary of the Sorachi and Yezo

groups, and the lower part of the Yezo Group are well cropped out.

The Shimonakagawa quarry is located in northern Nakagawa (Fig. 1). The uppermost part of the Sorachi Group and the lowermost part of the Yezo group is continuously cropped out without faults and lack of outcrops. The section is the best outcrops of the boundary between the Sorachi and Yezo groups throughout the Hokkaido area. Amber- and plant debris-concentrated turbidites which are intercalated the boundary sequence were also described in Chapter 1.

The Sakkotan area is 10 km to the south from the Shimonakagawa Quarry (Fig. 1). Litho-stratigraphy, radiolarian biostratigraphy, larger benthic foraminifera biostratigraphy has established in this area (e.g., Taketani and Kanie, 1992; Kawaguchi, 1997; Mitsugi and Hirano, 1998; Iba et al., 2005; Iba and Sano, 2007). A conglomerate bed has been reported in the lowermost part of the Yezo Group (e.g., Ijima and Shinada, 1952; Nagao, 1962; Kawaguchi, 1997; Mitsugi and Hirano, 1998; Iba et al., 2005). Based on its lithofacies, Iba et al. (2005) concluded that the conglomerate bed was deposited by high-concentrated gravity flow. There are three routes in Sakkotan area (Fig. 2-a); the north forest road, the Sakkotangawa Creek and the south forest road from north to south. These routes are parallel located within 500 m distance each (Fig. 2-a). The sequence from the uppermost part of the Sorachi Group and to the lowermost part of the Yezo Group is cropped out in all routes. The sequence in the north forest road is newly described in this study.

The Chirashinaigawa Creek is 20 km to the south from the quarry section (Figs. 1–2-b). The sequence from the Sorachi Group to the upper part of the Yezo Group is continuously exposed along the creek. Lithostratigraphy and chemostratigraphy are established (Ijima and Shinada, 1952; Nagao, 1962; Shimizu, et al., 2001; Taki et al.,

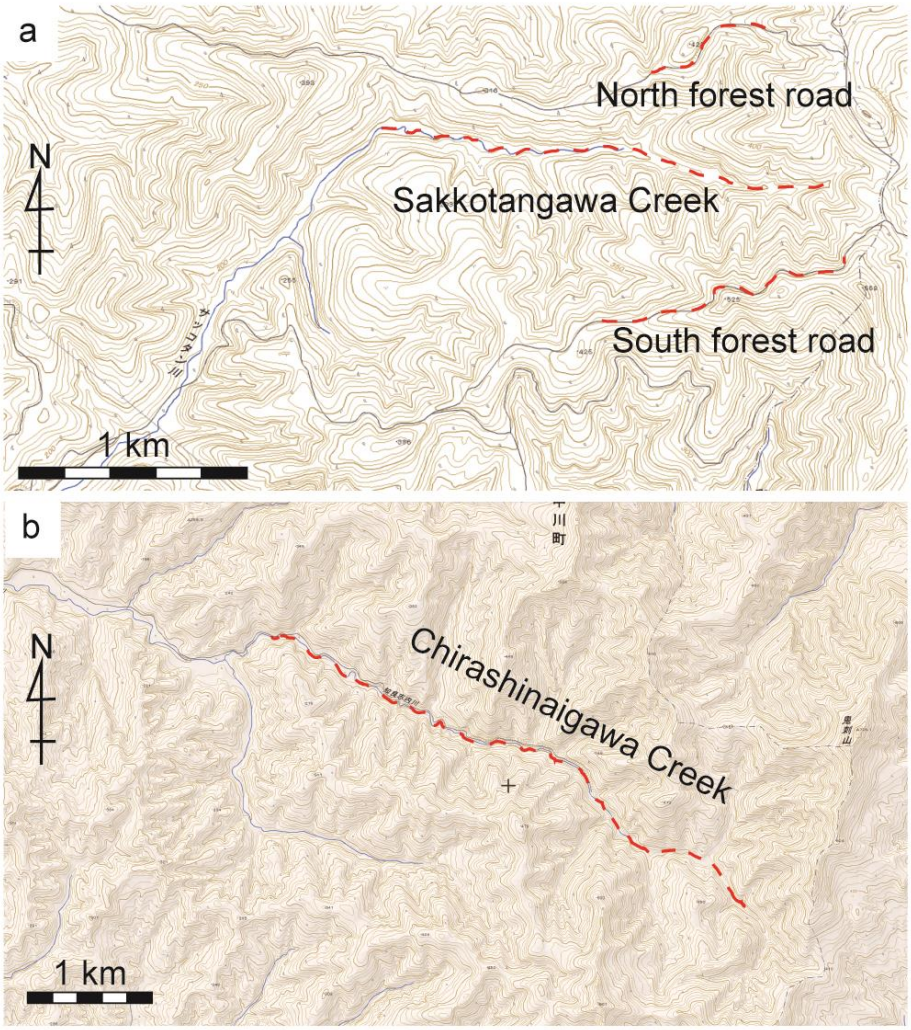

Fig. 2 Maps of the study area. a: Sakkotan area. b: Chirashinaigawa Creek. The dot lines indicate the route in the study area.

2011; Kobayashi et al., 2009). Slump deposits in the basal part of the Yezo Group have been reported although they are only a brief statement (Taki et al., 2011).

RESULTS

1. Shimonakagawa Quarry (Figs. 3–5)

In the Shimonakagawa quarry, complete succession from the uppermost part of the Sorachi Group and the lowermost part of the Yezo Group including their boundary were cropped out (Fig. 3). They were subdivided into four lithostratigraphy units.

Unit 1 (Figs. 3–4): It consists of dark green-, gray- and dark gray-colored claystone. Dark green-colored mudstone mainly consists of volcanic glass and radiolarian shells. Thin ash-fall tuff (typically less than 2 mm) are frequently intercalated. Dark green- and gray-colored claystone are dominant. In the uppermost part of the unit, the dark gray-colored claystones gradually increase. The total thickness of this unit is at least 350 m.

Unit 2 (Figs. 3 and 5): It consists of alternating beds of sandstone and dark gray-colored siltstone. The thickness is about 20 m. Throughout the unit, ambers, mud clasts, plant debris, and soft sediment deformation structures such as slump and sand injections frequently occur from beds. Sandstone beds are generally divided into two lithofacies. Most sandstone beds (type 1) are interpreted as distal turbidites. Other sandstone beds (type 2) are interpreted as cohesive debris-flow deposits (see details in Chapter 1). The thick planar amber (3-cm-thick)-bearing turbidite are distributed the base of the Unit 2.

Unit 3 (Fig. 5): It consists of dark green-, gray- and dark gray-colored claystone. The dark green-colored and non-bioturbated claystone with lamination of radiolarian

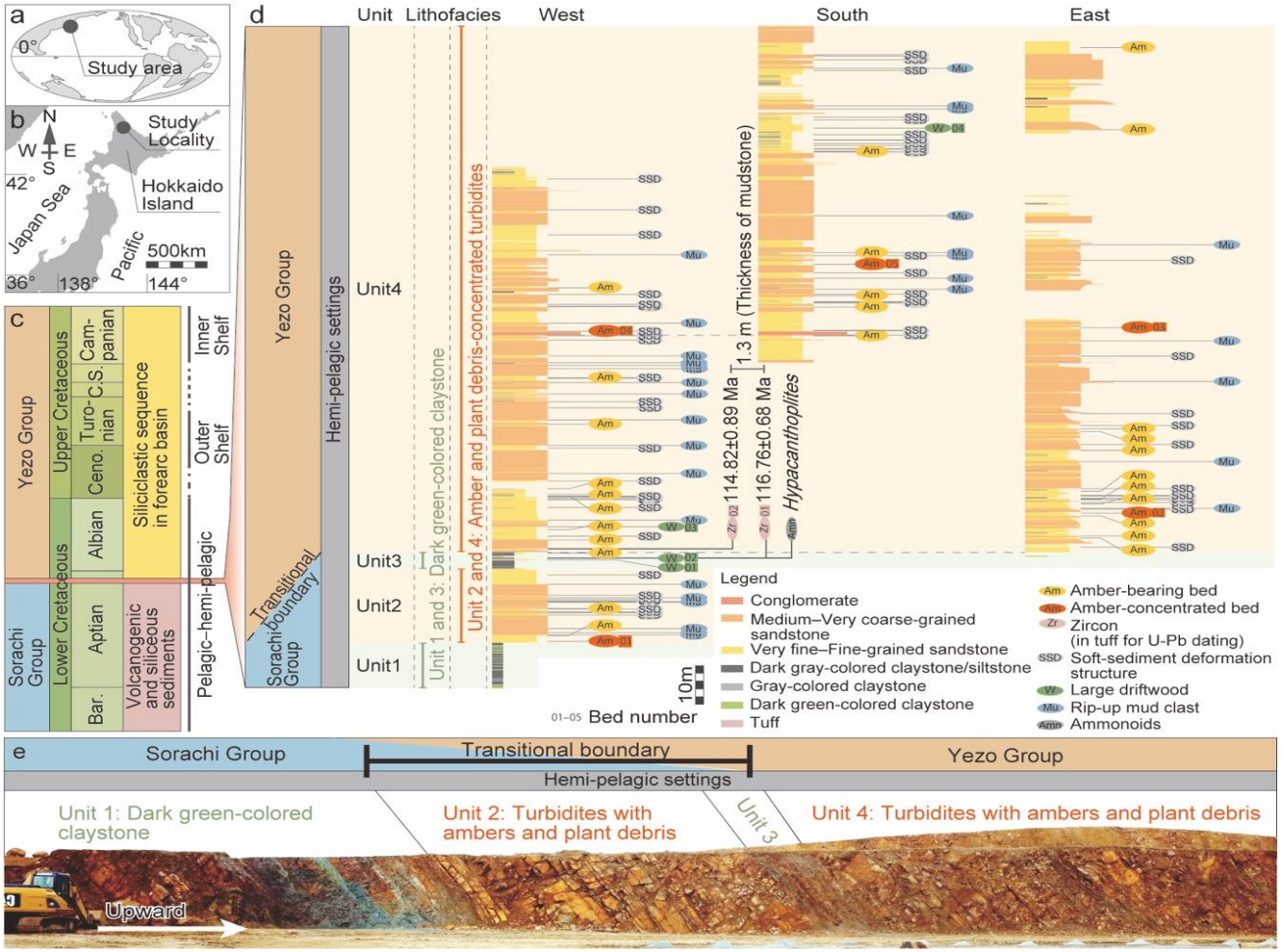

Fig. 3 Locality and stratigraphic distribution of amber-concentrated beds in the Shimonakagawa Quarry, Nakagawa area, northern Hokkaido, northern Japan. a–b: Locality map. Cretaceous paleomap is modified from Iba et al. (2011). c: Stratigraphic scheme and general trend of depositional settings of the Cretaceous siliciclastic sequence in the Nakagawa area (modified from Iba et al. (2011)). Bar.–Barremian. Ceno.–Cenomanian. C.–Coniacian. S.–Santonian. d: Columnar sections in the west, south, and east portions of the Shimonakagawa Quarry (Fig. 1). e: Outcrops representing the transitional boundary between the Sorachi and Yezo groups in the quarry.

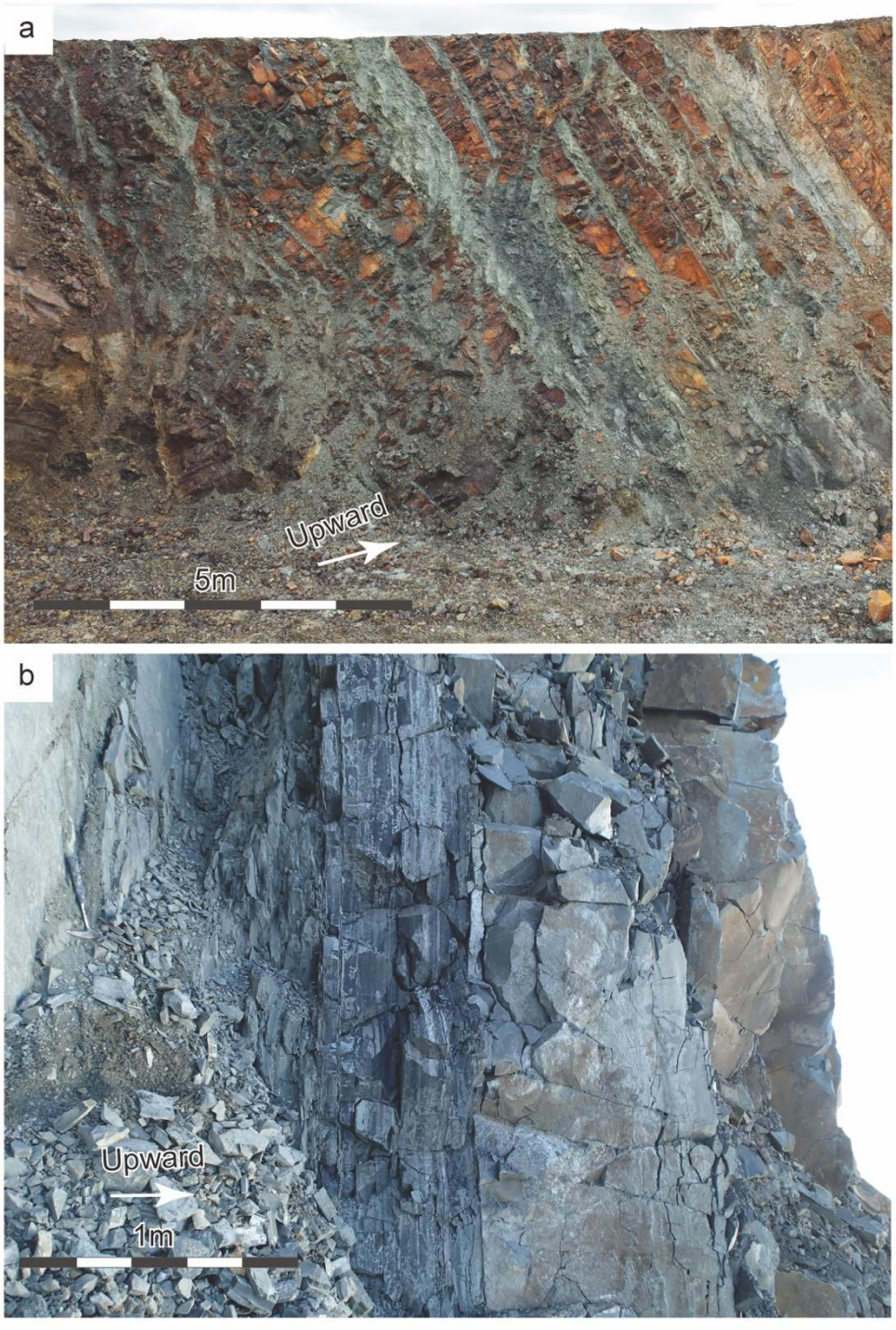

Fig. 4 Lithofacies of the uppermost part of the Sorachi Group in the Shimonakagawa quarry. Dark green-, gray- and dark gray-colored mudstone in Unit 1 (a) and 3 (b).

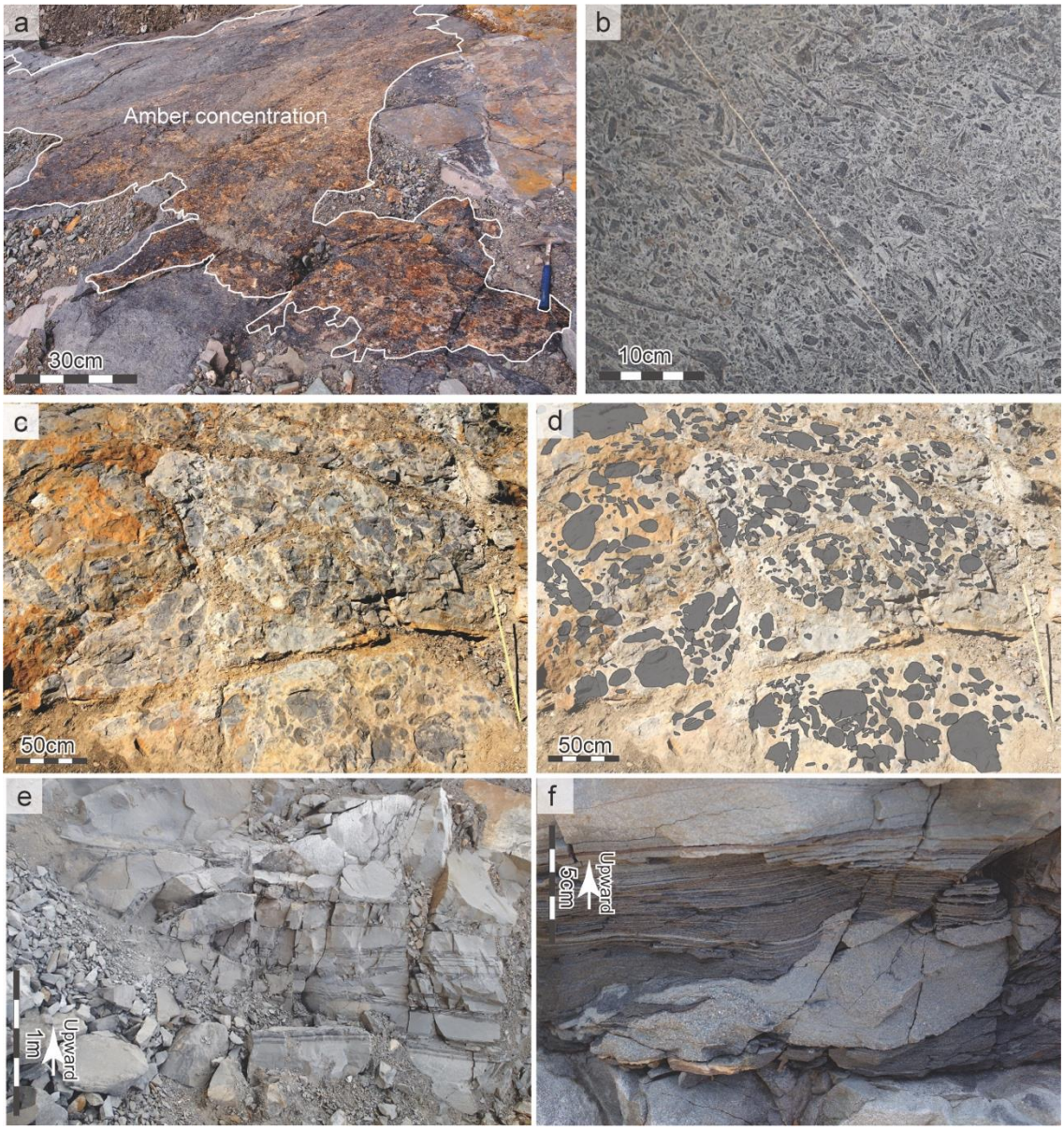

Fig. 5 Lithofacies of the lowermost part of the Yezo Group in the Shimonakagawa quarry. a: Amber-concentrated bed. b: Plant debris concentration. c–d: Mud clast concentration. e: Slump. f: Sand injection. a–d: Proximal side of the surfaces in photographs is upward.

shell concentration. Thin ash-fall tuff (typically less than 2 mm) is frequently intercalated. The Parahoplitid ammonoids concentrate in one horizon in the unit. The thickness is at least 20 m.

Unit 4 (Figs. 3–4): It consists of alternating beds of sandstone and dark gray-colored siltstone. The thickness is at least 130 m. Sandstone beds are generally divided into two lithofacies (type 1 and 2). The thinning upward cycles of occur every 5−20 m. In the lower to middle part of the unit is sandstone-dominated and upper is mudstone-dominated. Throughout the unit, ambers, mud clasts, plant debris, soft sediment deformation structures frequently occur from beds.

The boundary between the Sorachi and Yezo groups: The boundary between the Sorachi and Yezo groups is defined as the transitional one including Unit 2 and 3.

2. Sakkotan area (Figs. 6–7)

2-1. Sakkotan north forest road

Pechikunnai Formation: Dark green-colored and non-bioturbated claystone and very fine-grained sandstone are dominated (Fig. 7-a). Lamination of radiolarian shells concentration and tuff layers are developed in the dark green-colored mudstone. The total thickness is at least 240 m.

The group boundary and the Kamiji Formation: Gradual changes in the color of the mudstone from dark green to dark gray is unclear. Fine-grained laminated sandstone with plant debris, which lithofacies clearly differs to the ones below, is deposited just above the mudstone. Above the sandstone, dark gray-colored mudstone is deposited.
The boundary between the Sorachi and Yezo groups is just under the sandstone because it is intercalated between the dark green- to dark gray-colored mudstone. Above the

boundary, very fine- to medium-grained sandstone and dark gray-colored mudstone are distributed. Plant debris is occasionally included in sandstone. The total thickness is 610 m.

2-2. Sakkotangawa Creek

Pechikunnai Formation: Dark green-colored and non-bioturbated claystone and very fine-grained sandstone are developed. The total thickness is at least 30 m.

The boundary between the Sorachi and Yezo groups: Gradual transition from the dark green- to dark gray-colored mudstone occurs.

Kamiji Formation: The lowermost part of the formation consists of dark gray-colored mudstone (30 m thick), conglomerate, and very fine- to medium- grained sandstone. 6 m above the group boundary, medium-grained sandstone is deposited with folded mudstone (Fig. 7-c). The sandstone is not continuous between 1 m in a lateral side without faults. The sandstone holds dark gray-colored mudstone clasts in its lower part (7 cm in diameter). A conglomerate bed occurs 30 m above the group boundary (Fig. 7-b). Two conglomerate beds are distributed in 200 m thickness of the sequence. They are composed of round to sub-round pebbles of chert. The diameter of them is typically less than 10 mm. The lower conglomerate bed is 5.7 m in thickness. The upper conglomerate bed probably be divided into two beds because the dark gray-colored deformed mudstone is intercalated in them (Fig. 7-d). A slumping bed of mudstone is distributed 155 m above the boundary. A total thickness of the formation is at least 330 m.

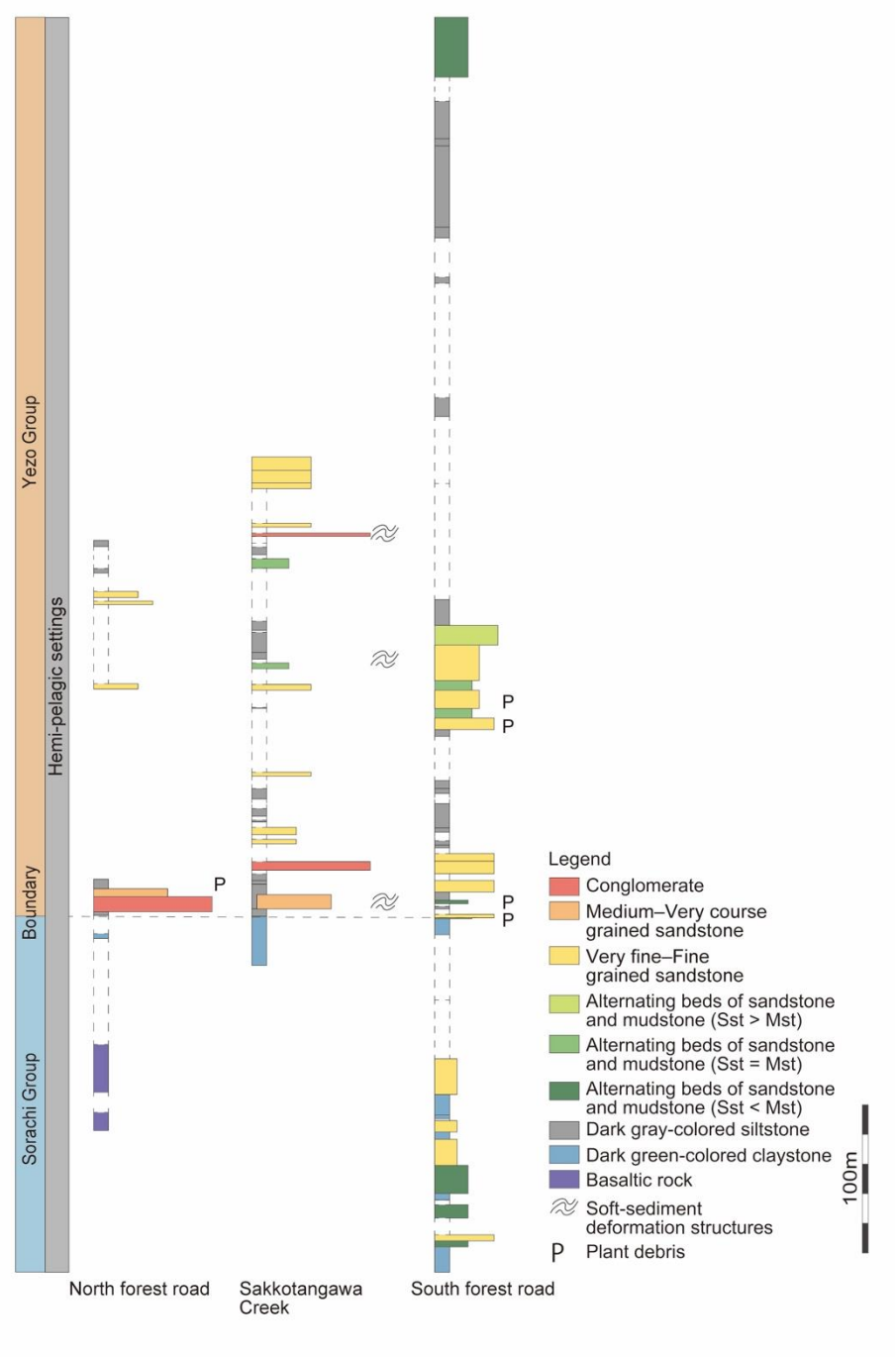

Fig. 6 Columnar sections in the Sakkotan area.

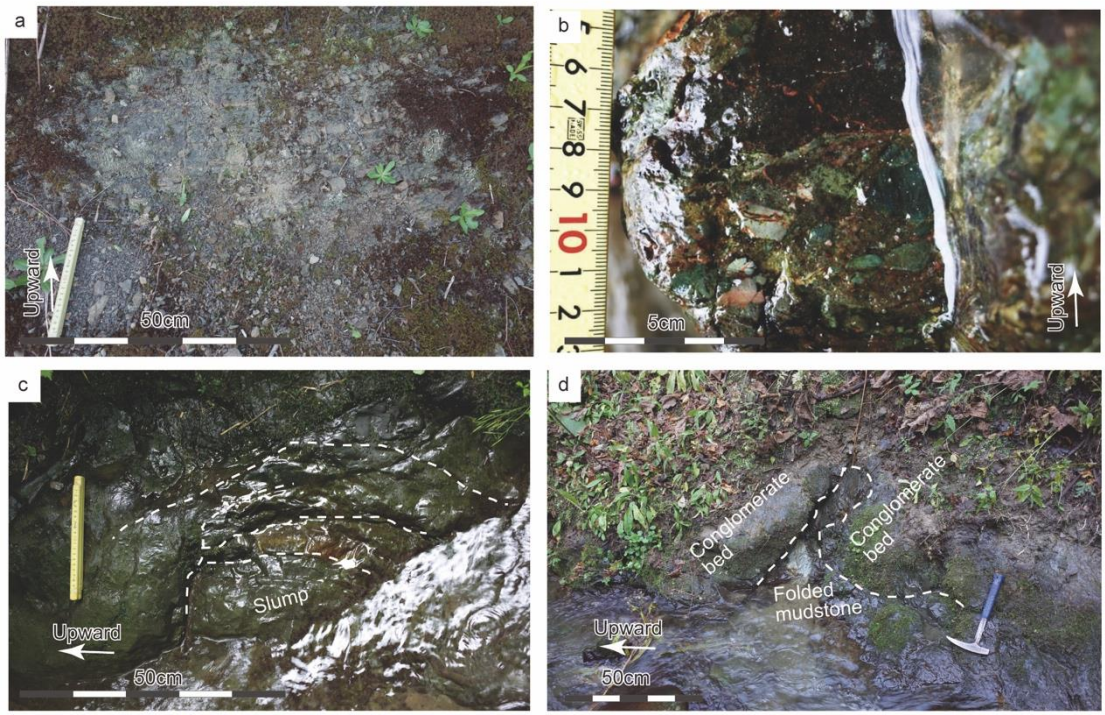

Fig. 7 The outcrop photos in the lower part of the Yezo Group in the Sakkotan area. a: Dark green-colored mudstone in the north forest road. b: Conglomerate bed. c: Slump deposit. d: Conglomerate bed (upper). b–d: The Sakkotangawa Creek.

2-3. Sakkotan south forest road

Pechikunnai Formation: It is composed of basaltic rocks and dark green-colored and non-bioturbated mudstone with well-developed parallel lamination of radiolarian shells. The total thickness of the formation is at least 100 m.

The group boundary and the Kamiji Formation: The boundary between the Sorachi and Yezo groups is not exposed. The base of the formation is defined as the first occurrence of dark gray-colored mudstone. Above the mudstone, 10 m thick conglomerate bed is deposited. The conglomerate bed is intercalated within non-bioturbated laminated mudstone and exhibits inverse grading in the basal part (1 m thick) and normal grading in its other parts (16 m thick). The gravel is typically 3 cm in diameter. The lower part consists of a clast-supported conglomerate with a poorly sorted matrix, in which pebbles show an imbrication structure. The upper part consists of matrix-supported conglomerate, in which three grading cycles are recognized. This conglomerate bed is interpreted to be a gravity flow deposit. The dark gray-colored mudstone which contact with the conglomerate conclude plant debris. The typical lithofacies of the Kamiji Formation is composed of the dark gray-colored mudstone, conglomerate, and very fine to medium-grained sandstone.

3. Chirashinaigawa Creek (Figs. 8–12)

Pechikunnai Formation: Dark green-colored mudstone with well-developed parallel lamination of radiolarian shells and tuff layers. The intensity of bioturbation is quite low. Total thickness is at least 60 m. The 30 cm below from the boundary, the sheath fold-like structure occurs.

The boundary between the Sorachi and Yezo groups: The boundary is defined

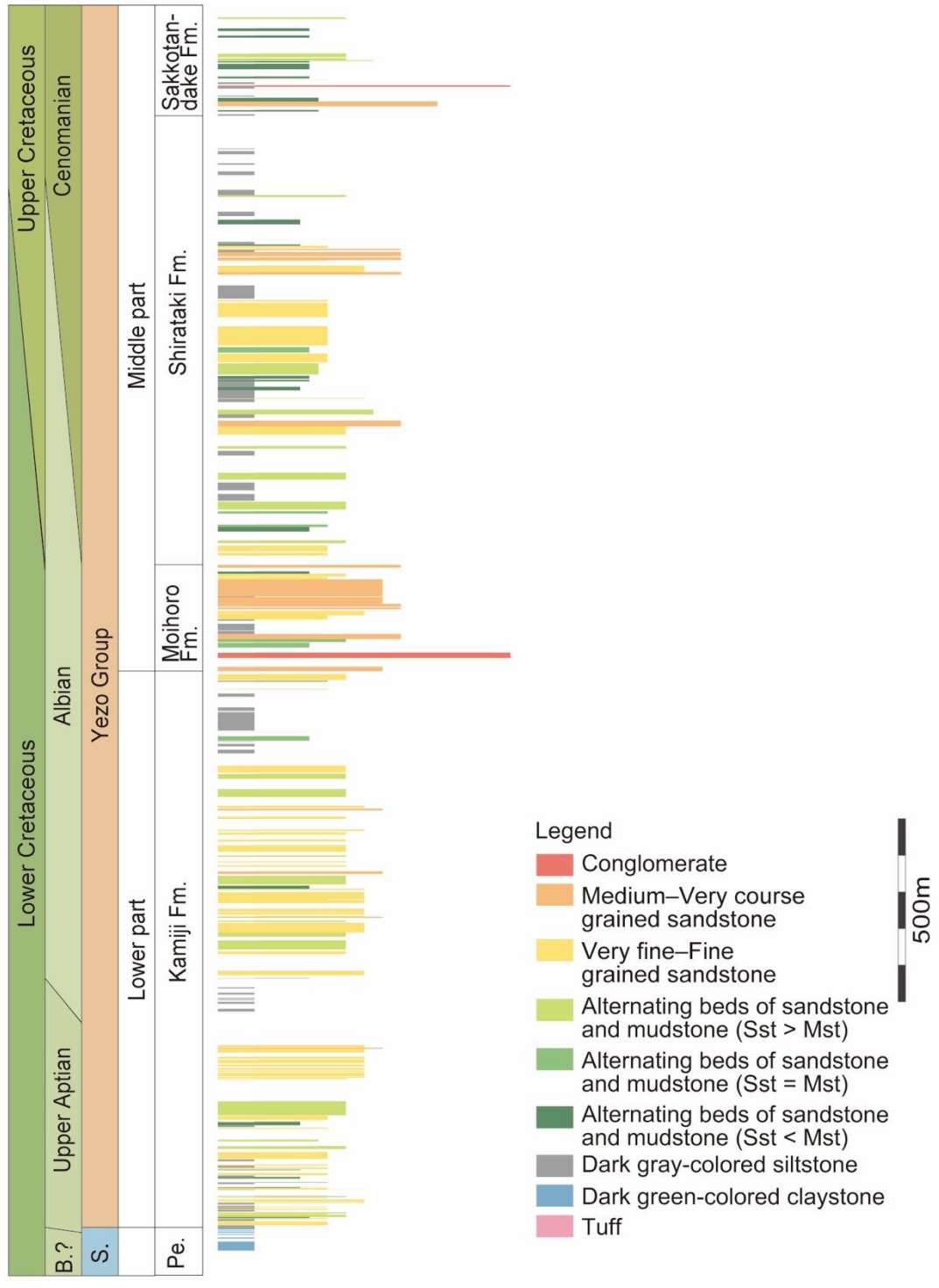

Fig. 8 Columnar section in the Chirashinaigawa Creek. B.–Barremian. S.–Sorachi Group.

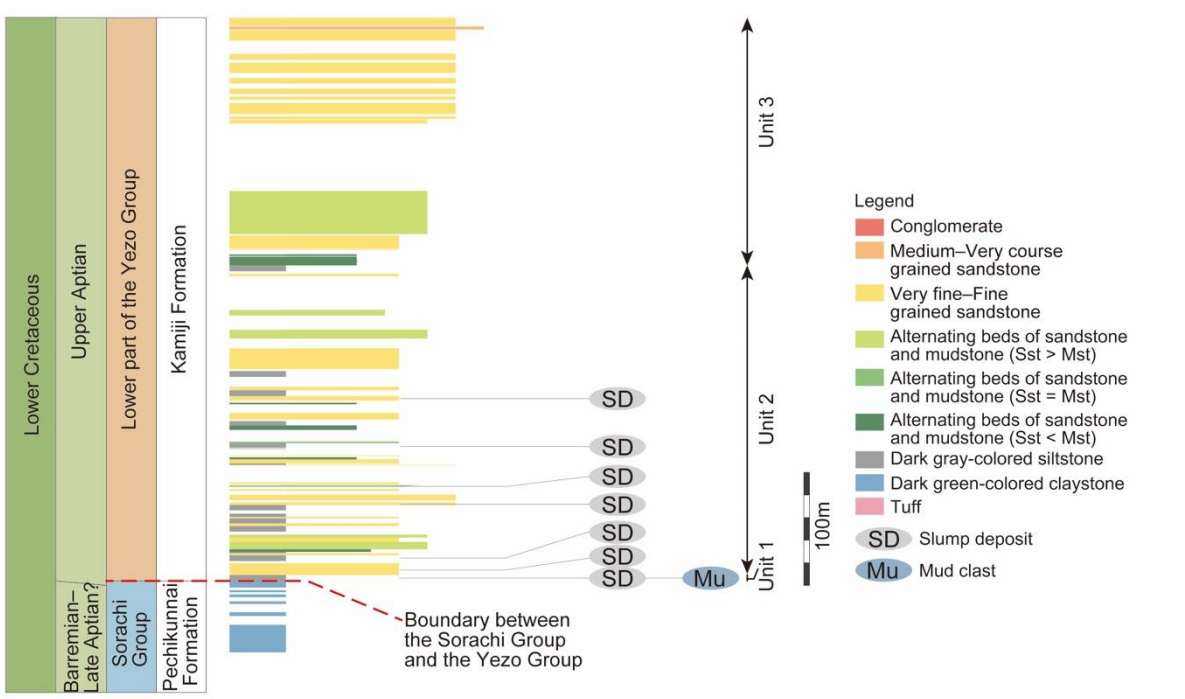

Fig. 9 Columnar section of the boundary between the Sorachi Group and the Yezo Group in the Chirashinaigawa Creek.

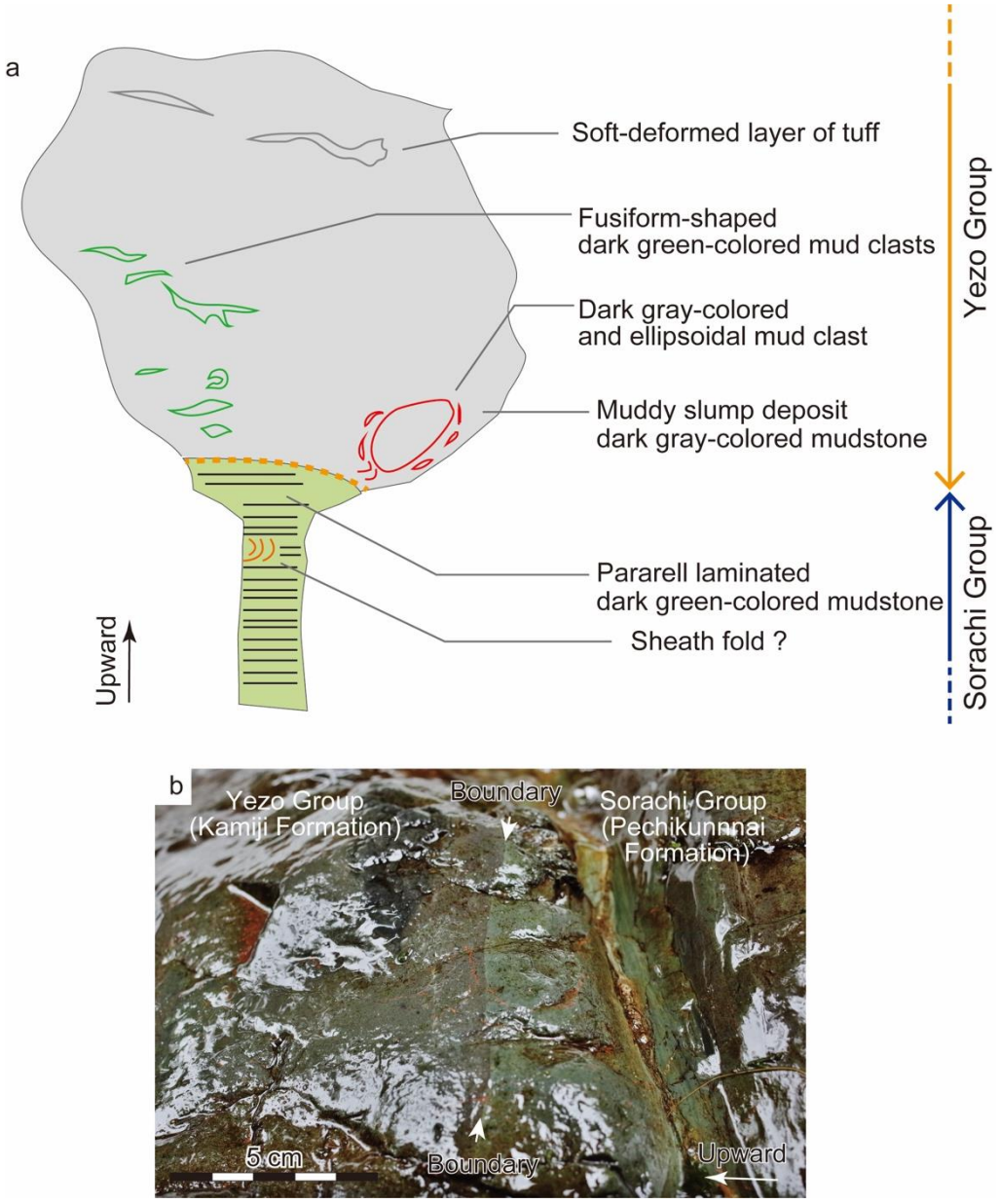

Fig. 10 Mode of occurrence of the boundary between the Sorachi and Yezo groups in the Chirashinaigawa Creek. a: The sketch of the boundary between the Sorachi Group and Yezo Group. b: The boundary between the Sorachi Group and the Yezo Group.

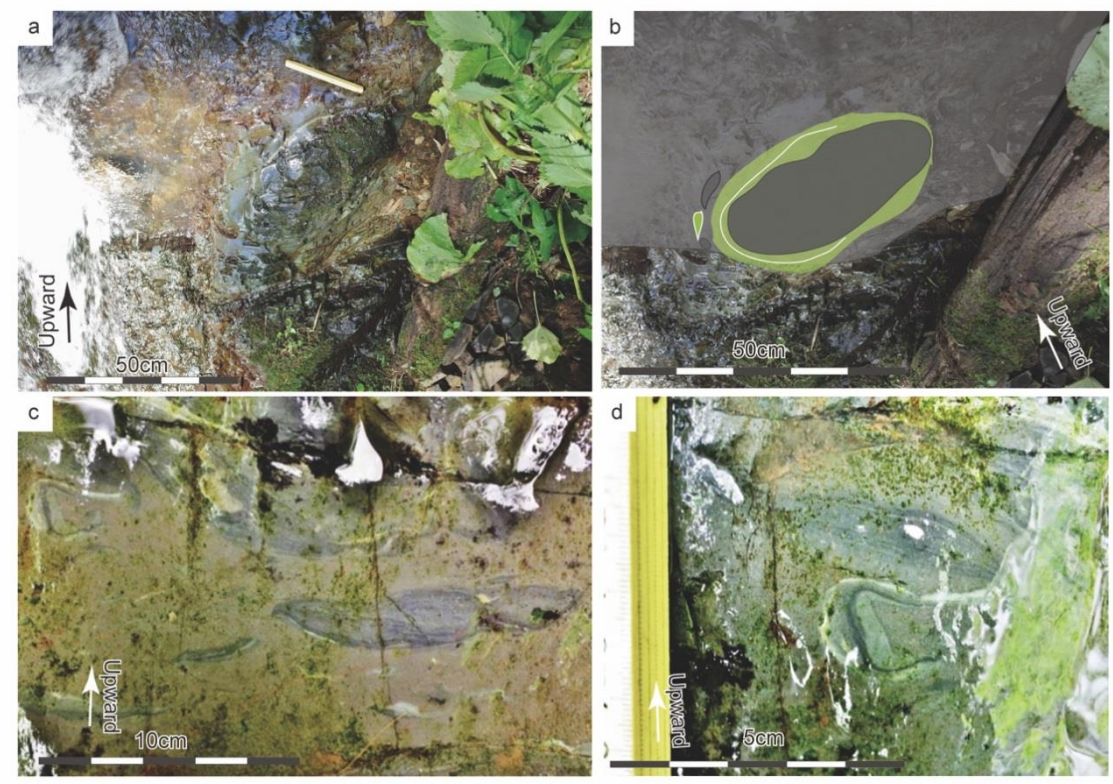

Fig. 11 The mode of occurrence of mud clasts. a: 30 cm-sized, dark gray-colored and ellipsoidal mud clast. b: The sketch of the mud clast. c: Fusiform-shaped dark green-colored mud clasts. d: Tightly folded mud clast.

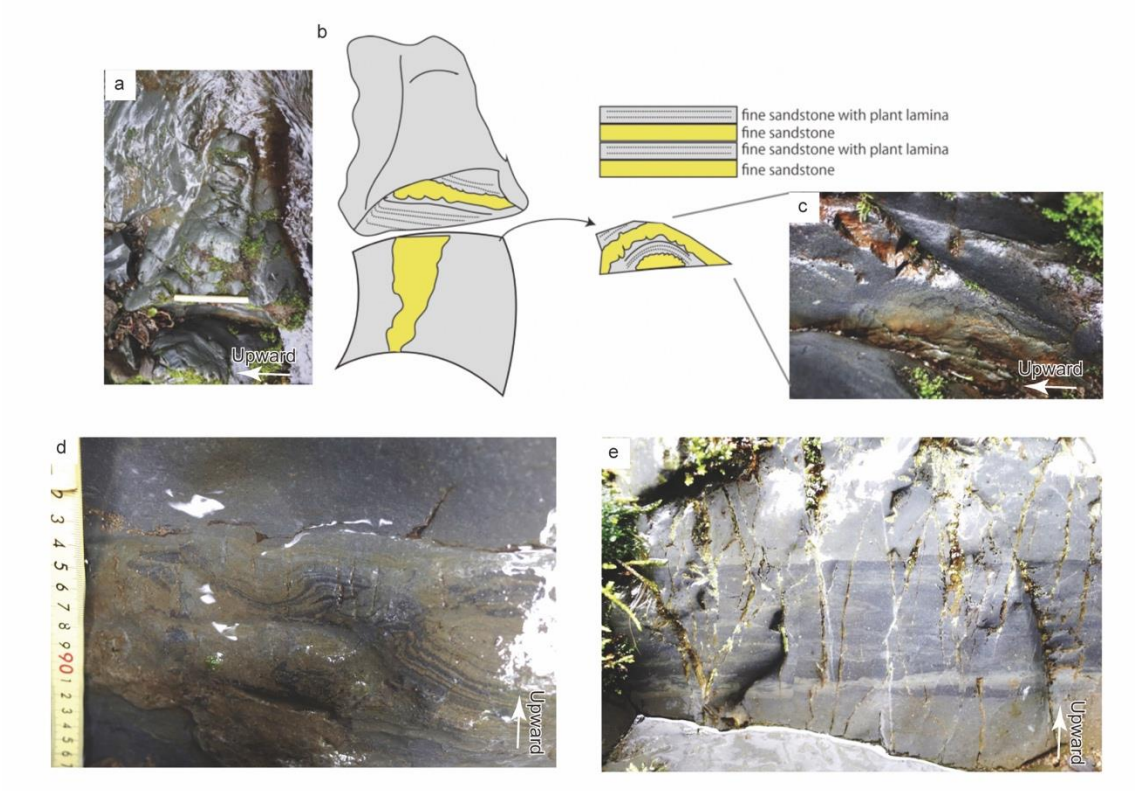

Fig. 12 The mode of occurrence of the slump deposits. a: The whole shape. b: Sketch of the slump deposit. c: Cross section of the rolling structures. d: Soft-sediment deformation structures with plant laminae. e: Soft-sediment deformation structures with mudstone.

between the dark green- and dark gray-colored mudstone. The boundary is clear and sharply cut by a scour-like structure (Fig. 10-b).

Kamiji Formation: The lowermost part of the formation is subdivided into three units focusing on the chaotic deposits; the muddy slump deposits in Unit 1: alternating beds of sandstone and mudstone with soft sediment deformation structures in Unit 2: and alternating beds of sandstone and parallel laminated mudstone in Unit 3.

Unit 1: Muddy slump deposits: The base of the Kamiji Formation is covered by the non-laminated dark gray-colored massive mudstone (5.3 m thick; Fig. 9). Just 30 cm above the base, two types of the mud clasts are concentrated (Figs. 10-a–11). One is the 30 cm sized dark gray-colored ellipsoidal mudstone clast (Figs. 10-a and 11-a–b). This mud clast is surrounded by dark green-colored claystone layer and several small mud clasts (Fig. 11-b). Another is the green-colored fusiform-shaped mud clasts (2 × 9 cm in maximum size; Figs. 10-a and 11-c–d). They are concentrated locally and some of them tightly twisted (Fig. 11-c) and folded (Fig. 11-d). The long axis of them is along with their inner lamination. In the upper part, deformed tuff layers occur but continuous in the lateral side.

Unit 2: Alternating beds of sandstone and mudstone with soft-sediment deformation structures: The alternating beds of sandstone and mudstone show irregular grain size distribution. Soft-sediment deformation structures are concentrated (Figs. 9 and 12). Massive sandstone beds are occasionally concluded plant debris. Total thickness is 270 m.

Unit 3: Alternating beds of sandstone and parallel laminated mudstone, sandstone, mudstone without soft-sediment deformation structures: Alternating beds of thin sandstone and parallel laminated mudstone are well-stratified. Massive sandstone beds

are occasionally concluded plant debris. Soft-sediment deformation structures are not observed in this part. Total thickness is 1080 m.

DISCUSSION AND CONCLUSIONS

1. Various lithofacies of the boundary between the Sorachi Group and the Yezo Group

The transition from green-colored mudstone to black-colored mudstone along the Pechikunnai Creek in the Nakagawa area are defined as the boundary between the Sorachi and Yezo groups (Kawaguchi, 1997). The transition is not alternating beds of green- and black-colored mudstones but occur gradually. Chemostratigraphy of mudstone through from uppermost part of the Sorachi Group (Osashima and Pechikunnai formations) to the lowermost part of the Yezo Group (Kamiji Formation) in the Nakagawa area clearly show the difference between the Sorachi and Yezo groups and support the onset of continental origin sediment supply on the base of the Yezo Group (Kobayashi et al., 2009). The irreversible transition of the mudstone and subsequent terrestrial siliciclastic sediments has been recognized as the general trend of the boundary sequence through the Nakagawa area.

In this study, the lithostratigraphy of the boundary between Sorachi and Yezo groups and lowermost part of the Yezo Group in three areas were descripted in detail. In the Shimonakagawa Quarry, complete sequence without faults from the uppermost part of the Sorachi Group and the lowermost part of the Yezo Group are reconstructed in this study. In the uppermost part of the Sorachi Group, dark green-, gray- and dark gray-colored claystone occur in turn in Unit 1. The dark gray-colored claystones are dominant in the uppermost part of the Unit 1. In addition, the 20-m-thick alternating

beds of the sandstone and dark gray-colored siltstone (Unit 2) are intercalated into the dark green-, gray-, and dark gray-colored claystone and siltstone (Unit 1 and 3). The lithofacies of the boundary sequence in the tree areas are different from the one of Kawaguchi (1997). In the Sakkotangawa Creek and the Chirashinaigawa Creek, the base of the Yezo Group is dark gray-colored slump deposit (Iba et al., 2005; Iba and Sano, 2007; Taki et al., 2011; this study). The lithofacies of the boundary sequence in the tree areas are different from the one of Kawaguchi (1997). The results propose that the lithofacies of the boundary between Sorachi and Yezo groups and lowermost part of the Yezo Group are various which are not typical one of Kawaguchi (1997).

2. The various chaotic deposits on the hemi-pelagic sediments in the boundary between the Sorachi and Yezo groups, and lowermost part of the Yezo Group in the Nakagawa area, northern Hokkaido

In addition to the boundary between the Sorachi and Yezo groups, the lithofacies of the lowermost part of the Yezo Group are various through the Nakagawa area, in contrast to the monotonous lithofacies of the uppermost of the Sorach Group. The features and interpretations of each lithofacies are mentioned below sections (discussion 2a–c). The depositional environment through the uppermost part of the Sorachi Group and the lowermost part of the Yezo Group are considered as the hemi-pelagic from the reasons of low sedimentation rate. Kobayashi et al. (2009) reported the high concentration of radiolaria from the uppermost part of the Sorachi Group in the Chirashinaigawa Creek, southern Nakagawa, and imply the low sedimentation rate as one of its cause. The quite low sedimentation rate is also estimated from claystone and siltstone of the transitional boundary between Sorachi and Yezo groups and lowermost

part of the Yezo Group (Unit 3 and lowermost part of the Unit 4) in the Shimonakagawa Quarry by U-Pb ages of two tuff layers (Chapter 1). This indicate that the depositional environment had not been changed and it was hemi-pelagic during the deposition of terrestrial organic-rich siliciclastic sediments (Unit 2 in Chapter 1).

2a. Amber- and plant debris-concentrated turbidites in the Shimonakagawa Quarry, northern Nakagawa

In the Shimonakagawa Quarry, ambers and plant debris-concentrated turbidites are distributed in the transitional boundary between the Sorachi and Yezo groups and lowermost part of the Yezo Group (Unit 2 and 4, respectively). The content rates of them are extra-ordinary high. The organic-rich deposits clearly indicate the presence of large supply from lands. The land forest destruction and mass-transportation of its remains from lands to oceans by large-scale tsunamis are reconstructed (Chapter 1).

2b. Conglomeratic gravity flow deposits in the Sakkotan area, central Nakagawa

The Sakkotan area is characterized by the conglomerate beds in the lowermost part of the Yezo Group (e.g., Iba et al., 2005). The conglomerate beds are classified as the Onodera Sandstone and Conglomerate Member (defined by Ijima and Shimada, 1952 as the Onodera Sandstone Formation; revised by Taki et al, 2011; Nagao, 1962 as the Onodera Formation; Hashimoto et al., 1967 as a part of the KJ1 Member) The member typically consists sandstone associated with thick conglomerate bed. The conglomerate beds have been sporadically distributed in the range of 20 km scale (Taki et al., 2011); the Shimonakagawa area in northern Nakagawa, the Sakkotan area and the Okahonaigawa Creek in central Nakagawa (e.g. Igi, 1959; Taki et al., 2011; Hashimoto

et al., 1967). In this study, it is clear that the thickness of the conglomerate bed gets thinner and grain size of the pebbles get smaller from south to north in the Sakkotangawa Creek and the south forest road. In the north forest road, the conglomerate bed does not occur. Remarkable lateral transition that thin out in a 1 km scale occur in a narrower range than has been thought in previous thought.

The conglomerate bed exposed in the Sakkotan south road has been well-described and considered as the conglomeratic gravity-flow deposits (Iba et al., 2005). Pebbles of shallow marine calcareous sediments (e.g., orbitolinid tests, rudist fragments and calcareous red algae) are included in the bed (Iba et al., 2005; Iba and Sano, 2006, 2007). They indicate that the origin of the deposit is shallow-marine. *Mesorbitolina parva*, which is described from the Okahonaigawa Creek indicate that the generation of the pebbles and their supply are also in the Late Aptian age (Iba et al., 2005; Iba and Sano, 2007).

2c. Muddy slump deposits in the Chirashinaigawa Creek, southern Nakagawa

The slump deposits in the lowermost part of the Yezo Group in the Chirashinaigawa Creek has been reported but not described in detail (Taki et al., 2011). In this study, it is clear that slump deposits are frequency occur in the Unit 1and 2 of lowermost part of the Yezo Group (275 m). In the Unit 1 of the muddy slump deposit just above the boundary between the Sorachi and Yezo groups, the sole large-scale mud clasts and concentration of the fusiform-shaped mud clasts are newly described (Fig. 10, 11). The shape of the mud clasts indicates the difference of hardness of them at the depositional time. The dark gray-colored ellipsoidal mud clasts should have passed the polishing process. This means that relatively semi- to mostly solidified mudstone block (Fig. 10,

11) had been generated by destruction of seafloors and submarine cliffs, where are shallower than the depositional area, and then polished during their transportation. Whereas, fusiform clasts show folding and twisted structures (Figs. 10 and 11). They are concentrated locally, not arranged along layers and not scattered in the muddy slump (Figs. 10 and 11). The distribution indicate that they had not much disturbed as to be scattered and sorted as to be arranged in the slump deposit. The mode of occurrence indicate that they had been peeled off from the seafloors relatively near the depositional area in the soft to semi-solidified condition. They had not dispersed because of the high viscosity of the muddy slump deposit. The mode of occurrence of large-scale mud clasts surrounded by the dark green-colored mudstone layer means that the dark green-colored mudstone on the surface of the sea floor in the depositional area had still been in a soft condition (Fig. 11). They had pushed up by the strike of the large-scale mud clast. From the evidence mentioned above, the origin of the muddy slump deposit is relatively far from the depositional area. They had related to the destruction of the sea bottom, not only reworking and failure of near seafloor sediments (Fig. 13).

3. The various chaotic deposits on the hemi-pelagic sediments in the lowermost part of the Yezo Group in the Nakagawa area, northern Hokkaido

The lowermost part of the Yezo Group in the Nakagawa area is characterized by various chaotic deposits; the amber- and plant debris-concentrated turbidites, conglomeratic gravity flow deposits with shallow-marine limestone pebbles and muddy slump deposit with large mud clasts (Fig. 14). The occurrence of the similar deposits over multiple horizons in each area, and significant difference between each area indicate that they depend on the source areas and supply route of the deposits.

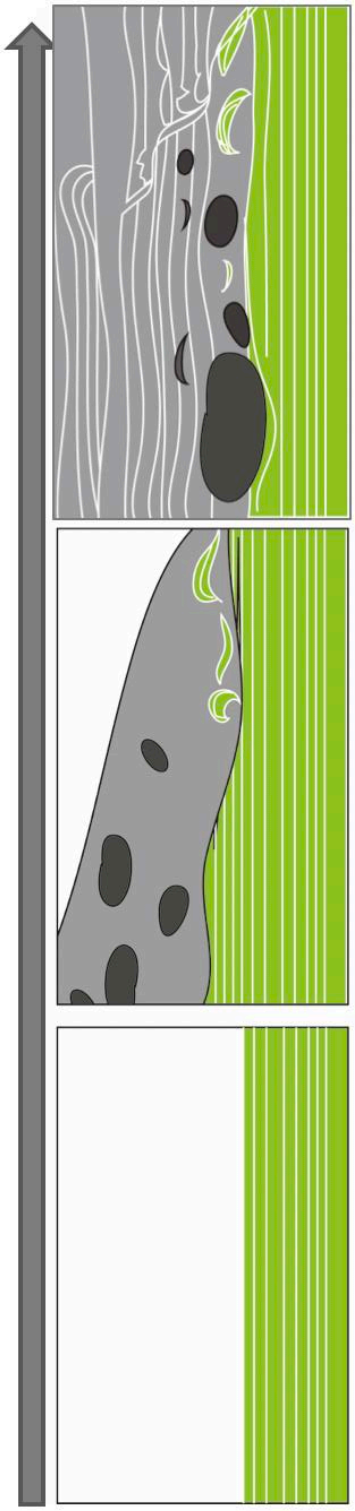

Fig. 13 The reconstruction of the depositional process of the muddy slump deposit focusing on mud clasts.

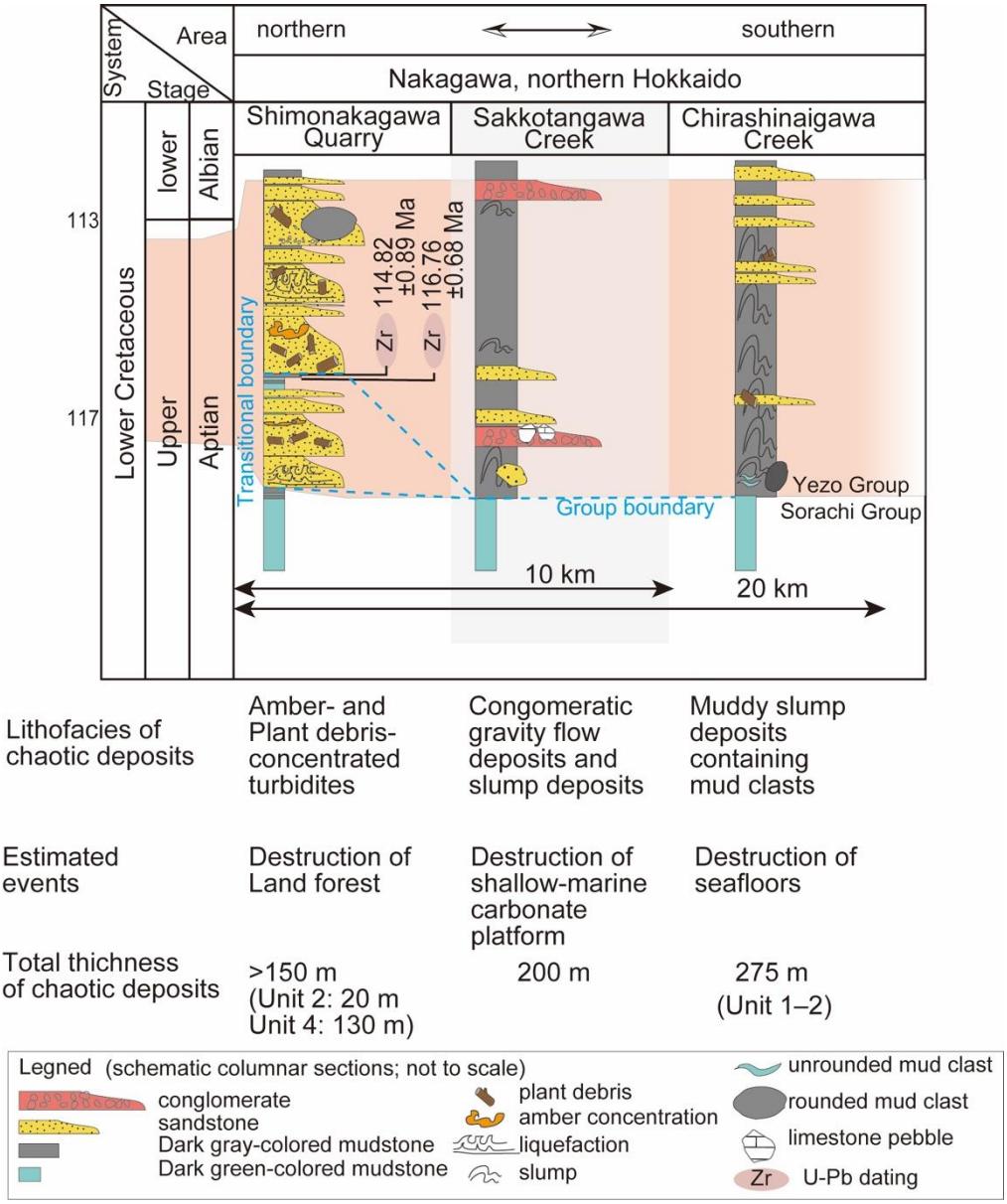

Fig. 14 The correlation of the chaotic deposits in the boundary between the Sorachi and Yezo groups and lowermost part of the Yezo Group, the Nakagawa area, northern Hokkaido, Japan.

The sources and processes of the chaotic deposits are reconstructed from their lithofacies. In the Shimonakagawa Quarry, extraordinary high-concentrated plant debris and amber in turbidites indicate that the wide destruction of the land forests by large-scale tsunamis (Chapter 1). In the Chirashinaigawa Creek, two types of the mud clasts in the muddy slump deposit (Fig. 11) indicate that they had related to the destruction of the seafloors which are far from the depositional area, not only reworking from near slopes. In the Sakkotan area, pebbles of the shallow-marine calcareous sediments included in the conglomeratic gravity flow deposit (Iba et al., 2005) indicate that the destruction of the shallow-marine area. As mentioned above, these deposits have common features that they are associated with the destruction of the hinterlands; lands, shallow-marine area, and seafloors.

4. The destruction of land, shallow marine and seafloors in the Nakagawa area

Based on the results, the chaotic deposits are concentrated in the lowermotst part of the Yezo Group and the boundary between the Sorachi and Yezo groups and reveal that the possibility of the destruction of the lands, shallow marine and seafloors (Fig. 14). It is unknown whether the sediments of slump deposits in the Chirashinaigawa creek and the conglomeratic gravity-flow deposits in the Sakkotan area are directly supplied from the source or had undergone multiple reworking. Iba and Sano (2006, 2007) discussed that both of destruction and supply of the conglomeratic gravity-flow deposits occurred in the same age, the Late Aptian. The unrounded and fusiform-shaped dark green-colored mud clasts (Fig. 11) included in the slump deposit indicate that they are eroded in the period that dark-green colored mudstone had are exposed on the seafloors or thinly-covered by dark gray-colored siltstone, and are still in unconsolidated

condition. The soft- “resin” deformation structures in planar amber (Chapter 1) are clearly indicate that the destruction of the land forest and direct mass-transportation of its remains into hemipelagic settings without any time to hardening of the resin in the air.

The slump deposits with large sized mud clast in the Chirashinaigawa Creek and slump deposit and subsequent conglomeratic deposits in the Sakkotan area, and a thick planar amber-bearing turbidite are deposited just above the Sorachi Group in each area. The remarkable chaotic deposits on the dark green-colored claystone indicate that the supply of the siliciclastic sediments started from the chaotic deposits, not gradual increase in three areas distributed in 20 km scale.

In conclusion, the tsunami deposit in the Shimonakagawa quarry (Chapter 1) frequently changes its lithofacies from amber-concentrated turbidite to muddy slump deposit (Chirashinai) via, thick conglomerate, at 100 m to 20 km. This occurrence of various lithofacies indicate various distraction/collapse happened from land to shallow-marine carbonate platform via slope.

In addition, the chaotic deposits are not only one bed in each area. In the Shimonakagawa Quarry, the plant debris-concentrated turbidites continue at least 150 m in thickness (Fig. 2). Amber occurs from 32 horizon in the sequence. The result of the age in Unit 3 and lowermost part of the Unit 4 indicate that there are 0.3–3.5 Myr interval in the claystone/siltstone sequence (Chapter 1). It indicates that the presence of two major event-concentrated period around 117–114 Ma, the latest Aptian. Slump deposits frequently occur in 275 m thick above the group boundary in the Chirashinaigawa Creek (Figs. 9 and 12). In the Sakkotan area, two conglomerate beds and several slump deposits occur in 280 m thick (Fig. 6). The sequence also shows the

presence of unstable period which occur the destruction and slope failure of the hinterland.

The boundary between the Sorachi and Yezo groups has been considered as a period of drastic tectonic changes, such as paleo-backland shifts by orogeny of hinterlands by westward subduction (e.g., Niida and Kito, 1986; Kiminami et al., 1992). The chaotic deposit sequences are located in the base of 8000-m-thick terrestrial siliciclastic sediments which supply into the Yezo for-arc basin from the latest Aptian to Paleocene. The frequent earthquakes and tsunamis would had been occurred in the early stage of the formation of the Yezo Group in the Nakagawa area, northern Hokkaido, in the latest Aptian.

5. The various lithofacies of the destruction events

Although it is clear that earthquakes and tsunamis affect various places such as lands to submarine, and make various sedimentary structures (e.g., Dawson and Stewart, 2007; Montenat et al., 2007), it is impossible to grasp their scale only by tracing and correlating of the single lithofacies. In this study, the trace of the chaotic deposits, which are distributed in the same lithostratigraphic horizon in 20 km scale. They have common features of destruction of their hinterland. The destruction would occur in lands, shallow marine and seafloors. Their destructions cannot be grasped by the trace of the single facies. It is also cleared that the deposits which are related to be destructive events change their lithofacies depending on the conditions of the source and the route even though in a narrow scale (20 km scale). This study provides the importance of the trace of the deposits which changing their lithofacies by extracting the common features focusing their formation process.

REFERENCES CITED

Dawson, A.G., and Stewart, I., 2007, Tsunami deposits in the geological record: Sedimentary Geology, v. 200, p. 166–183, doi: 10.1016/j.sedgeo.2007.01.002.

Dhondt, A.V., 1992, Palaeogeographic distribution of Cretaceous Tethyannon-rudist bivalves, *in* Kollmann, H.A., and Zapfe, H., eds., New aspecton Tethyan Cretaceous fossil assemblages: Schriften-reihe der Erdwissenschaftlichen Kommission der Österreichischen Akademie der Wissenschaften, v. 9, p. 75–94, doi: 10.1007/978-3-7091-5644-5_6.

Hashimoto, W., Nagao, S., Tono, S., and Taira, K., 1967, On the Stratigraphy of the Lower Yezo Group and Lower Part of the Middle Yezo Developed in the Nakagawamachi Area, Nakagawa County, Hokkaido: Commemorative Volume for Professor H. Shibata, p. 220–228.

Hayakawa, H., 1999, Occurrence of *Ammonoceratites ezoense* (Yabe) from the Albian of Nakagawa, Hokkaido: Bulletin of the Nakagawa Museum of Natural History, v. 2 p. 41–44.

Iba, Y., Taki, S., Yoshida, K., and Hikida, Y., 2005, *Orbitolina*-bearing limestone pebbles from the lowermost part of the Lower Yezo Group (Lower Cretaceous) in the Nakagawa area, northern Hokkaido, Japan, and its significance: Journal of the Geological Society of Japan, v. 111, p. 67–73, doi: 10.5575/geosoc.111.67.

Iba, Y., and Sano, S., 2006, *Mesorbitolina* (Cretaceous larger foraminifera) from the Yezo Group in Hokkaido, Japan and its stratigraphic and paleobiogeog raphic significance: Proceedings of the Japan Academy, Series B, v. 82, p. 216–223, doi: 10.2183/pjab.82.216.

Iba, Y., and Sano, S., 2007, Mid-Cretaceous step-wise demise of the carbonate platform

biota in the Northwest Pacific and establishment of the North Pacific biotic province: Palaeogeography, Palaeoclimatology, Palaeoecology, v. 245, p. 462–482, doi: 10.1016/j.palaeo.2006.09.008.

Ijima, S., and Shinada, Y., 1952, Geology of northern part of Abeshinai Oil Field: Hokkaido, Bulletin of the Geological Survey of Japan v. 3, p. 609–619.

Igi, S., 1959, Explanatory text of the geological map of Japan 'Pinneshiri' (scale1:50000): Geological Survey of Japan, 64p.

Kanie, Y., Taketani, Y., Sakai, A., and Y., Miyata, Y., 1981, Lower Cretaceous deposits beneath the Yezo Group in the Urakawa area, Hokkaido: The Journal of the Geological Society of Japan, v. 87, p. 527–533, doi: 10.5575/geosoc.87.527.

Kawaguchi, M., 1997, Lower Cretaceous strata around the River Onisashi, northern Hokkaido, *in* Kawamura, M., Oka, T. and Kondo, T., eds., Commemorative volume for Professor Makoto Kato: Hokkaido University, p. 121–134.

Kiminami, K., Komatsu, M., and Kawabata K., 1992, Composition of clastics of the Sorachi Group and the Lower Yezo Group in the Inushibetsu-gawa area, Hokkaido, Japan, and their significance: Memoir of the Geological Society of Japan, v. 38, p. 1–11.

Kobayashi, S., Ohta, T., and Hirano, H., 2009, Geochemical variation of mudstones across the Sorachi Group and Yezo Supergroup boundary at the Teshionakagawa area, northern Hokkaido, Japan: Bulletin of the Mikasa City Museum, Natural Science, v. 13, p. 21−34.

Matsumoto, T., 1942, Fundamental in the Cretaceous stratigraphy of Japan, Part Ⅰ: Memoirs of Faculty of Science, Kyushu Imperial University, Series D, v. 1, p. 129–280.

Matsumoto, T., 1943, Fundamental in the Cretaceous stratigraphy of Japan, Part Ⅱ: Memoirs of Faculty of Science, Kyushu Imperial University, Series D, v. 2, p. 98–237.

Matsumoto, T., 1984, A gigantic parahoplitid ammonite from northern Hokkaido: Report of the Geological Survey of Hokkaido, v. 55, p. 21–28.

Mitsugi, T., and Hirano, H., 1998, Radiolarian biostratigraphy of the Lower Cretaceous strata in the Nakagawa area, northern Hokkaido: Scientific Reports of Waseda University, v. 46, p. 19–32.

Montenat, C., Barrier, P., Ott d'Estevou, P., and Hibsch, C., 2007, Seismites: An attempt at critical analysis and classification: Sedimentary Geology, v. 196, p. 5–30, doi: 10.1016/j.sedgeo.2006.08.004.

Nagao, S., 1962, Explanatory text of the geological map of Japan 'Teshio–Nakagawa' (scale1:50000): Geological Survey of Hokkaido, 55p.

Niida, K., and Kito N., 1986, Cretaceous arc-trench system in Hokkaido: Monograph of the Association of Geological Collaboration, Japan, v. 31, p. 379–402.

Shimizu, K., Takeda, I., Mitsugi, T., and Hirano, H., 2001, Geochemical study of the Lower Cretaceous in the Nakagawa area, northern Hokkaido, Japan: Bulletin of Nakagawa Museum of Natural History, v. 4, p. 53–70.

Takahashi, A., Hirano, H., and Sato, T., 2003, Stratigraphy and fossil assemblage of the Upper Cretaceous in the Teshionakagawa area, Hokkaido, northern Japan: Journal of the Geological Society of Japan, v. 109, p. 77–95, doi: 10.557 5/geosoc.109.77.

Takashima, R., Kawabe, F., Nishi, H., Moriya, K., Wani, R., and Ando, H., 2004, Geology and stratigraphy of forearc basin sediments in Hokkaido, Japan:

Cretaceous environmental events on the north-west Pacific margin: Cretaceous Research, v. 25, p. 365–390, doi: 10.1016/j.cretres.2004.02.004.

Taketani, Y., and Kanie, Y., 1992, Radiolarian age of the Lower Yezo Group and the upper part of the Sorachi Group in Hokkaido *in* Ishizaki, K., and Saito, T., eds., Centenary of Japanese Micropaleontology: Tokyo, Terra Scientific Publishing Company, p. 365–373.

Taki, S., Iba, Y., Hikida, Y., and Yoshida, K., 2011, Lithostratigraphy of the Cretaceous in the upper reaches of the Chirashinai River, Teshionakagawa area, northern Hokkaido, Japan: Journal of the Faculty of Science Shinshu University, v. 43, p. 43–65.

Ueda, H., 2016, Hokkaido, *in* Moreno, T., Wallis, S., Kojima, T., and Gibbons, W., eds., The Geology of Japan: Geological Society, London, p. 201–221.

Yoshida, K., Iba, Y., Taki, S., Sugawara, M., Tsugane, T., and Hikida, Y., 2010, Deposition of serpentine-bearing conglomerate and its implications for Early Cretaceous tectonics in northern Japan: Sedimentary Geology, v. 232, p. 1–14.

Chapter 3

Earliest history of the Yezo Group revealed by the calcareous sandstone olistoliths in the Horokanai area, Hokkaido, northern Japan

ABSTRACT

The Yezo Group is a Cretaceous–Paleocene fore-arc basin deposit along the eastern margin of the Eurasia, and its middle to upper part has been regarded as a reference marine succession of the Upper Cretaceous in the circum-North Pacific regions. Geological age of the lower part of the Yezo Group, especially of its lowest part, is, however, still unclear due to lack of index fossils, though it recorded important information for understanding the early history of the Yezo fore-arc basin. Here we describe an olistostrome deposit including calcareous sandstone olistoliths, intercalated in the basal part of the Yezo Group in the Horokanai area, northern Hokkaido. We identify a well-preserved orbitolinid specimen in the olistolith as *Mesorbitolina parva*, which indicated that the lowest part of the Yezo Group in this area is assigned to the Late Aptian–Early Albian or later in age. This is much earlier than previously thought (the upper Valanginian to Barremian of the uppermost part of the Sorachi Group) This olistostrome bed can be considered as a key unit and correlated with the Kirigishiyama Olistostrome Member in the Yubari–Ashibetsu area (about 80 km south of Horokanai)

and the conglomerate in the lowest Yezo Group in the Nakagawa (about 90 km north of Horokanai). According to stratigraphic correlation among these areas, it is indicated that significant difference of the early history of the Yezo Group is present between central and northern Hokkaido: the basin was probably first formed in central Hokkaido in the earliest Aptian and then, expanded to northern Hokkaido in the Late Aptian or later. In the northern Hokkaido, the deposition of the Yezo Group started with the catastrophic deposition which occurred simultaneously with, and possibly caused by tectonic instability along the eastern margin of the Eurasia.

INTRODUCTION

The Yezo Group is about 8000-m-thick Aptian to Paleocene fore-arc basin deposit along the eastern margin of the Eurasia, which is distributed in the area from the offshore of North Honshu Island (Japan) to Sakhalin (Far East Russia) (Ando, 2003; Takashima et al., 2004) (Fig. 1). A high-resolution integrated stratigraphy of the middle to upper part of the Yezo Group, including macro-, micro-fossil, and carbon isotope stratigraphy, has been established (e.g., Matsumoto, 1942, 1943; Hirano et al., 1977; Toshimitsu, 1995; Hasegawa, 1997; Obradovich et al., 2002; Toshimitsu et al., 2003; Takashima et al., 2004; Shigeta and Maeda, 2005). It has been nowadays regarded as a reference marine succession of the Upper Cretaceous in the circum-North Pacific regions. On the contrary, geological age of the lower part of the Yezo Group (Lower Cretaceous), especially of its lowest part, is still unclear due to lack of index fossils, though it is important for understanding the early history of the Yezo fore-arc basin.

Olistostrome and its related gravity flow deposits, which contain shallow-marine carbonate olistoliths and/or pebbles, occur in the lower part of the Yezo Group in central (Yubari–Ashibetsu area) and northern Hokkaido (Nakagawa area) (Fig. 1-a) (Sano, 1995; Takashima et al., 2004; Iba et al., 2005; Iba and Sano, 2006). They have been recognized as the remarkable key unit in the lower part of the Yezo Group (Iba and Sano, 2006, 2007), and provides one of the most important clues for understanding the early history of the Yezo Group.

In this study, we discovered the above-mentioned key unit from the basal part of the Yezo Group in the Horokanai area, which is located between the Yubari–Ashibetsu and

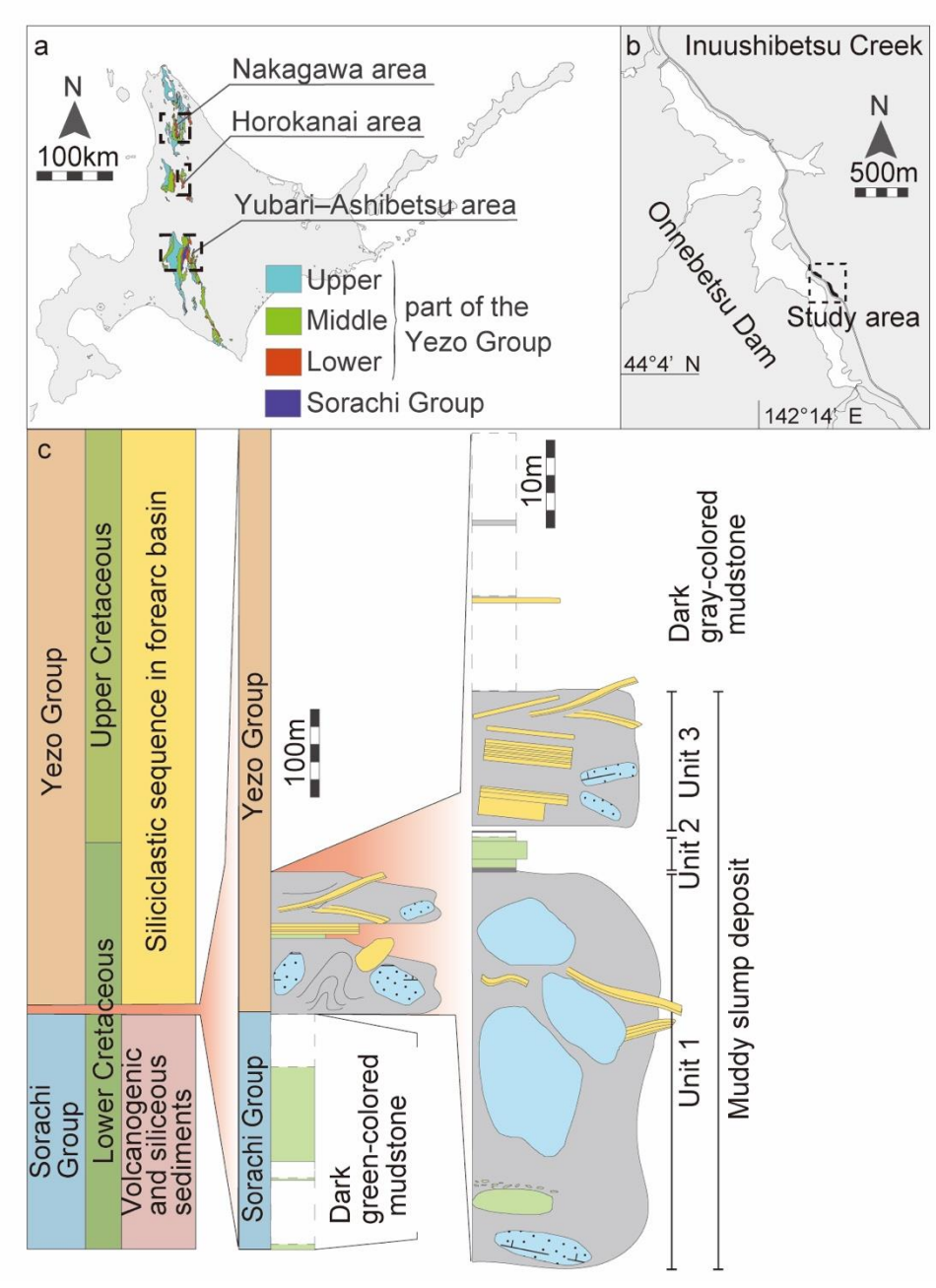

Fig. 1 Locality map and columnar section of the lowest part of the Yezo Group in the Horokanai area, Hokkaido, northern Japan. a–b: Locality map. c: Lithostratigraphic columnar section of the study route.

Nakagwa areas. Biostratigraphic study of the Lower Cretaceous sequence has not been established there. In this study, *Mesorbitolina parva* (larger foraminifer) from the calcareous sandstone olistolith in the lowest part of the Yezo Group are described and discussed its age and regional correlation, and the early history of the Yezo Group are reconstructed.

GEOLOGICAL SETTINGS

The Jurasso–Paleogene Sorachi and Yezo groups, widely-distributed in Hokkaido Island of northern Japan, is composed of ophiolite-based large fore-arc basin sequence (Ueda, 2016). This continuous sequence is composed of a piece of basaltic oceanic crust (Horokanai Ophiolite and the lower part of the Sorachi Group), volcanogenic and siliceous sediments (the upper part of the Sorachi Group), and thick, terrigenous siliciclastic sediments (the Yezo Group) in ascending order (Kiminami et al., 1992; Takashima et al., 2004 and 2017). The fore-arc basin is a part of an extensive (up to 1400 km) and continuous basin along the eastern margin of the Eurasia, from offshore of North Honshu Island of Japan in the South to Sakhalin Island, Russian Far East in the North (e.g., Ando, 2003; Takashima et al., 2004; Ueda, 2016).

In the Horokanai area, which is located between the Nakagawa and Yubari–Ashibetsu areas (Fig. 1-a), the Horokanai ophiolite, the Sorachi group, and the lower part of the Yezo Group, in ascending order, are distributed (Kiminami et al., 1992). The boundary between the Sorachi and Yezo groups has been considered as the unconformable (Igi et al., 1958). Kiminami et al. (1992) reported the conformable

boundary (forest road along the Rokusenzawa Creek) and the slump deposit on the base of the Yezo Group (eastern road along the Inuushibetsu Creek) around the Onnebetsu dam site. The study argued that the boundary between the Sorachi and Yezo Groups are conformable. The radiolarian assemblage from uppermost part of the Sorachi Group can be correlated with *Archaeodictyomitra laclimula* Zone and *Cecrops septemporatus* Zone, which is assigned to the upper Valanginian to Barremian (Kito, 1987; Kiminami et al., 1992; Taketani and Kanie, 1992). In contrast, age-diagnostic fossils are absent in the lower part of the Yezo Group.

RESULTS

1. Lithofacies and geological age of the lowest part of the Yezo Group in the Horokanai area

The upper part of the Sorachi Group and the lowest part of the Yezo Group are exposed along in the Onnebetsu dam site of the Inuushibetsu Creek (Fig. 1-b: 44°4’24.27, 142°14’29.83). The upper part of the Sorachi Group is composed of well-laminated dark green-colored claystone without bioturbation, and its thickness is about 165 m.

Lithofacies of the lowest part of the Yezo Group, which is about 130 m in thickness, can be divided into three units. Unit 1 consists of muddy slump deposits including large calcareous sandstone and bedded sandstone blocks, and dark green-colored mudstone blocks (Figs. 1–2). The matrix of slump deposit is dark gray-colored siltstone. The calcareous sandstone blocks are composed of massive fine-grained sandstone with

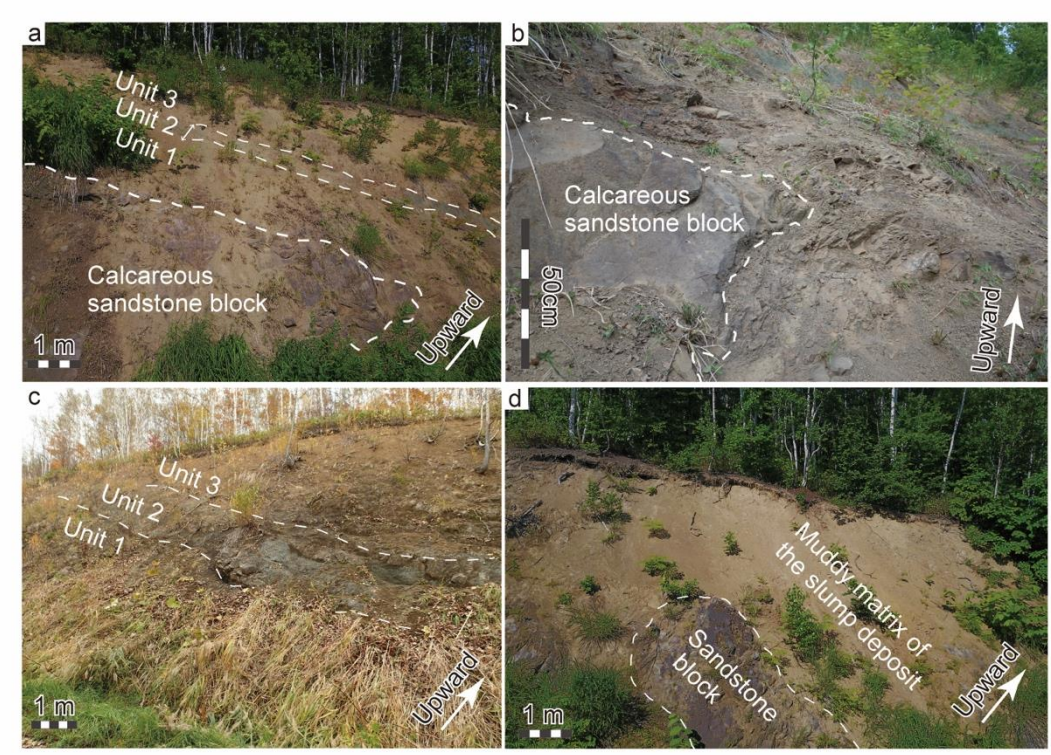

Fig. 2 Lithofacies of the lowerst part of the Yezo Group in the Horokani area. a: Calcareous sandstone block in the Unit 1. b: The mode of occurrence of the calcareous sandstone block. c: Well-stratified green-colored claystone and sandstone in the Unit 2. d: Sandstone block and muddy matrix of the slump deposit in the Unit 3.

carbonate mud matrix. Their maximum diameter is over 10 m. Well-rounded chert pebbles, limestone intraclasts, and ooids are abundant in the calcareous sandstone blocks (Fig. 3). Typical Cretaceous tropical shallow marine fauna (Masse, 1992a, b), such as orbitolinid foraminifers and calcareous red algae, occurs in the blocks (Figs. 3–4). An age diagnostic orbitolinid species, *Mesorbitolina parva* (Upper Aptian–Lower Albian), is identified in the calcareous sandstone block (Fig. 4).

Unit 2 is well-stratified green-colored claystone and sandstone, which is similar to the lithofacies of the uppermost Sorachi Group (Kawaguchi, 1997; Kiminami, et al., 1992) (Figs. 2–3). Unit 3 is composed of alternating beds of fine-grained sandstone and dark gray-colored mudstone and intercalates three muddy slump deposits (Figs. 2–3). These slump deposits also contain calcareous sandstone blocks and folded sandstone layers.

Systematic Paleontology

Family Orbitolinidae MARTIN 1890

Genus *Mesorbitolina* SCHROEDER 1962

Mesorbitolina parva DOUGLASS 1960

Fig. 4

Type specimen: Holotype P5494 deposited in the U.S. National Museum of the Natural History from the Peak Formation, Lower Albian, Grant County, New Mexico, USA.

Material: One axially sectioned specimen recovered from a shallow marine

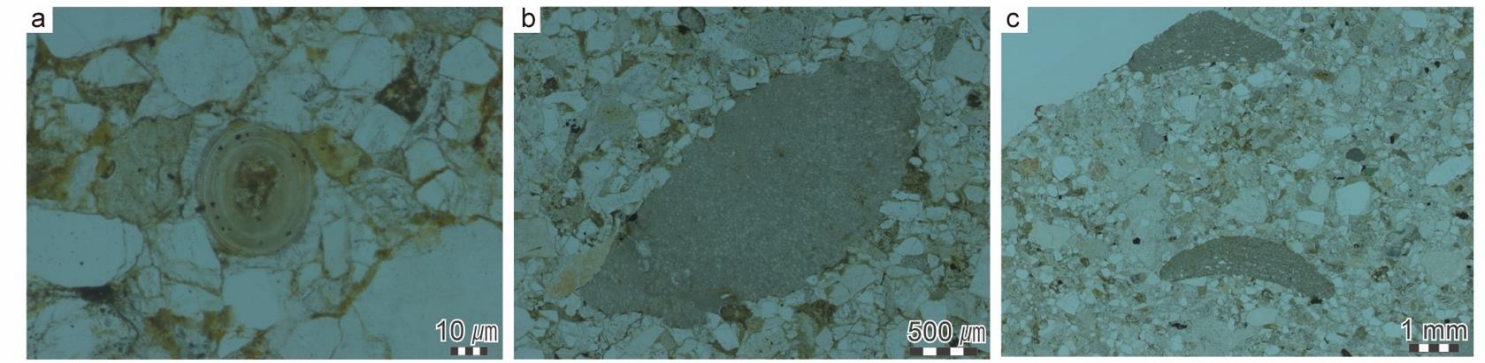

Fig. 3 Photomicrographs of calcareous sandstone olistoliths. a: ooid, b: calcareous algae, c: orbitolinid foraminifers.

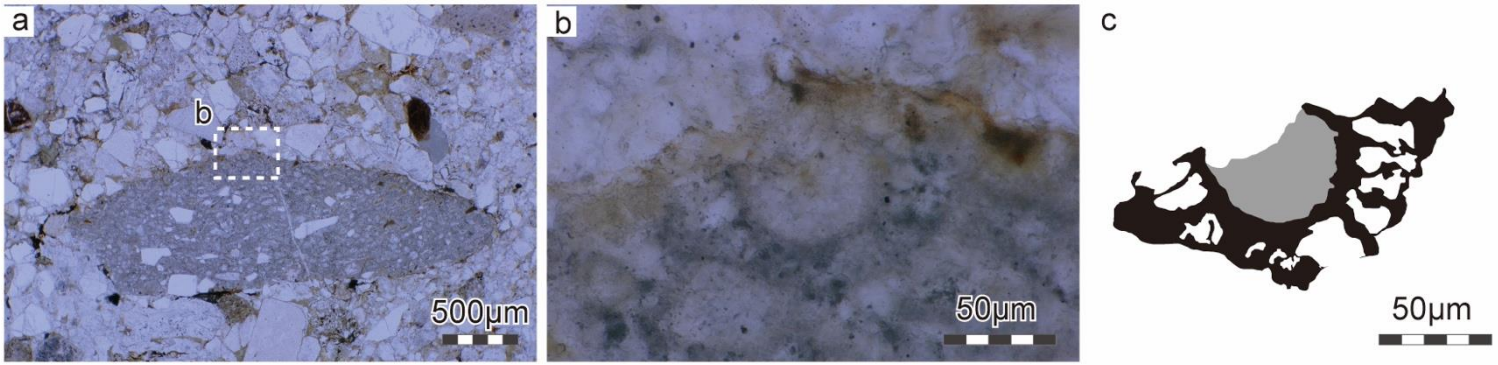

Fig. 4 Photomicrographs and drawing of *Mesorbitolina parva*. a: General view. b–c: Detail of the embryonic apparatus.

calcareous sandstone block from the lowest part of the Yezo Group in the Horokanai area, northern Hokkaido (Fig. 1).

Description: The test is small, low conical, the base of which is slightly convex (Fig. 4) . An embryonic apparatus is centrally situated in the tip of the test, and consists of a protoconch with a small subembryonic zone. The diameter of embryonic apparatus is 156.9 μm. The protoconch is globular, not ellipsoidal. The diameter of protoconch is 53.7 μm. The deuteroconch is eroded. The subembryonic zone is simple and divided by a small number of regular septa making a reticulum. The lower surface of the subembryonic zone is rounded.

Distribution: This species is widely distributed in circum-Mediterranean region, Middle East, India, Tibet, Pacific guyots, the Caribbean region, the southern part of the Western Interior Seaway, and Japan. In Japan, only three localities are previously known (Iba et al., 2011); limestone olistoliths of the Shuparogawa Formation (Upper Aptian) in the Yubari–Ashibetsu area, central Hokkaido, limestone pebbles of the lowest part of the Yezo Group (Upper Aptian) in the Nakagawa area, northern Hokkaido, and the Hiraiga Formation of the Miyako Group (Upper Aptian–Lower Albian) in Rikuchu, northern Honshu Island.

Age: Late Aptian–Early Albian

DISCUSSION

1. Age of lowest part of the Yezo Group in the Horokanai area

Slump deposits in the lowest part of the Yezo Group in the study area have been known previously (Kiminami et al., 1992). The occurrences of the calcareous sandstone olistoliths are, however, newly discovered in this study. Well-rounded pebbles of chert, carbonate intraclasts, ooids, and typical Cretaceous shallow-marine carbonate platform biota (e.g., orbitolinids and calcareous red algae) are abundant in the olistoliths (Fig. 3). It is indicated that these calcareous sediments originally deposited in a shallow-marine shelf, and were later transported into a deeper part of the basin by an olistostrome.

The Orbitolinidae is a larger benthic foraminiferal family, which was most diversified during the period of the Barremian to Cenomanian. Its species had short biochronological ranges and provide reliable chronostratigraphic information (Schroeder, et al., 2010). Orbitolinid species in the calcareous sandstone olithtolith is identified as *Mesorbitlolina parva*, which indicate the Late Aptian to Early Albian age (Schroeder et al., 2010; Iba et al., 2011). Now it is revealed that the lowest part of the Yezo Group in the study area is precisely assigned to the Upper Aptian or younger in age. Whereas, the Unit Ma of the base of the middle part of the Yezo Group in the Horokanai area is correlated to the Maruyama Formation (Igi et al., 1958; Takashima et al., 2004). The formation is the KY-2 of the widely traceable key units of the Yezo Group (Takashima et al., 2004) and can be traced from southern to northern Hokkaido. Its depositional age is considered as the Late Albian (Obradovich et al., 2002; Takashima et al., 2004). From these ages mentioned above, the lowermost part of the

Yezo Group is considered as the Late Aptian–Late Albian. The age of the lowermost part of the Yezo Group has been inferred from the upper Valanginian to Barremian of the uppermost part of the Sorachi Group by the radiolarian assemblage which can be correlated with *Archaeodictyomitra laclimula* Zone and *Cecrops septemporatus* Zone (Kiminami et al., 1992). This study is the first report of the geological age from the lowest Yezo Group in the Horokanai area which is much younger than previously thought.

Most remarkable tectonic change within the entire sequence of the Jurasso–Paleogene Sorachi and Yezo groups is recognized at the group boundary. Based on the differences geochemical composition of clastics between the uppermost Sorachi and the lowest Yezo groups, Kiminami et al. (1992) discussed the remarkable shift of the tectonic setting of the hinterland from an oceanic island arc to the active continental margin along the Eurasia continent at the boundary. Deposition of olistostrome at the basal part of the Yezo Group is probably influenced by tectonic instability during the period of such major shift of tectonic setting. It should be noted that deposition of the Yezo Group in this area started with catastrophic deposition, and subsequently siliciclastic sediments continuously deposited until the Paleogene.

2. Regional correlation and early history of the Yezo Group

2-1. Olistostrome and gravity flow deposits in the lowest part of the Yezo Group

Olistostrome and gravity flow deposits, which contain shallow-marine carbonates as olistoliths and/or pebbles, are well known from the lower part of the Yezo Group in

central (Yubari–Ashibetsu area) and northern Hokkaido (Nakagawa area) (Sano, 1995; Takashima et al., 2004; Iba et al., 2005; Iba and Sano, 2006) (Figs. 1 and 5). They have been considered as one of the most important key units in the Yezo Group (Iba and Sano, 2006), and the olistostrome reported herein can be correlated with this key unit.

In the Yubari–Ashibetsu area, the Kirigishiyama Olistostrome Member of the Shuparogawa Formation represents an olistostrome bed with many huge shallow-marine carbonate olistoliths, which contain carbonate platform biota such as orbitolinids, rudists, and calcareous algae (Iba and Sano, 2007). Largest carbonate olistolith represents slab-like shape (about 60 m in thickness and over 3 km in length) (Takashima et al., 2004). Iba and Sano (2006, 2007) identified specimens of *Mesorbitolina parva* (Late Aptian–Early Albian) from the carbonate olithtoliths. Ando and Kakegawa (2007) supposed that the Aptian–Albian boundary existed in the lower part of the Kasamori-zawa Member of the Shuparogawa Formation that directory overlies the Kirigishiyama Olistostorome Member. Thus, the Kirigishiyama Olistostrome Member should be the Late Aptian in age. It can be concluded that calcareous sediments were deposited in shallow-marine environment in the Late Aptian, and transported into a deeper part of the basin as olistoliths within the Late Aptian (Iba and Sano, 2006, 2007).

Iba et al. (2005) and Iba and Sano (2006, 2007) correlated this olistostrome bed with gravity-flow deposit in the lowest part of the Yezo Group in the Nakagawa area, which is located about 200 km north from the Yubari–Ashibetsu area (Fig. 1). In the Nakagawa area, the conglomerate bed (17 m thick), which interpreted to be gravity-flow deposit, is

intercalated in the lowest part of the Yezo Group (Iba et al., 2005; Iba and Sano, 2007). It contains abundant shallow-marine carbonate pebbles (Iba et al., 2005). Based on multiple biostratigraphic data, such as *Mesorbitolina parva* from the limestone pebble and an ammonoid about 100 m from the horizon above the orbitolinid-bearing bed, Iba and Sano (2006, 2007) concluded that calcareous sediment deposited in shallow-marine environment in the Late Aptian, and was later transported as pebbles by high-concentrated gravity flow into the deeper part of the basin also in the Late Aptian. Based on similarities of lithofacies, stratigraphic position, occurrence of calcareous olistoliths and its fossil assemblages, and geological age, olistostrome bed in study area seems to be correlated with the above-mentioned key unit in the Yubari–Ashibetsu and Nakagawa areas (Fig. 5).

2-2. Age and correlation of the uppermost part of the Sorachi Group

An important radiolarian datum plane: the last occurrence of *Cecrops septemporatus,* which is correlated to the Early Barremian time, was identified in the middle-to-upper part of the Shirikishimanaigawa Formation, the youngest formation of the Sorachi Group in the Yubari–Ashibetsu area (Takashima et al., 2001, 2006), and uppermost part of the Sorachi Group (Pechikunnai Formation) in the Nakagawa area (Fig. 5). In the Horokanai area, Kiminami et al (1992) also reported radiolarian assemblages from the uppermost part of the Sorachi Group and pointed out the similarity with *Cecrops septemporatus* Zone. Thus, the upper part of the Sorachi Group of three areas is almost synchronous based on radiolarian biostratigraphy (Fig. 5).

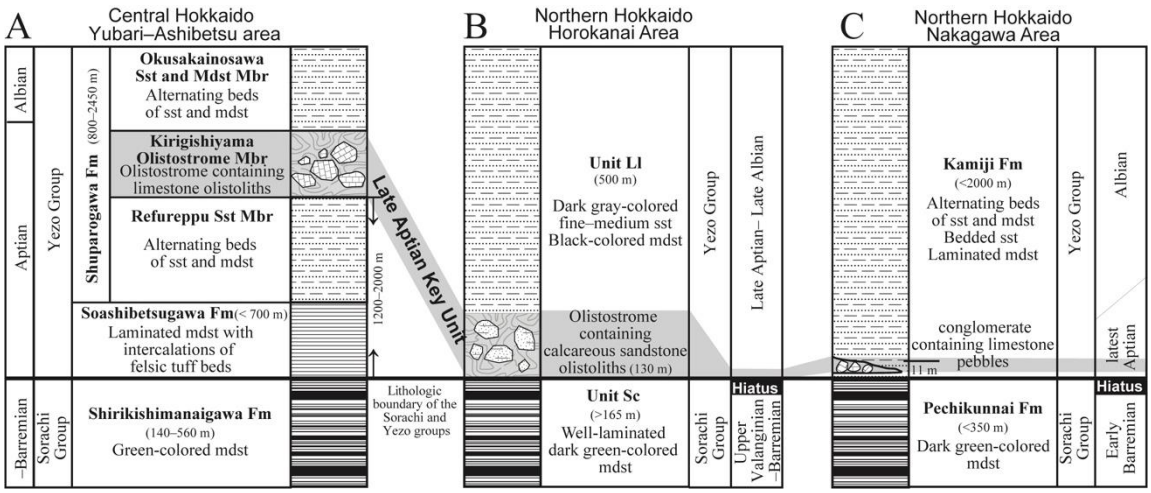

Fig. 5 Comparison of the lowest part of the Yezo Group between central to northern Hokkaido by the Late Aptian key unit (modified from the Iba and Sano, 2006). Geological data are based on Takashima et al. (2004, 2006) for the Yubari–Ashibetsu area, Igi et al. (1958), Kiminami et al. (1992) and this study for the Horokanai area, and Kawaguchi (1997), Iba et al. (2005) and this study (in Chapter 1 and 2) for the Nakagawa area.

2-3. Implication for early history of the Yezo Group

The Kirigishiyama Olistostrome Member is interacted at 1200 to 2000 m above the boundary between the Sorachi and Yezo groups (Takashima et al., 2004). On the other hand, in the Nakagawa and Horokanai areas, the conglomeratic gravity flow deposits and olistostrome is just above the boundary between the Sorachi and the Yezo groups (Fig. 5). In the Nakagawa and Horokanai areas, a hiatus, possible ranging from the Barremian to Early Aptian is supposed to occur around at group boundary. Such a huge hiatus is not recognized in the Yubari–Ashibetsu area (Fig. 5).

In summary, the upper part of the Sorachi Group in the three areas is similar in lithology and the depositional age. The early depositional history of the Yezo Group was, however, significantly different between the Yubari–Ashibetsu (central Hokkaido) and Horokanai–Nakagawa (northern Hokkaido) areas, although they were located within the same Yezo fore-arc basin. Thus the differentiation of regional sedimentary sub-basins within the Yezo fore-arc basin during the Aptian is inferred, when the deposition of the Yezo Group started. The deposition of the Yezo Group was probably first started in Central Hokkaido in the Late Barremian–Early Aptian, and then expanded to northern Hokkaido in the Late Aptian. In northern Hokkaido, the fore-arc basin sequence started with catastrophic deposition, such as olistostrome or conglomeratic gravity-flow deposits, which occurred simultaneously with, and possibly caused by tectonic instability along the eastern margin of the Eurasia (Fig. 5).

REFERENCES CITED

Ando, A., Kakegawa, T., Takashima, R., and Saito, T., 2002, New perspective on Aptian carbon isotope stratigraphy: Data from δ^{13}C records of terrestrial organic matter: Geology, v. 30, p. 227–230, doi: 10.1130/0091-7613(2002)030<0227:NPOACI>2.0.CO;2.

Ando, A., and Kakegawa, T., 2007, Carbon isotope records of terrestrial organic matter and occurrence of planktonic foraminifera from the Albian stage of Hokkaido, Japan: Ocean−atmosphere δ13C trends and chronostratigraphic implications: Palaios, v. 22, p. 417–432, doi:10.2110/palo.2005.p05‐104r.

Ando, H., 2003, Stratigraphic correlation of Upper Cretaceous to Paleocene forearc basin sediments in Northeast Japan: cyclic sedimentation and basin evolution: Journal of Asian Earth Sciences, v. 21, p. 921–935, doi: 10.1016/S1367-9120(02)00111-6.

Douglass, R.C., 1960, The foraminiferal genus *Orbitolina* in North America: Geological Survey Professional Paper, v. 333, p. 1–52, doi: 10.3133/pp333.

Hasegawa, T., 1997, Cenomanian-Turonian carbon isotope events recorded terrestrial organic matter from northern Japan: Palaeogeography, Palaeoclimatology, Palaeoecology, v. 130, p. 251–273, doi: 10.1016/S0031-0182(96)00129-0.

Hirano, H., Matsumoto, T., and Tanabe, K., 1977, Mid-Cretaceous stratigraphy of the Oyubari area, central Hokkaido: Palaeontological Society of Japan Special Papers, v. 21, p. 1–10.

Iba, Y., and Sano, S., 2006, *Mesorbitolina* (Cretaceous larger foraminifera) from the

Yezo Group in Hokkaido, Japan and its stratigraphic and paleobiogeographic significance: Proceedings of the Japan Academy, Series B, v. 82, p. 216–223, doi: 10.2183/pjab.82.216.

Iba, Y., and Sano, S., 2007, Mid-Cretaceous step-wise demise of the carbonate platform biota in the Northwest Pacific and establishment of the North Pacific biotic province: Palaeogeography, Palaeoclimatology, Palaeoecology, v. 245, p. 462–482, doi: 10.1016/j.palaeo.2006.09.008.

Iba, Y., Taki, S., Yoshida, K., and Hikida, Y., 2005, *Orbitolina*-bearing limestone pebbles from the lowermost part of the Lower Yezo Group (Lower Cretaceous) in the Nakagawa area, northern Hokkaido, Japan, and its significance: Journal of the Geological Society of Japan, v. 111, p. 67–73, doi: 10.5575/geosoc.111.67.

Iba, Y., Sano, S., and Miura, T. 2011, Orbitolinid foraminifers in the Northwest Pacific: their taxonomy and stratigraphy: Micropaleontology, v. 57, p. 163–171.

Igi, S., Tanaka, K., Hata, M., and Sato, H., 1958, Explanatory text of the geological map of Japan 'Horokanai' (scale1:50000): Geological Survey of Hokkaido, 55p.

Kawaguchi, M., 1997, Lower Cretaceous strata around the River Onisashi, northern Hokkaido, *in* Kawamura, M., Oka, T. and Kondo, T., eds., Commemorative volume for Professor Makoto Kato: Hokkaido University, p. 121–134.

Kiminami, K., Komatsu, M., and Kawabata K., 1992, Composition of clastics of the Sorachi Group and the Lower Yezo Group in the Inushibetsu-gawa area, Hokkaido, Japan, and their significance: Memoir of the Geological Society of

Japan, v. 38, p. 1–11.

Kito, N., 1987, Stratigraphic relation between greenstones and clastic sedimentary rocks in the Kamuikotan Belt, Hokkaido, Japan: Journal of the Geological Society of Japan, v. 93, p. 21–55, doi: 10.5575/geosoc.93.21.

Martin, K., 1889, Untersuchungen über den Bau von *Orbitolina* (Patellina Auct.) von Borneo: Sammlungen des Geologischen ReichsMuseums, Leiden, Series 14, p. 209–231.

Masse, J.P., 1992a, Lower Cretaceous Mesogean benthic ecosystems: palaeoecologic aspects and palaeobiogeographic implications: Palaeogeography, Palaeoclimatology, Palaeoecology, v. 91, p. 331–345, doi: 10.1016/0031-0182(92)90075-G.

Masse, J.P., 1992b, The Lower Cretaceous Mesogee: A state of the art, *in* Kollmann, H.A. and Zapfe, H. eds., New Aspect on Tethyan Cretaceous Fossil Assemblages: Schriftenreiche der Erdwissenschaftlichen Kommissionen der Österreichischen Akademie der Wissenschaften, p. 15–33, doi: 10.1007/978-3-7091-5644-5_2.

Matsumoto, T., 1942, Fundamentals in the Cretaceous stratigraphy of Japan, Part I: Memoirs of Faculty of Science, Kyushu Imperial University, Series D, v. 1, p. 129–280.

Matsumoto, T., 1943, Fundamentals in the Cretaceous stratigraphy of Japan, Parts II–III: Memoirs of Faculty of Science, Kyushu Imperial University, Series D, v. 2, p. 98–237.

Obradovich, J.D., Matsumoto, T., Nishida, T., and Inoue, Y., 2002, Integrated biostratigraphic and radiometric study on the Lower Cenomanian (Cretaceous) of Hokkaido, Japan: Proceedings of the Japan Academy, Series B, v. 78, p. 149–153, doi: 10.2183/pjab.78.149.

Sano, S., 1995, Lithofacies and biofacies of Early Cretaceous rudist- bearing carbonate sediments in northeastern Japan: Sedimentary Geology, v. 99, p. 179–189, doi: 10.1016/0037-0738(95)00043-8.

Schroeder, R., 1962, Orbitolinen des Cenomans Südwesteuropas: Paläontologische Zeitschrift, v. 3, p. 171–202.

Schroeder, R., van Buchem, F.S.P., Cherchi, A., Baghbani, D., Vincent, B., Immenhauser A., and Granier B., 2010, Revised orbitolinid biostratigraphic zonation for the Barremian – Aptian of the eastern Arabian Plate and implications for regional stratigraphic correlations, *in* van Buchem, F.S.P., Al-Husseini, M.I., Maurer F., and Droste H.J., eds., Barremian − Aptian stratigraphy and hydrocarbon habitat of the eastern Arabian Plate: GeoArabia Special Publication 4, Gulf PetroLink, Bahrain, v. 1, p. 49–96.

Shigeta Y., and Maeda H., 2005, Yezo Group research in Sakhalin‐a historical review, *in* Shigeta, Y. and Maeda H., eds., The Cretaceous System in the Makarov area, southern Sakhalin, Russian Far East: National Science Museum Monographs 31, p. 1–24.

Takashima, R., Yoshida, T., and Nishi, H., 2001, Stratigraphy and sedimentary environment of the Sorachi and Yezo groups in the Yubari–Ashibetsu area,

Hokkaido, Japan: Journal of the Geological Society of Japan, v. 107, p. 1–20, doi: 10.5575/geosoc.107.359.

Takashima, R., Nishi, H., and Yoshida, T., 2006, Late Jurassic-Early Cretaceous intra-arc sedimentation and volcanism linked to plate motion change in northern Japan: Geological Magazine, v. 143, p. 753–770, doi:10.1017/S0016756806 00255X.

Takashima, R., Kawabe, F., Nishi, H., Moriya, K., Wani, R., and Ando, H., 2004, Geology and stratigraphy of forearc basin sediments in Hokkaido, Japan: Cretaceous environmental events on the north-west Pacific margin: Cretaceous Research, v. 25, p. 365–390, doi: 10.1016/j.cretres.2004.02.004.

Takashima, R., Nishi, H., and Yoshida, T., 2017, Stratigraphic and petrological in sights into the Late Jurassic–Early Cretaceous tectonic framework of the Northwest Pacific margin. Dynamics of arc migration and amalgamation-ar chitectural examples from the NW Pacific margin: InTech., doi: 10.5772/in techopen.68289.

Taketani, Y., and Kanie, Y., 1992, Radiolarian age of the Lower Yezo Group and the upper part of the Sorachi Group in Hokkaido, *in* Ishizaki, K., and Saito, T., eds., Centenary of Japanese Micropaleontology: Terra Scientific Publishing Company, Tokyo, p. 365−373.

Toshimitsu, S., 1995, Towards an integrated mega-, micro-and magnetostratigraphy of the Upper Cretaceous in Japan: Journal of the Geological Society of Japan, v. 101, p. 19–29, doi: 10.5575/geosoc.101.19.

Toshimitsu, S., Hirano, H., Matsumoto, T., and Takahashi, K., 2003, Database and species diversity of Japanese Cretaceous ammonoids: Journal of Asian Earth Sciences, v. 21, p. 887–893, doi: 10.1016/S1367-9120(02)00074-3.

Ueda, H., 2016, Hokkaido, *in* Moreno, T., Wallis, S., Kojima, T., and Gibbons, W., eds., The Geology of Japan: Geological Society, London, p. 201–221.

Chapter 4

Shallow-marine carbonate platform collapsed alive in the latest Aptian: a factor in a major extinction event in the Northwest Pacific coast?

ABSTRACT

In the mid-Cretaceous, the extreme warmth created by superplume activities caused the poleward expansion of reef lines. The carbonate platform had developed linearly along the Asian continental margin from central Kyushu Island in Japan to Sakhalin Islands and it was the largest in Cretceous North Pacific.

An olistostrome bed has been known from the Upper Aptian fore-arc basin deposit in Hokkaido, northern Japan. This olistostrome contains many huge carbonate olistoliths. Its detail of sedimentary process has been, however, uncleared due to the difficulty of age determination. Here we reveal that the carbonate platform collapsed when reefal biota still alive, and its transportation directly into the deeper part of the ocean by geochronological and sedimentological methods. Such large-scale living carbonate platform collapse has not been recognized both in the geological record and modern analogue. This event coincides with an enigmatic the latest Aptian extinction event of carbonate platform biota in the Northwest Pacific, and can be considered as one of the possible factors, as physical habitat loss in coast to shallow-marine area.

INTRODUCTION

The Yezo Group, which is 8000 m-thick Cretaceous fore-arc basin sequence, extends from southern Hokkaido Island to Sakhalin Island (Fig. 1). The lower part of the Yezo Group in central Hokkaido, an olistostrome bed containing huge shallow-marine carbonate olistoliths in a muddy matrix has been previously well known (Yabe, 1901; Takashima et al., 1997, 2004) (Figs. 1–2). The largest carbonate olistoliths extend 60 m in thick and 3 km for length (Takashima et al., 2004) (Fig. 3). A rimmed shelf developed along the eastern margin of Eurasia has been reconstructed by bio- and litho-facies of the carbonate olistoliths (Sano, 1995), and is considered being the largest shallow-marine carbonate platform in the Cretaceous of North Pacific. An olistostrome bed is also regarded as the largest catastrophic event and an important key unit throughout the Yezo Group (see Chapter 3). However, their sedimentary process has been uncleared. This is due to the limitation of age-diagnostic fossil occurrence from olistoliths itself and also from strata just above the olistostrome bed indicating the age of the carbonate platform collapse and its mass transportation, respectively.

The purpose of this study is that reconstruct the entire sedimentary process including shallow-marine carbonate sedimentation, and its collapse and subsequent mass transportation into the deep sea by multiple geochronological evidence and facies analysis with special attention to soft-sediment deformation structures (SDSS) of carbonate. This study is divided into three steps; (1) determining age of carbonate platform in shallow-marine environments by Sr isotope stratigraphy, (2) and depositional age of olistostrome by U-Pb aging, (3) and confirm synchrony between carbonate sedimentation at shallow-marine and its collapse and subsequent reworking processes by multiple chronological data and SDSS.

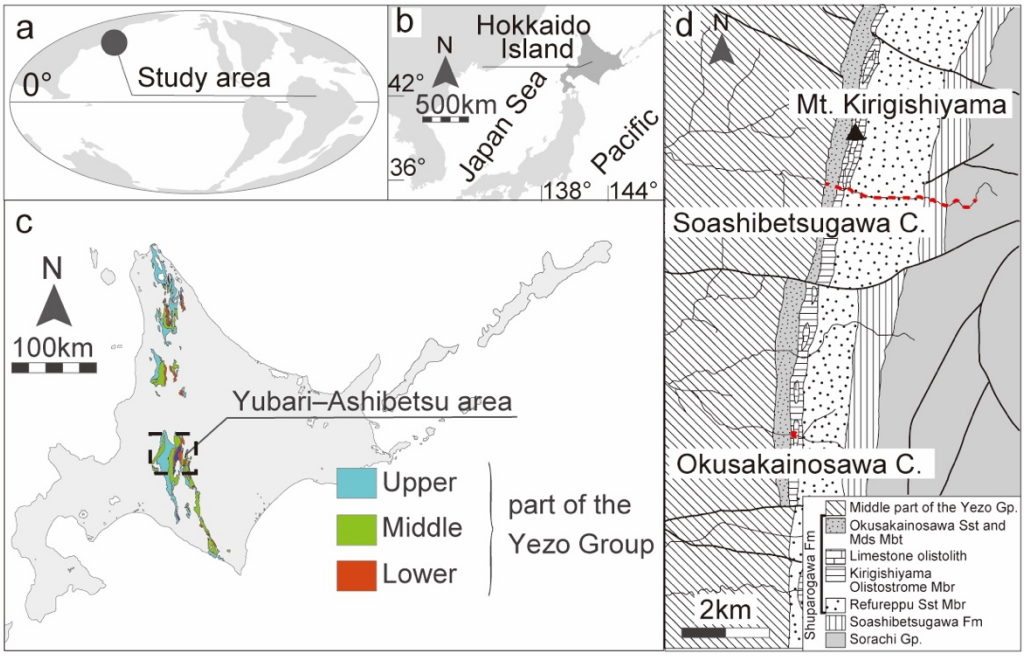

Fig. 1 The map of the Yubari-Ashibetsu area, central Hokkaido. d: Study routes. Red dot lines show the study route in the Soashibetsugawa Creek and the Okusakainosawa Creek. modified from Iba and Sano (2006).

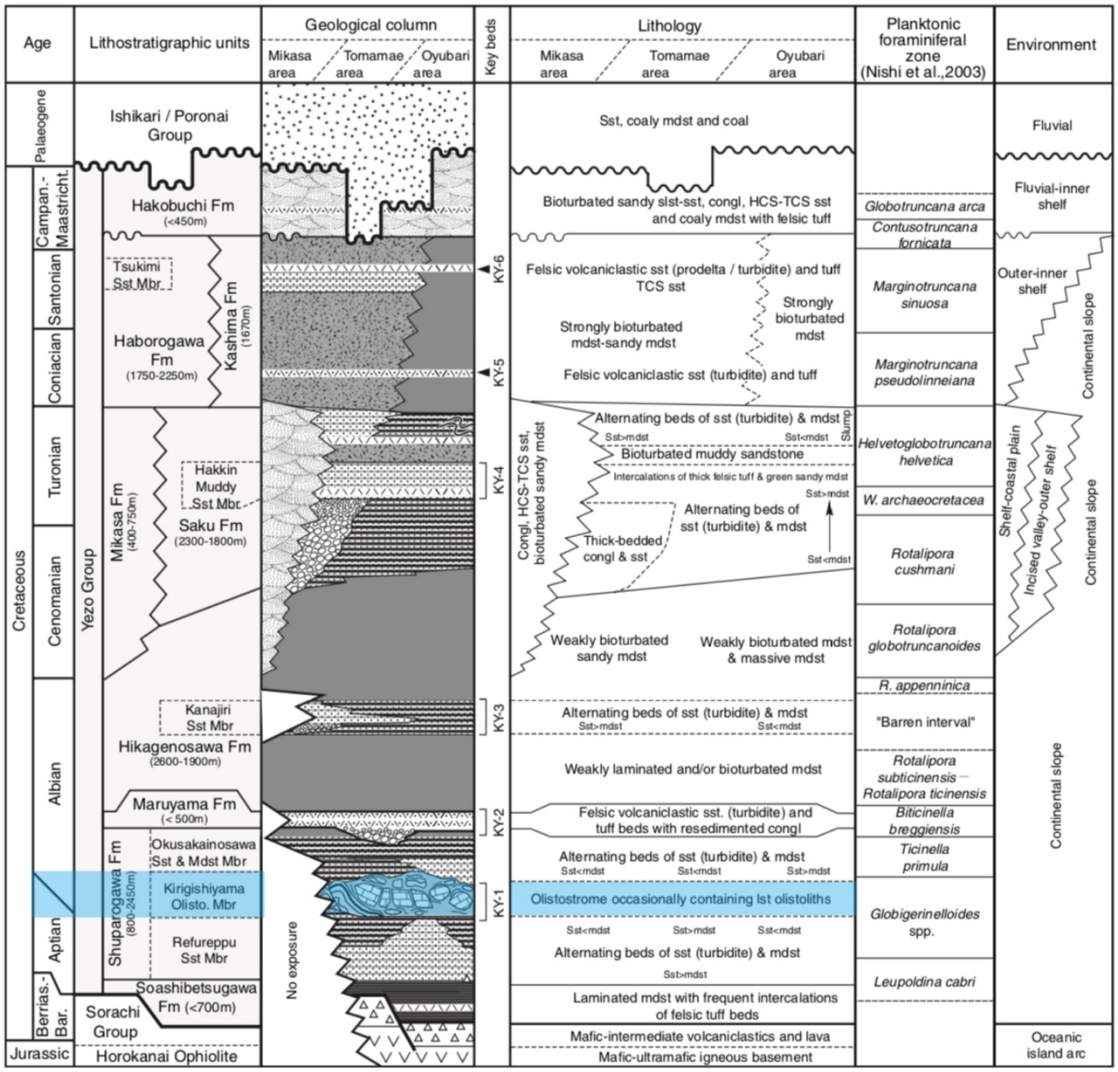

Fig. 2 Integrated columnar section of the Yezo Group in central Hokkaido. Modified from Takashima et al. (2004).

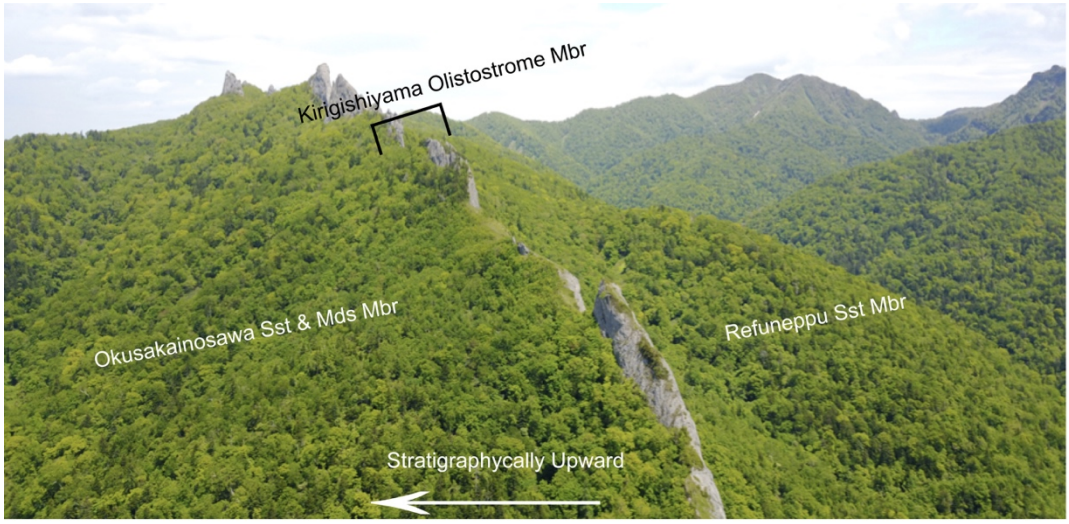

Fig. 3 The outcrop photo of the largest carbonate olistoliths in the Mt. Kirigishiyama.

GEOLOGICAL SETTINGS

Many carbonate olistoliths are intercalated in the Kirigishiyama Olistostrome Member of the Shuparogawa Formation, in the lower part of the Yezo Group in central Hokkaido (Takashima et al., 2004; Figs. 1–2). Abundant carbonate platform biota, consisting of rudists (requieniids, a monopleurid, a radiolitid and others), a dasycladacean alga, orbitolinid, and miliolid foraminifers, a stromatoporoid and other sponges, hermatypic corals, and calcareous red algae, nerineacean gastropods occur in the carbonate olistoliths (e.g., Sano, 1995, 2000; Iba and Sano, 2007). Based on the spatial distribution of litho- and bio-facies of the olistoliths, a rimmed shelf was inferred to be the original carbonate depositional environment (Sano, 1995, 2000). This platform has been regarded as the largest carbonate platform in the Cretaceous North Pacific (Iba and Sano, 2007).

The Kirigishiyama Olistostrome Member is well-exposed in several sections in Central Hokkaido. Best two sections: the Okusakainosawa Creek (Fig. 1) and the Soashibetsugawa Creek (Fig. 1) in the Yubari-Ashibetsu area are selected in this study by following reasons (Fig. 2). *Insitu* ash-fall tuff layers are intercalated in the lowermost part of the Okusakainosawa Sandstone and Mudstone Member that overlies Kirigishiyama Olistostrome Member along the Soashibetsugawa Creek. It is suitable for determining the age of olistostrome event by U-Pb aging (Fig. 4). A carbonate olistoliths contains well-preserved rudistid bivalves (*Toucasia*) which available for Sr isotope analysis (Fig. 5). In the Okusakainosawa Creek, well-preserved and continuous carbonate sequence are well-preserved. The contact between the uppermost part of the Kirigishiyama Olistostrome Member and the Okusakainosawa Sandstone and Mudstone

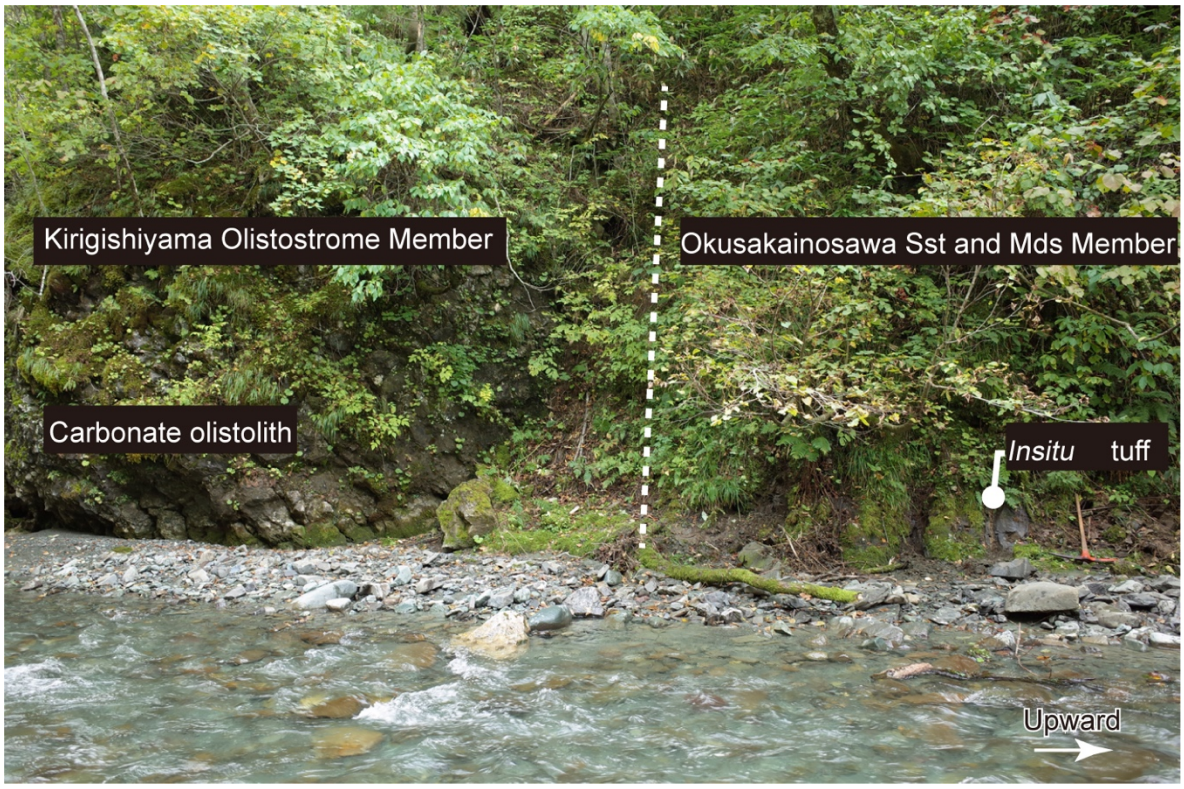

Fig. 4 The outcrop photo of the boundary of the Kirigishiyama Olistostrome Member, the Okusakainosawa Sandstone and Mudstone Member along the Soashibetsugawa Creek. The horizon of tuff for SHRIMP U-Pb dating is indicated.

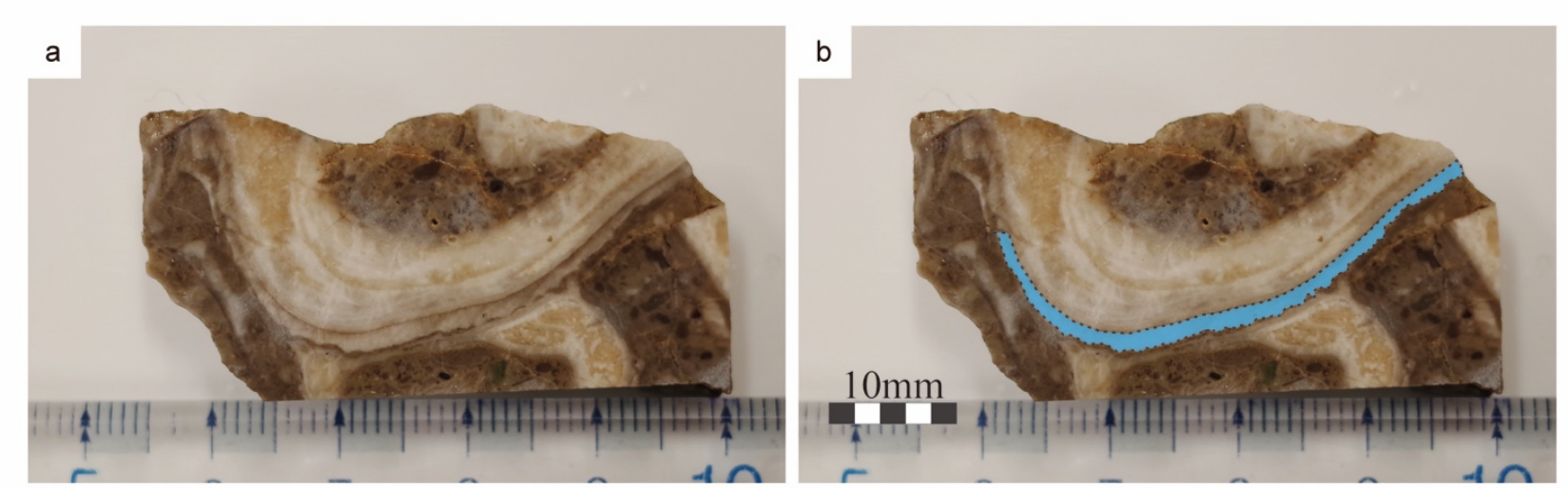

Fig.5 The rudist bivalve (*Toucasia*) sample for Strontium isotope stratigraphy. Blue indicate sampled shell layer.

Member are also well-exposed. Soft-sediment deformation structures of carbonate rocks can be observed in the Okusakainosawa Creek.

MATERIAL AND METHODS

1. Strontium isotope stratigraphy

The calcitic outer shells layers of *Toucasia*, a requieniid rudist bivalves from the Kirigishiyama Olistostrome Member from the Soashibetsugawa Creek were analyzed for strontium isotopes ($^{87}Sr/^{86}Sr$). One sample was drilled with tungsten instruments from a thick section of well-preserved outer shell layers of a requieniid rudist bivalves. Areas in which recrystallization or bio-erosion was visible were avoided.

Samples powders weighed in the range of 3.3–4.8 mg. They were decomposed with acetic acid and HNO_3, in Teflon vessels. Strontium was separated from the major elements using by passing the dissolved sample through cation exchange resin columns with an HCl carrier. Sr isotopic compositions were measured with a VG Sector thermal ionization mass spectrometer (a VG Sector 54-30) in Nagoya University. The trace elements (Ca, Na, Mg, Sr, Mn, and Fe) of the samples were analyzed for the evaluation of diagenesis by the ICP-MS (Agilent technologies 7700 series).

2. U-Pb data analysis

The depositional age of olistostrome unit is determined by U-Pb age data of zircon from *insitu* ash-fall tuff layer intercalated basal part of the Okusakainosawa Sandstone and Mudstone Member of the Shuparogawa Formation (0922-01 in Fig. 4).

Zircon grains were separated by crushing of rock samples, sieving, heavy mineral separation by heavy liquid and hand-picking under a binocular microscope. Zircons

were mounted for each sample in epoxy and polished to expose approximate centers of the zircon grains. Backscattered electron and cathodoluminescence images of individual zircon grains were obtained using a JEOL JSM-6610LV scanning electron microscope at the Korea Basic Science Institute (KBSI, Ochang, Republic of Korea), and were used for choosing analytical spots.

The zircons were analyzed for U-Pb isotopes using SHRIMP Ⅱ-e/MC (sensitive high- resolution ion microprobe) at the KBSI following standard procedures (Williams, 1998 and references therein). FC1 (1099.0 Ma; Paces and Miller, 1993) and SL13 (U = 238 ppm) standard zircon were used for calibrating of measured $^{206}Pb/^{238}U$ ratio and U concentrations, respectively. A primary negative ion oxygen beam (O_2^-) was 2–5 nA in intensity and ca. 25 μm in spot size. Each analysis consisted of five scans through mass measurements for each element. Common Pb contributions were corrected using the measured ^{207}Pb amount using the model common Pb composition (Stacey and Kramers, 1975). SQUID 2.50 and ISOPLOT programs (Ludwig, 2008, 2009) were used for reduction and plotting of the U-Pb data.

3. Facies analysis and visualization of soft-sediment deformation structures

The lithostratigraphic and sedimentological information were obtained from outcrops along two creeks (Fig. 2). Three-dimensional mode of occurrences and internal sedimentary structures of the carbonate block–sandstone interface was reconstructed by using a novel technique, named “Grinding Tomography” (see details for Chapter 1).

This method is based on automatic serial grinding and the subsequent serial full-color imaging. This technique using automatic serial grinding and imaging is recently applied for fossil materials, and its basic mechanism was well explained in

pioneering studies of Götz (2007) and Pascual-Cebrian et al (2013). Rock samples have been grinded down by an automatic machine, new surfaces have been photographed with a high-resolution digital camera (Canon 5Ds: 50.6-megapixel) in 40 μm intervals. Each photo was taken under white light. Total 1126 full-size images (Raw image formats) are archived as digital specimens in the Kyushu University Museum.

RESULTS

1. Geological age

1-1. Formation age of shallow-marine carbonate platform (Fig. 6 and Table. 1–2)

In splits of the samples which were analyzed for $^{87}Sr/^{86}Sr$ values, Mn concentrations are below 300 ppm, Sr/Mn is above 2 ppm (Table. 2). This composition range show typical for well-preserved low-Mg calcite (Jacobsen and Kaufman, 1999; Denison et al., 1994). The results tend to shift the low range of ratio. The spot of SR23 AK with the lowest effect of diagenesis is comparable to the LOWESS curve with 2σ error (Fig. 6 and Table 1–2). The estimated age of the rudist bivalves is 113.88−114.08 Ma, the uppermost Aptian.

1-2. Depositional age of the carbonate olistostrome bed (Fig. 7 and Table. 3)

Zircon grains from the tuff layer of 0922-01 range from about 30 to 50 μm in short axis and euhedral, subhedral in morphology. The weighted mean of $^{206}Pb/^{238}U$ zircon ages of a tuff layer (0922-01) is 114.58±0.59 Ma (n = 32, MSWD = 1.3), which can be correlated with the uppermost Aptian and *Acanthohoplites nolani* Zone (Ogg et al., 2016) (Fig. 7 and Table 1).

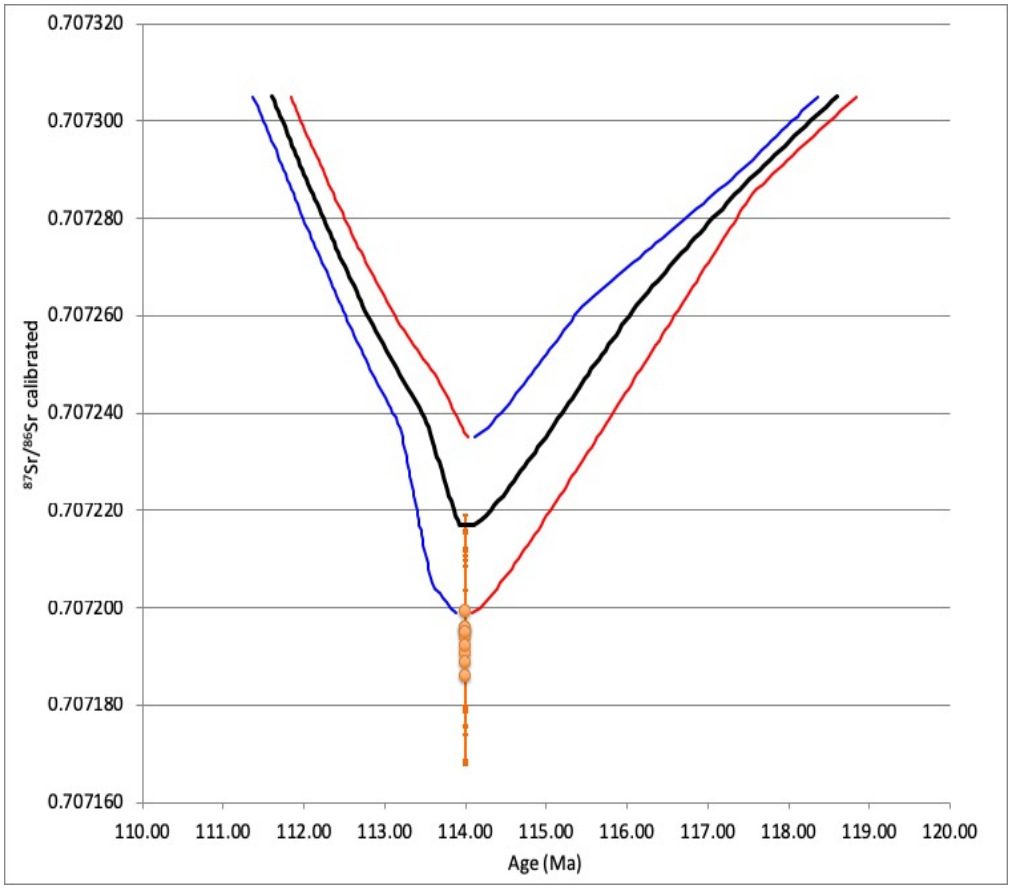

Fig. 6 The result of $^{87}Sr/^{86}Sr$. Dots and error bar: the analysis data with 2σ error. Black: LOWEES curve version 3 (McArther et al., 2001). Blue and Red: 95% Confidence limit line.

Table 1 The results of $^{87}Sr/^{86}Sr$.

Sample No.	$^{87}Sr/^{86}Sr$	Sd. Err.	**$^{87}Sr/^{86}Sr$ (calibrated)**
Sr21 AK	0.707197	0.000010	**0.707189**
Sr22 AK	0.707194	0.000009	**0.707186**
Sr23 AK	0.707208	0.000010	**0.707199**
Sr24 AK	0.707201	0.000009	**0.707192**
Sr25 AK	0.707203	0.000008	**0.707195**

Table 2 The results of trace elements analysis.

Sample No.	Na [ppm]	Mg [ppm]	Ca [%]	Ca [%]	Mn [ppm] ([Mn]>300 ppm)	Fe [ppm]
Sr21 AK	728.48	640.16	36.63	35.98	2.04	84.51
Sr22 AK	752.84	654.19	43.96	43.83	4.28	234.01
Sr23 AK	527.30	657.61	40.80	40.71	2.36	143.92
Sr24 AK	536.27	626.27	36.82	36.32	3.26	128.36
Sr25 AK	796.74	537.96	40.81	40.41	2.11	58.00

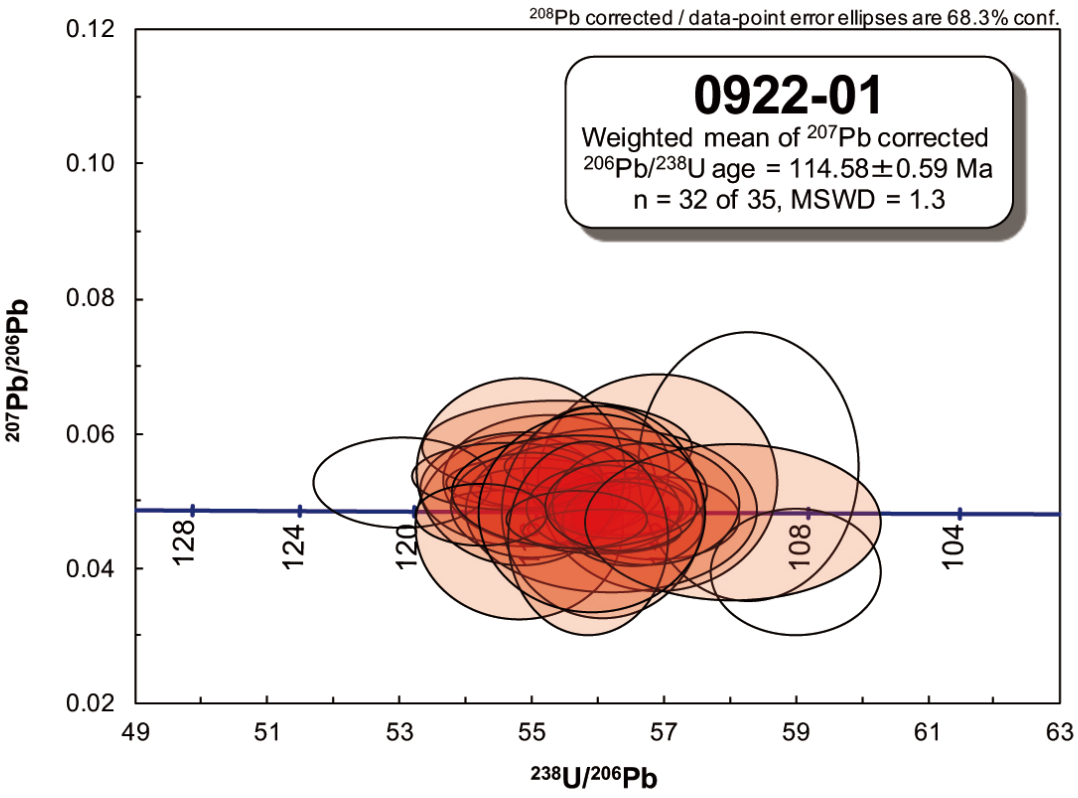

Fig. 7 U-Pb zircon ages by SHRIMP Ⅱ-e. Concordia plots of 0922-01.

Table 3 Summary of SHRIMP U-Pb isotopic compositions of zircon of 0922-01.

Spot number	Common ^{206}Pb (%)	U (ppm)	Th (ppm)	$^{206}Pb/^{238}U$ Age (Ma)*	$^{238}U/^{206}Pb^{\dagger}$	± (%)‡	$^{207}Pb/^{206}Pb^{\dagger}$	± (%)‡
0922-01_1.1	--	671	1127	117 ±2	54.8	1.9	0.0448	20.7
0922-01_2.1	0.05	539	778	115 ±2	55.3	1.9	0.0519	12.6
0922-01_3.1	0.02	390	374	116 ±1	54.9	1.5	0.0515	4.9
0922-01_4.1	0.06	464	761	112 ±2	56.9	2.1	0.0515	21.1
0922-01_5.1	0.20	304	357	114 ±2	55.4	2.4	0.0569	8.3
0922-01_6.1	0.01	1558	759	116 ±1	54.9	1.4	0.0489	2.2
0922-01_7.1	0.10	1546	2428	116 ±2	54.9	1.9	0.0506	11.3
0922-01_8.1	--	297	282	113 ±1	56.4	1.2	0.0484	6.5
0922-01_9.1	0.06	369	416	113 ±1	56.9	1.5	0.0462	9.0
0922-01_10.1	0.17	290	370	113 ±1	56.0	1.3	0.0537	11.7
0922-01_11.1	0.05	574	550	116 ±1	55.1	1.2	0.0507	4.0
0922-01_12.1	--	1189	1751	120 ±2	53.0	1.7	0.0515	8.8
0922-01_13.1	0.10	264	282	114 ±2	56.2	2.6	0.0474	17.3
0922-01_14.1	0.07	917	1170	116 ±2	54.6	1.8	0.0525	6.3
0922-01_15.1	0.12	672	664	114 ±1	55.6	1.2	0.0540	4.3
0922-01_16.1	0.07	1006	1494	116 ±1	55.0	1.5	0.0482	10.9
0922-01_17.1	0.07	593	885	109 ±1	58.3	1.9	0.0540	25.0
0922-01_18.1	--	339	411	116 ±2	54.8	1.9	0.0532	17.7
0922-01_19.1	0.11	559	950	114 ±1	56.1	1.8	0.0471	22.5
0922-01_20.1	0.01	526	642	113 ±1	56.5	1.2	0.0455	9.6
0922-01_21.1	0.20	526	649	114 ±1	56.1	1.4	0.0476	9.1
0922-01_22.1	0.31	506	520	114 ±1	56.3	1.2	0.0474	6.0
0922-01_23.1	--	329	267	115 ±1	56.1	1.4	0.0441	5.0
0922-01_24.1	0.12	499	664	110 ±1	59.0	1.4	0.0380	16.7
0922-01_25.1	0.02	474	657	113 ±1	56.7	1.6	0.0482	12.6
0922-01_26.1	0.02	326	406	114 ±2	55.7	2.3	0.0501	11.2
0922-01_27.1	0.12	2762	3658	118 ±1	54.2	1.2	0.0467	6.7
0922-01_28.1	0.06	154	124	115 ±1	55.7	1.3	0.0459	6.3
0922-01_29.1	0.23	146	141	113 ±1	56.3	1.3	0.0480	9.4
0922-01_30.1	--	345	432	115 ±1	55.8	1.4	0.0431	22.5
0922-01_31.1	5.89	497	643	111 ±2	58.0	2.5	0.0455	17.2
0922-01_32.1	--	401	635	114 ±2	55.9	2.0	0.0469	21.3

*Common Pb corrected by assuming 206Pb/238U-207Pb/235U age-concordance

†Common Pb corrected by assuming 206Pb/238U-208Pb/232Th age-concordance

‡All errors are percent, 1σ errors.

2. Soft-sediment deformation structures in carbonate olistoliths

The litho-facies of the uppermost part of the Kirigishiyama Olistostrome Member and the lowermost part of the Okusakainosawa Sandstone and Mudstone Member in the Okusakainosawa Creek, subdivided into four units (Figs. 8–9). Unit 1, which is uppermost part of the carbonate sequence (Iba and Sano, 2007) is consist of orbitolinid packstone (Fig. 10) which contain numerous orbitolinid tests, coated grains, and bioclasts such as cidarid spines and crinoids. This unit is covered directory by the basal part of the Okusakainosawa Sandstone and Mudstone Member (=Unit 2).

Unit 2 and 3 consist of fine-grained sandstone with normal grading, and alternating beds of sandstone and mudstone (Fig. 9). Sandstone beds (10–20 cm thick) commonly show sedimentary structures of proximal turbidites such as flute casts, convoluted laminations and climbing ripples (Fig. 11). The dark blueish green-colored sandstone beds occur occasionally. No carbonate platform biota has been found in Units 2 and 3. Unit 4 is composed of the well-stratified dark gray-colored mudstone with tuff layers (Fig. 9).

Soft-sediment deformation structures are concentrated in Unit 1 and 2 (Figs. 9–12). At the boundary of Unit 1 and 2, many irregularly-shaped carbonate clasts (0.5 to 25 cm in diameter) are observed (Figs. 10 and 12). Many carbonate clasts are un-rounded but their rims are along the individual orbitolinid tests and bioclasts (Fig. 10). Individual orbitolinid tests which are derived from the underlying orbitolinid-packstone peeled off and float in the sandstone (Figs. 10 d–f and 12-c, d). The sandstone just above Unit 1 are not stratified but liquefied (Fig. 10). The sandstone fills up the space between carbonate clasts. The admixture of bioclasts, orbitolinid tests, and sand grains frequently occur (Figs. 10-c and 12).

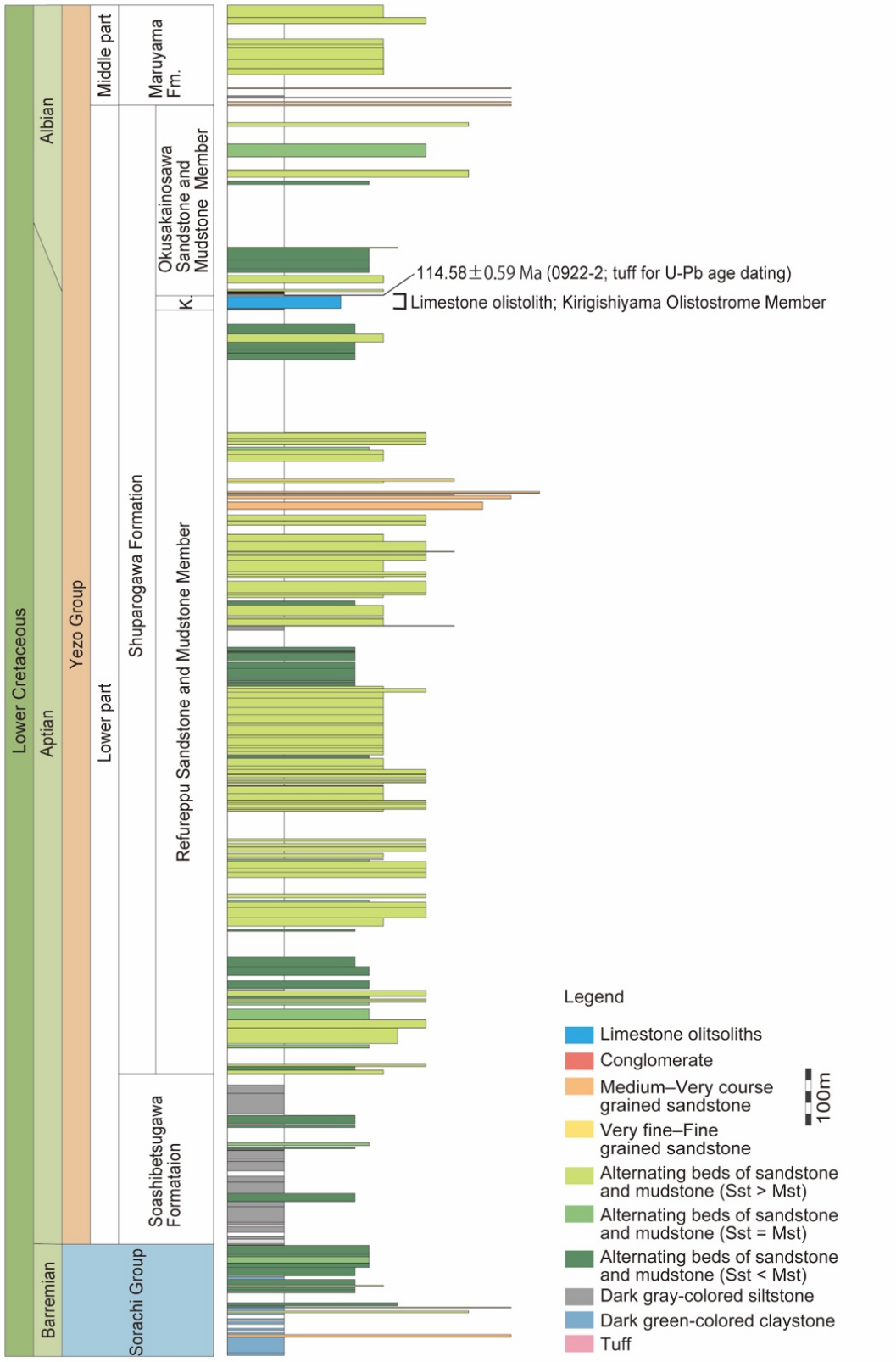

Fig. 8 Columnar section of the lower part of the Yezo Group in the Soashibetsugawa Creek.

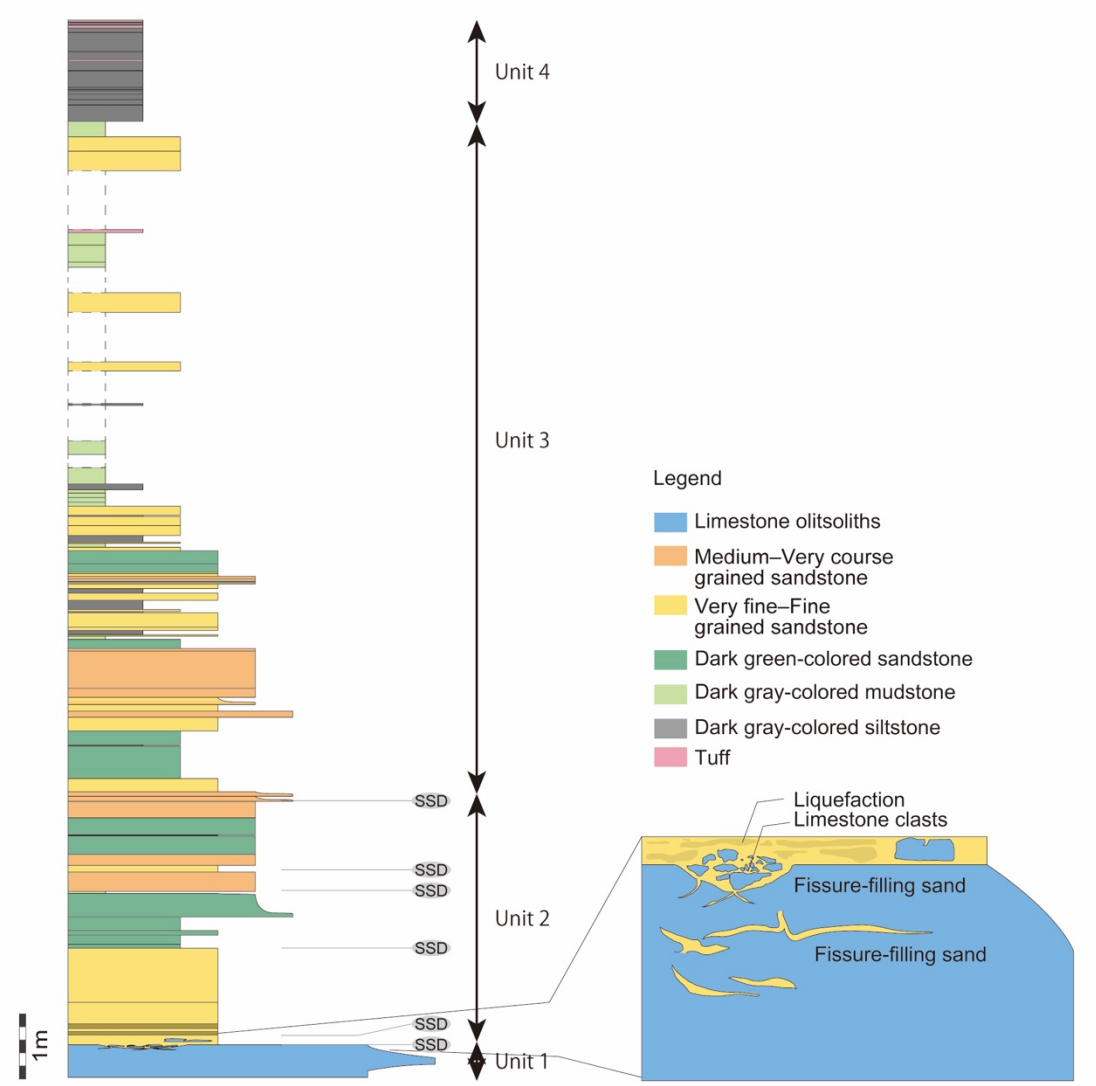

Fig. 9 Columnar section of the uppermost part of the Kirigishiyama Olistostrome Member, the lowermost part of the Okusakainosawa Sandstone and Mudstone Member in the Okusakainosawa Creek.

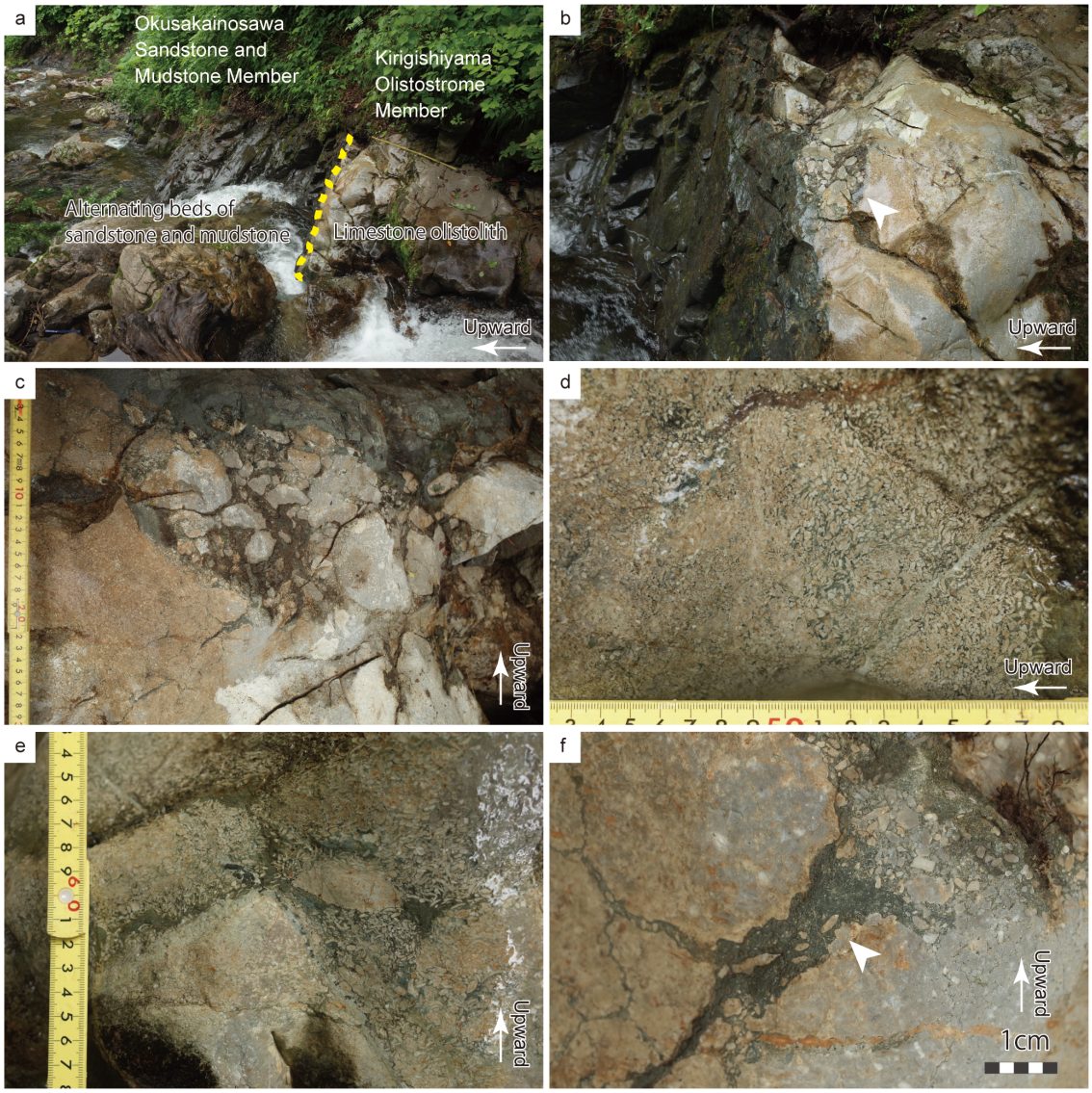

Fig. 10 The outcrop photos of the carbonate olilstoliths–sandstone interface. a–c: The boundary between the Kirigishiyama Olistostrome Member and the Okusakainosawa Sandstone and Mudstone Member. d–f: Orbitolinid packstone. f: An individual orbitolinid test floating in the sandstone.

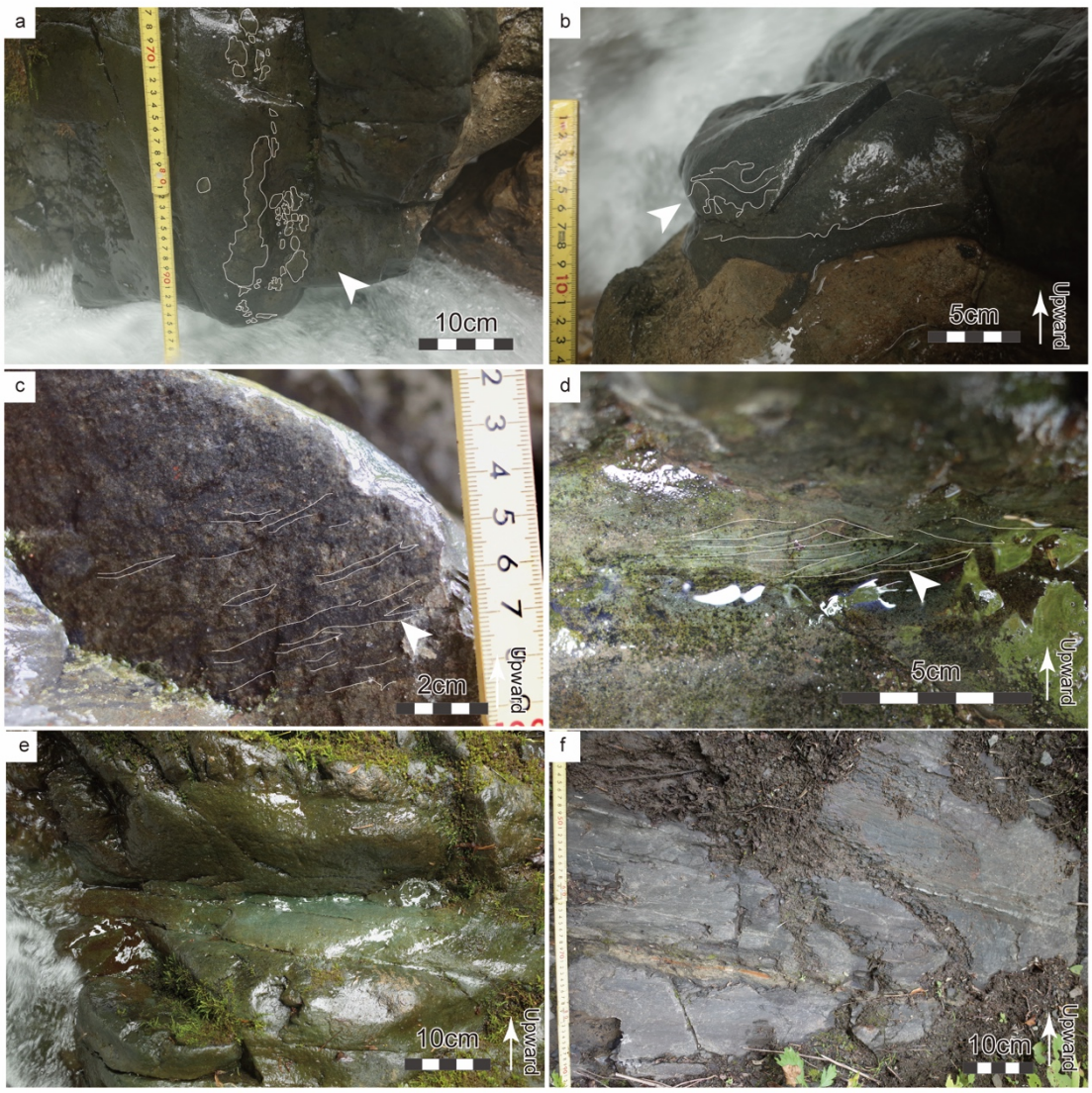

Fig. 11 The outcrop photos of the Okusakainosawa Sandstone and Mudstone Member. a–b: Liquefaction structures in sandstone just above the limestone. c: Deformation of laminae. d: Cross lamination. e: dark blueish green-colored sandstone. f: Stratified dark gray-colored mudstone.

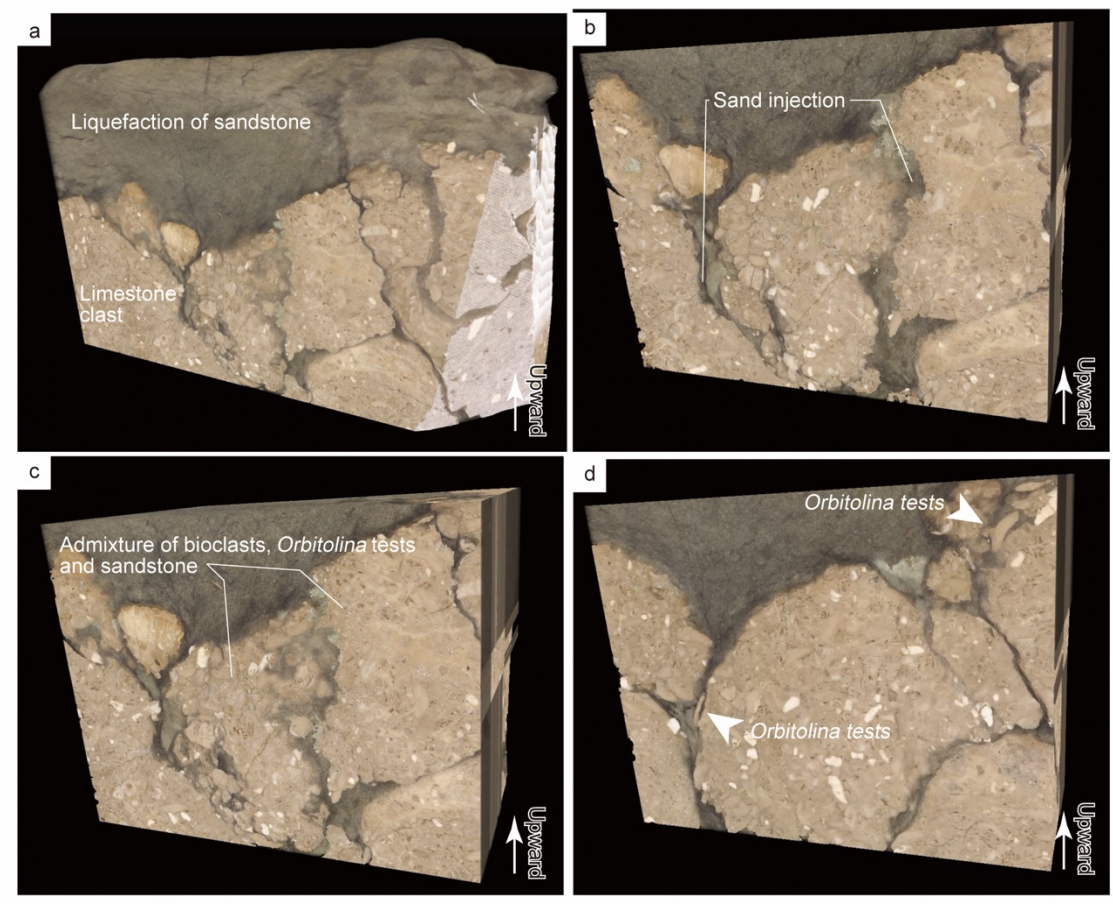

Fig. 12 The cross section of the three-dimensional mode of occurrence of the carbonate olilstoliths–sandstone interface. a–b Liquefaction and injections of sandstone. c. Admixture of bioclasts, orbitolinid tests and sandstone. d. Individual orbitolinid tests floating in sandstone.

DISCUSSION AND CONCLUSION

1. The collapse of living carbonate platform and its mass transportation in the latest Aptian

The formation age of the shallow-marine carbonate itself is estimated as 113.88–114.08 Ma (latest Aptian) by Strontium isotope analysis (Table 1 and Fig. 12). This result is consistent with the occurrence of *Mesorbitolina parva* indicating the Late Aptian to the Early Albian from carbonate olistoliths (Iba and Sano, 2007; Iba et al., 2011). On the contrast, the depositional age of the olistostrome bed is estimated in 114.58±0.59 Ma (latest Aptian) by U-Pb age dating of the basal part of Okusakainosawa Sandstone and Mudstone Member (Fig. 8). These two ages overlapped including their errors. These results clearly indicate that there is no geological time gap between the formation of rimmed shelf carbonate platform in the shallow-marine environment and their collapse-mass transportation by olistostrome into the deeper part of the basin in the geological time scale.

The liquefaction structures and sand injection mix the sand and bioclasts including tests of orbitolinid foraminifers and coated-grains are observed at the boundary between Units 1 and 2. The mud-rich fissure filling sand is similar sedimentary structures which are the admixture of sand and mud (Kawakami and Kawamura, 2002). These structures occur when the mud has not been solidified. From the series of the evidence, the top part of the carbonate olistolith had been in soft condition when they had been collapsed and transported into the deep-sea bottom. Liquefaction had occurred and disturbed in the interface of the carbonate block and sandstone.

The solidification of sedimentary carbonate rocks by their rapid cementation is confirmed by modern experiments in Bahama (Friedman, 1998). The results show that

the oolitic sand in shallow marine environments solidified in one year. Sedimentary environment of orbitolinid packstone is similar to that of modern experiment This supposes that the carbonate platform was living when they collapsed.

The evidence of age determination and soft-sediment deformation structures suggest that the collapse of "living" reef directly transported into the deeper part of the basin in the latest Aptian. The maximum size of carbonate olistolith in the study area is 60 m in thick and 3 km in length (Takashima et al., 2004). This latest Aptian carbonate olistostrome bed and or debris flow deposit including carbonate olistoliths and pebbles widely distributed over 200 km from central to northern Hokkaido (see Chapter 3). This is the largest carbonate platform in the Cretaceous of North Pacific (Iba and Sano, 2007). It is concluded that that the largest carbonate platform in the Cretaceous North Pacific collapsed alive and simultaneously transported into the deep ocean in the latest Aptian (114.58±0.59 Ma). Such scales of living platform collapse have not yet been recognized both in the geological record and modern analogue.

2. A habitat loss as extinction of carbonate platform biota in the latest Aptian in the Northwest Pacific

A step-wise demise of the carbonate platform biota transpired in the latest Aptian to latest Albian in the Northwest Pacific. This extinction occurred step-wisely: large benthic reef dwellers such as rudists, dasycladasean algae, hermatypic corals, stromatopotoids, nerineacean gastropods extinct Aptian/Albian boundary and then epibiota on calcareous sediments such as orbitolinid foraminifers and calcareous red algae disappeared at the Albian/Cenomanian boundary. After this extinction event, the carbonate platform biota, did not appear in the Northwest Pacific during the Middle

Albian to Paleocene interval, more than 50 million years in duration (Iba and Sano, 2007). Such a drastic disappearance of the carbonate platform biota has never been recognized in the Mediterranean, Caribbean and other Tethyan regions. This demise event is the reverse of the mid-Cretaceous global warming climatic trend, and its cause is still debatable (Iba and Sano, 2007). The collapse of carbonate, presented this study can be one of the causes of extinction as habitats loss (Fig. 13).

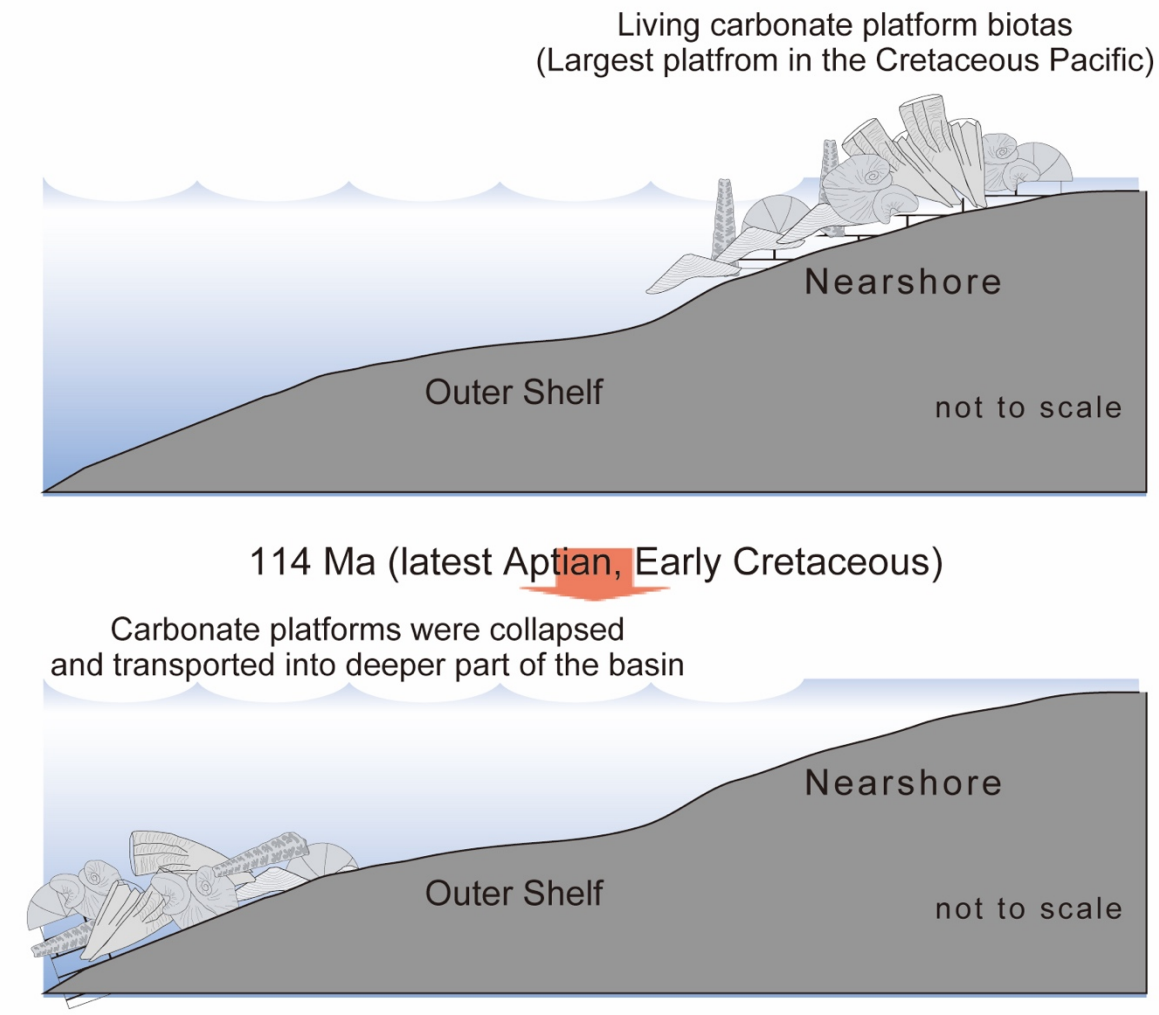

Fig. 13 Reconstruction of the collapse of carbonate platform in the latest Aptian, mid- Cretaceous.

REFERENCES CITED

Denison, R.E., Koepnick, R.B., Fletcher, A., Howell, M.W., and Callaway, W.S., 1994, Criteria for the retention of original seawater 87Sr/86Sr in ancient shelf limestones: Chemical Geology (Isotope Geoscience Section), v. 112, p. 131–143.

Friedman, G.F., 1998, Rapidity of marine carbonate cementation — implications for carbonate diagenesis and sequence stratigraphy: perspective: Sedimentary Geology, v. 119, p. 1–4, doi: 10.1016/S0037-0738(98)00075-X.

Götz, S., 2007, Inside rudist ecosystems: growth, reproduction and population dynamics, *in* Scott, R.W., ed., Cretaceous Rudists and Carbonate Platforms: Environmental Feedback, SEPM Special Publication, Society for Sedimentary Geology, v. 87, p. 97–113.

Iba, Y., and Sano, S., 2007, Mid-Cretaceous step-wise demise of the carbonate platform biota in the Northwest Pacific and establishment of the North Pacific biotic province: Palaeogeography, Palaeoclimatology, Palaeoecology, v. 245, p. 462–482, doi: 10.1016/j.palaeo.2006.09.008.

Iba, Y., Sano, S., and Miura, T. 2011, Orbitolinid foraminifers in the Northwest Pacific: their taxonomy and stratigraphy: Micropaleontology, v. 57, p. 163–171.

Jacobsen, S.B., and Kaufman, A.J., 1999, The Sr, C and O isotopic evolution of Neoproterozoic seawater: Chemical Geology, v. 161, p. 37–57, doi: 10.101 6/S0009-2541(99)00080-7.

Kawakami, G., and Kawamura, M., 2002, Sediment flow and deformation (SFD) Layers: evidence for intrastratal flow in laminated muddy sediments of the Triassic Osawa Formation, northeast Japan: Journal of sedimentary research, v.

72, no. 1, p. 171–181, doi: 10.1306/041601720171.

Ludwig, K.R., 2008, User's manual for Isoplot 3.6: a geochronological toolkit for Microsoft Excel: Berkeley Geochronology Center Special, Publication, v. 4, p. 77.

Ludwig, K.R., 2009, User's manual for Squid 2.50: Berkeley Geochronology Center Special, Publication, v. 5, p. 110.

Ogg, J., Ogg, G., and Gradstein, F., 2016, A Concise Geologic Time Scale 2016: Amsterdam, Netherlands, Elsevier, 234 p., doi: 10.1016/B978-0-444-59467-9.00001-7.

Paces, J.B., and Miller Jr., J.D., 1993, Precise U-Pb ages of Duluth Complex and related mafic intrusions, northeastern Minnesota: Geochronological insights to physical, petrogenetic, paleomagnetic, and tectonomagmatic processes associated with the 1.1 Ga Midcontinent Rift System: Journal of Geophysical Research, Solid Earth, v. 98, p. 13997–14013, doi: 10.1029/93JB01159.

Pascual-Cebrian, E., Hennhöfer, D.K., and Götz, S., 2013, 3D morphometry of polyconitid rudist bivalves based on grinding tomography: Facies, v. 59, p. 347–358, doi:10.1007/s10347-012-0310-8.

Sano, S., 1995, Lithofacies and biofacies of Early Cretaceous rudist- bearing carbonate sediments in northeastern Japan: Sedimentary Geology, v. 99, p. 179–189, doi: 10.1016/0037-0738(95)00043-8.

Sano, S., 2000, Reconstruction of carbonate platform from olithtolis embedded in Lower Yezo Group: Gekkan Chikyu (Earth Monthly), Special Issue 29, p. 45–60.

Stacey, J.S., and Kramers, J.D., 1975, Approximation of terrestrial lead isotope

evolution by a two-stage model: Earth and Planetary Science Letters, v. 26, p. 207–221, doi: 10.1016/0012-821X(75)90088-6.

Takashima, R., Nishi, H., Saito, T., and Hasagawa, T., 1997, Geology and planktonic foraminiferal biostratigraphy of Cretaceous strata distributed along the Shuparo River, Hokkaido, Japan: Journal of the Geological Society of Japan, v. 103, no. 6, p. 543–563, doi: 10.5575/geosoc.103.543.

Takashima, R., Kawabe, F., Nishi, H., Moriya, K., Wani, R., and Ando, H., 2004. Geology and stratigraphy of forearc basin sediments in Hokkaido, Japan: Cretaceous environmental events on the north- west Pacific margin: Cretaceous Research v. 25, p. 365–390.

Williams, I.S., 1998 U-Th-Pb geochronology by ion micro probe, *in* McKibben, M.A., Shanks III, W.C., and Ridley, W.I., eds., Applications of microanalytical techniques to understanding mineralizing processes: Reviews in Economic Geology, v. 7, p. 1–35.

Yabe, H., 1901. The discovery of *Orbitolina* limestone from Hokkaido: Journal of the Geological Society of Japan, v. 8, p. 187–190.

Chapter 5

General Discussion and Summary:

The mid-Cretaceous coastal catastrophe along the eastern margin of Eurasia reconstructed by sedimentological analysis and chronostratigraphic correlation

1. The stratigraphic correlations of the chaotic deposis in the lowermost part of the Yezo Group

The lower part of the Yezo Group is a good example for understanding the earliest history of the fore-arc basin. Geological age of the sequence, has, however, been still unclear due to a lack of age-diagnostic fossils. The problem has been an obstacle to regional correlations. The various chaotic deposits, which are distributed in the lower part of the Yezo Group in five areas in 200 km scale from northern to central Hokkaido, each was described in detail in this study. For their correlation, lithostratigraphy, larger benthic foraminifer biostratigraphy, U-Pb geochronology and strontium isotope stratigraphy were examined in five areas in 200 km scale from northern to central Hokkaido (Chapter 1–4; Fig. 1).

In this study, the depositional age of the amber- and plant debris-concentrated turbidites in the boundary between the Sorachi and Yezo Group and lowermost part of the Yezo Group in the Nakagawa area, northern Hokkaido, and huge carbonate rock-containing olistostrome in the Kirigishiyama Olistostrome Member in the lower

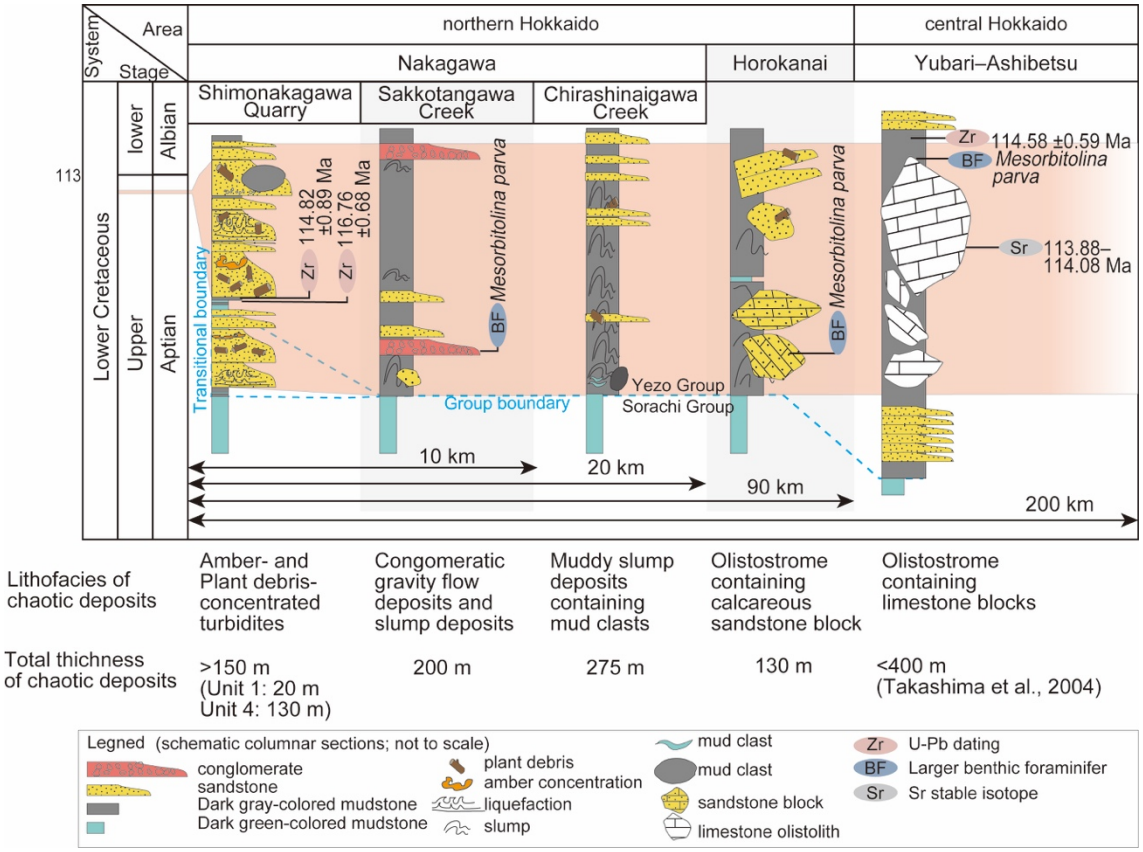

Fig. 1 Correlation of chaotic deposits distributed in northern–central Hokkaido.

part of the Yezo Group are dated by the U-Pb dating. The U-Pb age of the tuff in the lowermost part of the Yezo Group (Unit 4) in the Nakagawa area, and tuff in the mudstone 6-m-above the Kirigishiyama Olistostrome Member of the lower part of the Yezo Group in the Yubari–Ashibetsu area are dated. Their ages are 114.82±0.89 Ma and 116.76±0.68 Ma, respectively. The estimated age of strontium isotope analysis of rudist bivalves (113.88–114.08 Ma) and biostratigraphy of *Mesorbitolina parva* (Late Aptian–Early Albian; Iba and Sano, 2007; Schroeder et al., 2010) from limestone olistoliths in the Kirigishiyama Olistostrome Member in the Yubari–Ashibetsu area are also concordant to the age. The results of the ages show that the lowermost part of the Yezo Group in the Nakagawa area and the Kirigishiyama Olistostrome Member can be correlated.

In this study, age-diagnostic larger benthic foraminifer *Mesorbitolina parva* were newly extracted from the calcareous sandstone olistoliths in the lowermost part of the Yezo Group in the Horokanai areas, northern Hokkaido, intermediate between the Nakagawa and Yubari-Ashibetsu areas. The orbitolinid-containing limestone is one of the key units of the Yezo Group (KY-1 in Takashima et al., 2004). Iba and Sano (2006) propose that the lowermost part of the Yezo Group in Nakagawa area, northern Hokkaido and Kirigishiyama Olistostrome Member of the lower part of the Yezo Group. The results in this study show that the olistostrome in the lowermost part of the Yezo Group in the Horokanai areas can be correlated to the key unit and their chaotic event deposits in Nakagawa and Yubari–Ashibetsu areas. In conclusion, the chaotic deposits in the Nakagawa, Horokanai and Yubari–Ashibetsu area can be correlated to be latest Aptian (around 115 Ma).

In the Nakagawa area, amber- and plant debris-concentrated turbidites intercalate the 20-m thick claystone/siltstone unit (Unit 3). The U-Pb age dating from two tuff layers shows that there are 0.3–3.5 Myr interval in the sequence. The result shows that the amber- and plant debris-concentrated turbidite indicate the presence of two event-concentrated periods around 117–114 Ma. The former period is in 117.44–116.08 Ma, or older (Unit 2) and latter one is in 115.71–113.93 Ma, or younger (Unit 4), latest Aptian. The depositional age of the limestone olistostrome in the Yubari–Ashibetsu area are estimated as 114.58±0.59 Ma, and it can be correlated to the amber- and plant debris-concentrated turbidites of Unit 4 (latter period) in the Nakagawa area.

2. Coastal catastrophic events in the Latest Aptian

In central Hokkaido, a huge limestone olistostrome has been reported in previous studies (e.g., Yabe, 1901; Takashima et al., 2004). In the Horokanai area, an olistostrome which contains the calcareous sandstone blocks are described in this study (Chapter 3). The olistostrome can be correlated to the huge limestone olistostrome in the Yubari–Ashibetsu area (central Hokkaido) by *Mesorbitolina parva* and it indicates that olistostrome had occured in 100 km scale through central and northern Hokkaido, 114.58±0.59 Ma, the latest Aptian. This limestone olistostrome can be traced to 200 km as the debris-flow deposit including limestone pebbles in the Nakagawa area (Iba and Sano, 2006). The olistostrome and limestone pebbles-including debris-flow deposits show the largest carbonate platform in the Cretaceous North Pacific collapse when they still alive, and immediately transported into the deep ocean in the latest Aptian. Such scales of living carbonate platform collapse have not yet been recognized both in the geological record and modern analogue.

In the Nakagawa area, northern Hokkaido, amber- and plant debris-concentrated turbidites are newly described from the boundary between the Sorachi and Yezo groups and lowermost part of the Yezo Group (Chapter 1). Their sedimentary features indicate that the destruction of the land forests and rapid transportation of its remains into hemi-pelagic environments by large-scale tsunamis. Some chaotic deposits such as the conglomeratic gravity flow deposits and muddy slump deposits with large mud clast also occur from the lowermost part of the Yezo Group in the Nakagawa area (Chapter 2). Large-scale tsunamis and earthquakes are one of the plausible causes of the formation of these chaotic deposits.

The study clear that chaotic deposits are concentrated around 114–117 Ma, the latest Aptian from central to north Hokkaido. Each deposit indicates the destruction of hinterlands, such as land forests, carbonate platform and shallow-marine seafloors. These results show the collapse of the "living" largest carbonate platform Cretaceous North Pacific occurred over 200 km, land forest destruction by large-scale tsunamis and submarine slope failure occurred in the same period. These are the 200 km scale coastal catastrophe along the eastern margin of Eurasia in the latest Aptian, Early Cretaceous (Fig. 2).

3. As possible cause for an extinction event of carbonate platform biota

In the late Aptian of northern Hokkaido, the occurrence of high concentration of the plant debris and ambers through the turbidite sequence and U-Pb dating indicate the wide and repeatable destruction of the land forests. They had lasted at least 0.3−3.5 Myr with one interval. Their recovery would be supported by enormous biomass on the continent. Whereas, the drastic disappearance of typical Cretaceous Tethyan biota

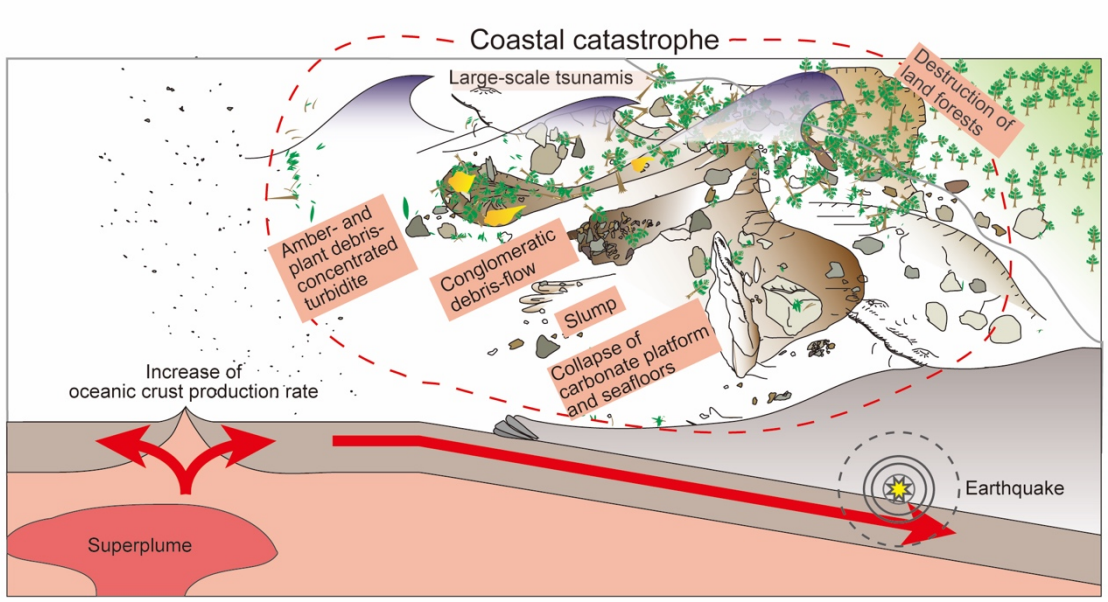

Fig. 2 The reconstruction of the coastal catastrophe along the eastern margin of Eurasia, latest Aptian.

occurred in Northwest Pacific (Iba and Sano, 2007) and it is assumed that the catastrophe was related to the biotic event.

In the mid-Cretaceous, the extreme warmth due to superplume activities (Larson 1991a, b) caused the poleward expansion of reef lines (Jhonson et al., 1996). The carbonate platform had developed linearly along the Asian continental margin (from central Kyushu Island to Sakhalin Islands) and it was the largest in Mesozoic North Pacific (e.g., Simo et al., 1993; Iba and Sano, 2007, Takashima et al., 2007). In the Late Aptian, the drastic disappearance of typical Cretaceous Tethyan biota occurred in Northwest Pacific (Iba and Sano, 2007). They are considered as the step-wise extinction of carbonate platform biota during the latest Aptian to middle Albian interval (Iba and Sano, 2006, 2007, 2008; Iba, 2009). The disappeared carbonate platform biota did not appear in the Northwest Pacific during the Middle Albian to the Paleocene interval, more than 50 million years in duration. In this extinction event, “Mesogean key taxa” (rudists and dasycladacean algae), some “Mesogean indicator” (e.g., hermatypic corals and stromatoporoids) (Masse, 1992a, b) and nerineacean gastropod disappearance (last occurrence) corresponds the periods of the coastal catastrophe including collapse of carbonate platform in central–northern Hokkaido.

Destruction events of the coral reefs in a present period, are typically caused by hurricanes and tsunamis. The hermatypic coral recolonization greatly depends on their damages and environment but typically slow on a scale of decades (e.g., Grigg and Maragos, 1974). In the example of the destruction of reefs by Holocene tsunami in the southern Caribbean, the coral reef did not regenerate in 3100 years (until present) and the shift of ecosystem from coral- to algae-dominant (Scheffers et al., 2006). The study argues that the presence of the serious influence of corals by tsunamis in pre-historic

records larger than the present ones. In this study, the collapse of the carbonate platform in central–northern Hokkaido would be more devastating damage to the carbonate platform biota, especially hermatypic ones. Its cause may not be tsunamis and hurricanes, but rather the complete destruction and sink of the carbonate platform should have given considerable damages. In addition, the presence of tsunamis in northern Hokkaido at least 0.3−3.5 Myr support the repeatable occurrence for the coastline and they also prevent their recovery in the periods. The calcareous red algae, coated grains and Tethyan bivalves occur from calcareous turbidites from the Kj3 Member in the Kamiji Formation (Early Albian) in the Chirashinai Creek of the Nakagawa area. Some species (Rudists, Dasycladacea, hermatypc corals, stromatopoloids and Nerineacea), however, would not occur since the Late Aprian Key Unit KY-1 which is the huge limestone Olistostrome sequence (Kirigishiyama Olistostrome Member in the Yubari–Ashibetsu area) (Iba and Sano, 2007). The collapse of the carbonate platform would give fatal damages that make the survival of the species impossible. The distribution of the carbonate platform in central–northern Hokkaido was mostly northern limit of the belt-like carbonate platform along the Eurasian continental margin. It is assumed that the distribution also makes the hermatypic biota to be difficult to recover against their habitat destruction due to lack of their recovery source nearby places. The wide and repeatable destruction of their habitats would be one of the conceivable factors of the biotic event.

4. The period of instability in the stage of the terrigenous sediment supply into the fore-arc basin

The boundary between the Sorachi and Yezo groups is considered as the transition period of the supply system of terrigenous sediments into fore-arc basin as the consequences of tectonic activities (e.g., Kito et al., 1986; Okada, 1983). In Early Cretaceous, orogeny and volcanic activities had been caused by the westward subduction. The subduction had caused the trap of the oceanic crust (the lower part of the Sorachi Group), activated the activity of volcanic arc in the west side (Rebun-Kabato belt) and supply of volcanic clastic sediments and form of pillow lava had occurred (the upper part of the Sorachi Group). The orogeny of the wide range of hinterlands (Sothern and North Kitakami Belt and Oshima Belt) had been also caused and that is considered as the factor of the transition of the supply from volcanic clastic sediments to terrigenous sediments in the boundary between the Sorachi and Yezo groups.

The U-Pb age data in the Nakagawa area shows that land forest catastrophe (large-scale tsunamis) had lasted about 0.3−3.5 Myr with one inactive period. In the latter event-concentrated period (115.71–113.93 Ma), the collapse of the carbonate platform occurred in a 200 km scale through central–northern Hokkaido. The drastic changes of the hinterlands such as orogeny are the plausible cause of these events. They should had been driven as the earliest stage of the supply system of terrigenous sediments into a fore-arc basin which had lasted from the latest Aptian to the Paleogene and had supplied the terrigenous sediments 8000 m in total thickness.

5. Originality of the study

5-1. Correlation of chaotic deposits for revealing the catastrophe

All the deposits studied in this study have various lithofacies (amber-concentrated turbidites, large mud clast-containing muddy slump deposits, limestone pebbles-containing gravity flow deposits, meter-order shallow-marine calcareous sandstone block-concentrated olistostrome and kilometer-order huge carbonate blocks-concentrated olistostrome; Fig. 1). The various lithofacies changes might be caused by the settings of the hinterlands and the distance from their causes. Although some deposits have been reported in previous studies, they have been interpreted as the consequences of a local phenomenon and overlooked. This is because conventional stratigraphic correlations have been based on the trace of the same litho- and bio-facies. Some enigmatic materials have been focused as the evidence of large-scale catastrophe and/or global events (e.g., the high-concentration of Iridium for bolide impact and organic carbon-rich sediments for Oceanic Anoxic Events; Alvarez et al., 1980; Shlanger and Jenkyns, 1976). In this study, chaotic deposits with various lithofacies were focused as the trace of the destructive events by sedimentological analysis and correlated with strict constraining of age by geochronostratigraphic methods. The way of the various lithofacies correlation with focusing on the detail sedimentological features with strict constraining of ages is the new aspect of view which unveil the catastrophic event.

5-2. Novel approach for reconstructing the sedimentary process by soft-sediment deformation structures

Soft-sediment deformation structures such as slump deposit and liquefaction structures are commonly used to the structures formed in sediments which were still in

unlithified condition. These structures in siliciclastic sediments are useful for interpretation of their sedimentation process, however, it is difficult to constrain their formation time because they can be formed until the matrix is in soft condition.

In this study, resins and sedimentary limestone has the features of rapid consolidation. The soft-sediment deformation structures of resins, which are typically hardening in one week in the air and unconsolidated in the water, reveal the process of destruction of the land forests by water and rapid transportation from land to hemi-pelagic seafloor. The soft sediment deformation structures of sedimentary limestone (orbitolinid-ooid packstone), which are considered to be hardening by rapid cementation in one year (Friedman, 1998), indicate the destruction of the "living" carbonate platform and transportation of its remains into the deeper part of the basin nearly coinstantaneous occur. These descriptions by soft-sediment deformation structures over the conventional discussion in a geologic time scale by stratigraphy, geochemistry, and geochronology. This can be a novel approach for reconstructing the sedimentary process (erosion, transportation and sedimentation) by soft-sediment deformation structures.

REFERENCE CITED

Alvarez, L.W., Alvarez, W., Asaro, F., and Michel, H.V., 1980, Extraterrestrial cause for the Cretaceous-Tertiary extinction: Science, v. 208, p. 1095-1108, doi: 10.1126/science.208.4448.1095.

Friedman, G.F., 1998, Rapidity of marine carbonate cementation — implications for carbonate diagenesis and sequence stratigraphy: perspective: Sedimentary Geology, v. 119, p. 1–4, doi: 10.1016/S0037-0738(98)00075-X.

Grigg, R.W., and Maragos J.E., 1974, Recolonization of hermatypic corals on submerged lava flows in Hawaii: Ecology, v. 55, p. 387–395, doi: 10.2307/1935226.

Iba, Y., 2009, An Early Albian Arctic-type ammonite Arcthoplites from Hokkaido, northern Japan, and its paleobiogeographic and paleoclimatological implications: Journal of Asian Earth Sciences, v. 3, p. 46–50, doi: 10.1016/j.jseaes.2008.03.007.

Iba, Y., and Sano, S., 2006, *Mesorbitolina* (Cretaceous larger foraminifera) from the Yezo Group in Hokkaido, Japan and its stratigraphic and paleobiogeographic significance: Proceedings of the Japan Academy, Series B, v. 82, p. 216–223, doi: 10.2183/pjab.82.216.

Iba, Y., and Sano, S., 2007, Mid-Cretaceous step-wise demise of the carbonate platform biota in the Northwest Pacific and establishment of the North Pacific biotic province: Palaeogeography, Palaeoclimatology, Palaeoecology, v. 245, p. 462–482, doi: 10.1016/j.palaeo.2006.09.008.

Iba, Y., and Sano, S., 2008, Paleobiogeography of the pectinid bivalve Neithea, and its pattern of step-wise demise in the Albian Northwest Pacific: Palaeogeography,

Palaeoclimatology, Palaeoecology, v. 267, p. 138–146, doi: 10.1016/j.palaeo.2008.07.002.

Johnson, C.C., Barron, E.J., Kauffman, E.G., Arthur, M.A., Fawcett, P.J., and Yasuda, M.K., 1996, Middle Cretaceous reef collapse linked to ocean heat transport: Geology, v. 24, p. 376–380, doi: 10.1130/0091-7613(1996)024<0376:MCRCLT>2.3.CO;2.

Kito, N., Kiminami, K., Niida K., Kanie, Y., Watanabe, T., and Kawaguchi, M., 1986, The Sorachi Group and the Yezo Supergroup: Late Mesozoic ophiolites and forearc sediments in the axial zone of Hokkaido: Journal of the Geological Society of Japan, v. 31, p. 81-96.

Larson, R.L., 1991a, Latest pulse of Earth: Evidence for a mid-Cretaceous superplume: Geology, v. 19, p. 547–550, doi: 10.1130/0091-7613(1991)019<0547:LPOEEF>2.3.CO;2

Larson, R.L., 1991b, Geological consequences of superplumes: Geology, v. 19, p. 963–966, doi: 10.1130/0091-7613(1991)019<0963:GCOS>2.3.CO;2.

Masse, J.P., 1992a, Lower Cretaceous Mesogean benthic ecosystems: palaeoecologic aspects and palaeobiogeographic implications: Palaeogeography, Palaeoclimatology, Palaeoecology, v. 91, p. 331–345, doi: 10.1016/0031-0182(92)90075-G.

Masse, J.P., 1992b, The Lower Cretaceous Mesogee: A state of the art, *in* Kollmann, H.A. and Zapfe, H. eds., New Aspect on Tethyan Cretaceous Fossil Assemblages: Schriftenreiche der Erdwissenschaftlichen Kommissionen der Österreichischen Akademie der Wissenschaften, p. 15–33, doi: 10.1007/978-3-7091-5644-5_2.

Okada, H., 1983, Collision orogenesis and sedimentation in Hokkaido, Japan, *in* Hashimoto, M., and Uyeda, S., eds., Accretion Tectonics in the circum-Pacific Regions: Tolyo, Terrapub, p. 91-105, doi: 10.1007/978-94-009-7102-8_7.

Simo, J.T., Scott, R.W., and Masse, J.P., 1993, Cretaceous Carbonate Platforms: An Overview, in Simo, J.T., Scott, R.W., and Masse, J.P., eds., Cretaceous Carbonate Platforms: American Association of Petroleum Geologists Memoir, v. 56, p. 1–14.

Scheffers, S., Scheffers, A., Radtke, U., Kelletat, D., Staben, K., and Bak, R., 2006, Tsunamis trigger long-lasting phase-shift in a coral reef ecosystem: Zeitschrift für Geomorphologie NF, Suppl, v. 146, p. 59–79.

Schlanger, S.O., and Jenkyns, H.C., 1976, Cretaceous oceanic anoxic events: causes and consequences: Geologie en mijnbouw, v. 55, p. 179–184.

Schroeder, R., van Buchem, F.S.P., Cherchi, A., Baghbani, D., Vincent, B., Immenhauser A., and Granier B., 2010, Revised orbitolinid biostratigraphic zonation for the Barremian – Aptian of the eastern Arabian Plate and implications for regional stratigraphic correlations, *in* van Buchem, F.S.P., Al-Husseini, M.I., Maurer F., and Droste H.J., eds., Barremian − Aptian stratigraphy and hydrocarbon habitat of the eastern Arabian Plate: GeoArabia Special Publication 4, Gulf PetroLink, Bahrain, v. 1, p. 49-96.

Takashima, R., Kawabe, F., Nishi, H., Moriya, K., Wani, R., and Ando, H., 2004, Geology and stratigraphy of forearc basin sediments in Hokkaido, Japan: Cretaceous environmental events on the north-west Pacific margin: Cretaceous Research, v. 25, p. 365–390. doi: 10.1016/j.cretres.2004.02.004.

Takashima, R., Sano, S., Iba, Y., and Nishi, H., 2007, The first Pacific record of the Late

Aptian warming event: Journal of the Geological Society, v. 164, p. 333–339, doi: 10.1144/0016-76492006-006.

Yabe, H., 1901, The discovery of *Orbitolina* limestone from Hokkaido: Journal of the Geological Society of Japan v. 8, p. 187–190.

Acknowledgment

I would like to thank deeply the following people. My supervisor Professor Yasuhiro Iba discussed, advised and supported my research work night and day for six years. He always gave me chance to advance my research and my perspective. I learned a lot from him about study, field research and philosophy of geology. He was a chief referee of defense of my doctoral thesis. Professor Yoshitsugu Kobayashi gave precise advice for my study. He was a sub-chief referee of defense of my doctoral thesis. Professor Noriyuki Suzuki encouraged me every time and gave me useful advice about sedimentology as a sub-chief referee of defense of my doctoral thesis. Professor Toru Takeshita was as a sub-chief referee of defense of my doctoral thesis. He gave me opportunity for U-Pb dating at KBSI, Korea. The U-Pb data were very important in my doctoral thesis.

Professor Shinichi Sano of Toyama University gave me many advices about paleontology and geology. He read and corrected my manuscript many times. His discussion was always deeply-conceived and promoted my study. Professor Makoto Kawamura of Hokkaido University discussed with me and lots of exciting advices based on his deep knowledge about sedimentology, geology and the history of the Sorachi and Yezo Groups. The concept of soft-sediment deformation structures which I learned from him were most important point of view in my doctoral thesis. Professor Hayato Ueda of Niigata University gave me advice about geology and attitude for field works. Professor Jörg Mutterlose read my manuscripts, gave me advices and corrected to the text. Professor Haruhumi Nishida of Chuo University gave me advice about paleobotany and encouraged my study.

Ms. Yumi Adachi deeply-supported my field works around Japan, analysis and my paper works for five years. Ms. Minami Murakami in Toyama University supported my field research. I could not work in the Chirashinaigawa Creek, the Sakkotangawa area and Soashibetsugawa Creek without her. Mr. Sanwu An always actively discussed with me our study, paleontology and geology. Mr. Shin Ikegami support my field works with his great ability for field observation. Ms. Miho Hama supported my study, especially for Strontium isotope analysis. Mr. Keisuke Nakamoto, Mr. Tomo Ozaki, Mr. Tomonori Tanaka, Mr. Ryuji Takasaki, Mr. Junki Yoshida, Mr. Masaya Iijima, Mr. Hidetoshi Sonobe, Mr. Takumi Sakakiyama, Mr. Yusuke Umemura, Mr. Shohei Ando, Mr. Satoshi Furota, Mr. Hideto Nakamura of Hokkaido University and Mr. Kotaro Katsuie of Shinshu University supported the field research around Hokkaido. Mr. Shintaro Sasaki operated the Grinding tomography for my analysis and instructed me how to use the machine. Mr. Yusuke Takeda made amazing 3D models of amber and limestone and instructed me about three-dimensional analysis. He gave me a rare opportunity for visiting SPring-8 and analysis of samples.

Professor Keewook Yi allowed me to U-Pb age analysis for three times and instructed me about U-Pb dating. Ms. Sookju Kim, Ms. Shinae Lee and Mr. Hui Je Jo, staffs and students of KBSI, supported my work and stay in KBSI for U-Pb data aging. Professor Julien Legrand of Chuo Universty discussed paleobotany and palynology. Professor Yoshinori Hikida of Nakagawa Eco Museum discuss my study, supported my field research at the Shimonakagawa Quarry for six years. Mr. and Mrs. Toyama allow me to work in the Shimonakagawa Quarry and kindly supported during my field research for six years. Mr. Tsuchida also supported my field research, especially for sampling by an excavator. Mr. and Mrs. Saito of the accommodation of Hokkaido

University in Nakagawa, gave me kind, warm and deep support for everything during the stay in Nakagawa for my field research for six years. Mr. Hojo and staffs of the Nakagawa experimental forest center allow me to work in the Nakagawa experimental forest and support my field work. The staffs of the Furano Quarry helped me when an emergency occurred in the field. Mr. Tun Ba kyu, Ms. Phyu Pann Ei, Mr. Ko Nyi Nyi Naing supported kindly my work about amber in Myanmar. Professor Jun Liu supported my fieldwork in China. Mr. Saw Mu Tha Lay Paw and Ms. Tin Tin Latt support the great field research in Myanmar. Mr. Kosuke Nakamura and Mr. Hidehiko Nomura made great thin sections of rock samples. Professor Hideko Takayanagi of Tohoku University and Professor Yoshihiro Asahara of Nagoya University deeply-supported for Strontium isotope analysis. Ms. Etsuko Uchiyama supported the management of laboratory. Ms. Chisako Sakata, of National Museum of Nature and Science, Tokyo help me for CT of amber samples. Professor Kentaro Uesugi and Professor Masato Hoshino of SPring-8 instructed me how to operate the Synchrotron at SPring-8. Mr. Shinohara and staffs in Campany Tsuji-sekizai cut my rock samples for many times. The cut sample were important for advancing my study. Mr. Kei Nakano, Mr. Ishibashi Volunteers and Staffs at the Hokkaido University Museum encouraged and helped my works. Mr. Koji Kato of Zeiss gave me abundant knowledge about a microscope.

Ms. Minami Kuroda, Ms. Mio Terada, Ms. Megumi Mori, Ms. Ayumi Okamoto, Ms. Michiru Kamibayashi, Ms. Yoshie Nakai, Mr. Yuma Miyata, Mr. Ryohei Abe, Ms. Moeko Nagata, Ms. Shiika Makinae, Ms. Kimi Takahashi, Ms. Wako Hashimoto, Ms. Yuka Sato, Mr. Daiki Yamamoto, Sato family, Staffs of Ponpira Drive Inn and Ms. Mami Iwasa greatly supported and encouraged during works. The members in

Paleobiology laboratory and course of Earth and Planetary System Science gave me advice and encouragement for a long time.

This research was supported by JSPS KAKENHI Grant 16J05629. Finally, I greatly thank my parents, sister, grandparents and my friends for their deep encouragement and supporting for everything.